TUNABLE PROPERTIES AND MORPHOLOGIES OF BIODEGRADABLE POLYMER THIN FILMS

by

JOE BROWN GRUBBS III

(Under the Direction of Jason Locklin)

ABSTRACT

In this dissertation, homopolymer and block copolymer (BCP) brushes were fabricated using surface-initiated ring-opening polymerization (SI-ROP) of polycaprolactone (PCL) and polylactide (PLA). These two polymer brush coatings exhibited controlled degradation rates. PCL brushes were polymerized from hydroxyl-terminated monolayers utilizing the bifunctional catalyst triazabicyclodecene (TBD). A brush thickness of 40 nm was achieved with a reproducible and unique crystalline morphology. The organocatalyzed PCL brushes were chain extended using lactide in the presence of zirconium n-butoxide to successfully grow PCL/PLA block copolymer (PCL-b-PLA) brushes with a final thickness of 55 nm. The degradation properties of the "grafted to" and "grafted from" brushes were probed using aqueous methanol solutions with elevated pH. Degradation kinetic studies elucidated that the brush density plays a major role in the rate of hydrolysis for the different PCL-based systems.

In addition, BCPs using polylactide as a biodegradable sacrificial component and polystyrene (PS) (PS-b-PLA) were studied in order to produce patterned thin films. The PS-b-PLA polymers were prepared using the bifunctional initiator 2-hydroxyethyl 2-bromoisobutyrate

(HEBIB). Atom transfer radical polymerization (ATRP) was utilized to synthesize the PS macroinitiator with low dispersity from the bromine end of HEBIB. PLA was then synthesized using the hydroxyl end of HEBIB to fabricate a diblock copolymer that consisted of immiscible covalently attached homopolymers. The covalently attached molecules enabled the formation of phase separated morphological cylinders to create a framework for nanoporous membranes. Solvent annealing using THF was employed to create the highly ordered perpendicular cylinder domains needed to develop nanopores that are desirable in applications such as drug delivery and water filtration. Film thicknesses ranging from 20 to 130 nm were investigated to elucidate the role of thickness in the long-range ordering of cylinders during solvent annealing. In addition, two stereoisomers of lactide were studied as sacrificial components to probe morphological changes in the thin films due to the addition of amorphous and crystalline lactide isomers.

Degradation studies of the BCP brushes and phase separated films were carried out using a basic solution (pH 14) in order to promote degradation of the polyester backbone by hydrolysis that yields selective etching of only the biodegradable component. This framework also enables tunability over the degradation kinetics.

INDEX WORDS: Block copolymer, SI-ROP, ATRP, ROP, Degradation, Phase Separated, Morphology, Annealing, Polymer Brush, Thin Film

TUNABLE PROPERTIES AND MORPHOLOGIES OF BIODEGRADABLE POLYMER THIN FILMS

by

JOE BROWN GRUBBS III

AA, Bainbridge College, 2003

BS, Georgia Southwestern State University, 2003

A Dissertation Submitted to the Graduate Faculty of The University of Georgia in Partial Fulfillment of the Requirements for the Degree

DOCTOR OF PHILOSOPHY

ATHENS, GEORGIA

2014

TUNABLE PROPERTIES AND MORPHOLOGIES OF BIODEGRADABLE POLYMER THIN FILMS

by

JOE BROWN GRUBBS III

Major Professor: Jason Locklin

Committee: Jon Amster
Ian Hardin

Electronic Version Approved:

Julie Coffield
Interim Dean of the Graduate School
The University of Georgia
December 2014

DEDICATION

My dissertation is dedicated to my beloved family: Melanie, Jake, Amelia, and Luciana. This journey would not have been possible without the love and unconditional support y'all have provided. I cannot thank you guys enough for the sacrifices you made. I love each of you with all my heart!

ACKNOWLEDGEMENTS

I would like to start out by thanking my Dad, Mom, David, and Jordan, for the wonderful childhood memories that we experienced together. I am truly blessed to have you guys in my life. Thanks for all the love and support.

To Kenny, Lynn, and Kendall, it was truly a blessing to marry into such a wonderful family. You guys have truly been a blessing in my life, and I am forever indebted to you for taking me in as a son and brother. Thanks for all the love and support over the past 13 years.

I would also like to thank Dr. Daniel Carraway for giving me the opportunity to earn a PhD in polymer chemistry. Thanks for providing financial support throughout my UGA tenure and believing in me. I appreciate all the hard work you did through DaniMer to make this possible. I am so thankful that we crossed paths back in 2006. I would also like to thank Dr. Steve Wann who took me in and mentored me at DaniMer for two years before I started my PhD. I appreciate the time you spent teaching me the fundamentals of polymer chemistry. It really helped my transition from Biology to Chemistry be a little smoother. I miss you two guys. Not a day goes by that I don't reflect on the memories we shared from our short time together at DaniMer.

Next, I would like to thank Dr. Jason Locklin, for being a great mentor and friend. I could search the whole world over and never find another advisor that is as hardworking and supportive as you. Thanks for your guidance over the past 5 years. You are truly blessed with many talents and I am very thankful for the skills you have taught me. I hope someday that I can pay you back for all you have done for me. I would also like to thank my committee members

Dr. Jon Amster and Dr. Ian Hardin. Dr. Amster, I really enjoyed your Mass Spec and Electronics class. They were really helpful and I appreciate your guidance in those courses. Dr. Hardin, thanks for being so inquisitive. It has really helped me to question and think about anything I pick up. The meeting in Riverbend South hallway, with the pack of crackers, really taught me a valuable lesson. Thanks guys!

Lastly, I would like to thank all of Locklin's graduate students both past and present that I have had the wonderful pleasure to work with. You guys are awesome. I hope you guys are all blessed with a bright and prosperous career. Kyle Sontag, I appreciate the long runs and fellowship. Anandi Roy, you are definitely the best Indian I have ever met. Eric Huddleston, you might be one of the coolest guys I have ever had the opportunity to hang out with. Rachelle Arnold, if I had a sister, you would be a clone. I look forward to working with you at DaniMer, and I appreciate all your help over the years. Evan White, thanks for setting the tone in BCP phase separation. The first image you obtained really made me work harder to fabricate my own. I hope you and Lauren are blessed with many years of happiness. Jenna Bilbrey, I really appreciate the time you put into helping a brother out.

TABLE OF CONTENTS

LIST OF TABLES

LIST OF FIGURES

Page

LIST OF SCHEMES

Page

CHAPTER 1

INTRODUCTION AND LITERATURE REVIEW

Introduction to Biodegradable Polymers:

Over the past decade, the human race has come to realize that we must be better stewards of our planet. Previously, this necessity has been centered on the premise of conserving our petroleum resources, but recently, advancements in the design and manufacture of specific biodegradable monomers (Table 1.1) from non-petroleum resources have engaged a worldwide interest in becoming a more bio-friendly planet. Two of the main culprits spawning this interest are polylactide/polylactic acid (PLA) [1-96], a biodegradable aliphatic polymer, and polycaprolactone (PCL) [97-165], a biodegradable polyester.

PLA is a biodegradable polymer that has garnered much attention since the turn of the century. PLA is a thermoplastic derived from renewable materials such as corn starch and sugarcane that has a melt temperature around 180 °C and a glass transition of 55 °C. PLA, due to its good mechanical properties, biocompatibility, and biodegradability, has been explored for a wide range of applications in the medical field, including bone tissue engineering [6, 59, 166-173] and drug delivery [53, 174-185]. PLA is also an ideal replacement for non-degradable polymers in numerous applications, such as trash bags, plastic food storage containers, agricultural films, adhesives, wax replacements, and plant containers. However, PLA homopolymers are usually brittle and lack flexibility because of their crystalline nature, which limits homopolymer processing. Therefore, most PLA-based materials are processed in

conjunction with other materials in order to achieve the desired physical properties for injection molding, extrusion lamination, and film formation.

Table 1.1 Structures of the most common biodegradable monomers.

Lactic Acid	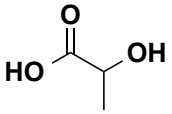
Lactide	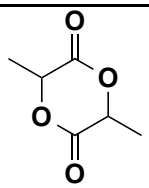
ε-caprolactone	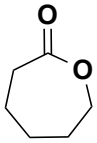
Glycolide	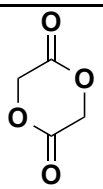

Poly(caprolactone) is another biodegradable polymer that has received a significant amount of interest over the last decade. PCL is a hydrophobic, low melting crystalline (60 °C) polymer that has been extensively researched since the seminal work of Wallace Carothers in the 1930s. PCL offers very good barrier properties such as oil and water holdout. It is also used in many applications to improve processing conditions of higher melting biopolymers such as PLA and to improve the impact resistance of brittle polymers like PLA. Recently, PCL has found its niche in tissue engineering [66, 99, 106, 108, 111, 113, 115, 120, 122, 125, 147, 186-204] due to its superior viscoelastic properties, which supersede those of PLA and polyglycolide (PGA). PCL networks are unique in their ability to be degraded by enzymes present outside of the body

such as various lipases. In contrast, the process is drastically slowed inside of the body due to insufficient degradation enzymes. This makes PCL an ideal candidate for applications such as bone scaffolds that require extended regeneration or healing time.

In this work, PLA was incorporated into block copolymers (BCPs) as a sacrificial component that allowed for the tailoring of nanoporous membranes to specific pore diameters. The majority of this work focused on the controlled polymerization of PLA in conjunction with other monomers to form block copolymers. Copolymerization of PLA was carried out using styrene and lactide to form partially biodegradable polymers. PCL was also utilized in conjunction with PLA to form block copolymer brushes with increased thicknesses and tunable degradation rates to modulate surface coatings.

Strategies Towards the Synthesis of Block Copolymers:

The principal synthetic strategy for obtaining PLA and PCL is by the ring-opening polymerization (ROP) of lactide (Scheme 1.1) and ε-caprolactone using a metal catalyst. The most common of these metal catalysts are tin, titanium, germanium, and zirconium. ROP of lactide is preferred over condensation polymerizations of lactic acid (Table 1.1) because the molecular weight of PLA can be controlled by using the ROP chain growth mechanism, while achieving conversion close to 100%. The coordination/insertion mechanism first involves metal catalyst coordination to the ester carbonyl, which generates electrophilic character on the carbonyl carbon. Next, the initiator inserts and opens the ring. The metal catalyst proceeds to activate another monomer, and this coordination/insertion continues, where one metal catalyst remains bound to the growing chain end. This process allows for precise control of molecular weight by controlling the monomer/catalyst ratio. Lactide has several enantiomers: D-lactide, L-

lactide, racemic-lactide, and meso-lactide. Racemic-lactide is a 50:50 mixture of D and L enantiomers of a chiral molecule, while meso-lactide is an achiral compound that has chiral centers. The enantiomers allow PLA to exhibit many unique properties after polymerization. Both PDLA from D-lactide and PLLA from L-lactide are very crystalline. PLA can also be amorphous if racemic-lactide or meso-lactide is polymerized to form PDLLA. Although lactic acid has these same chiral enantiomers, condensation polymerization is an equilibrium type polymerization that offers very little control. Condensation polymers typically yield molecular weights less than 10 kDa, whereas, ROP of lactide yields molecular weights that can reach several orders of magnitude higher if performed under anhydrous conditions. Another drawback to condensation polymerization is the higher polymer dispersity, which is generally around 2.0. ROP can achieve very low polymer dispersity usually around 1.1 to 1.3, which makes it an ideal polymerization technique for creating BCPs that have very uniform chain lengths, a criterion that is critical to successfully fabricating phase separation morphologies and uniform surface coatings.

Scheme 1.1 Mechanism for the ring-opening polymerization (ROP) of lactide.

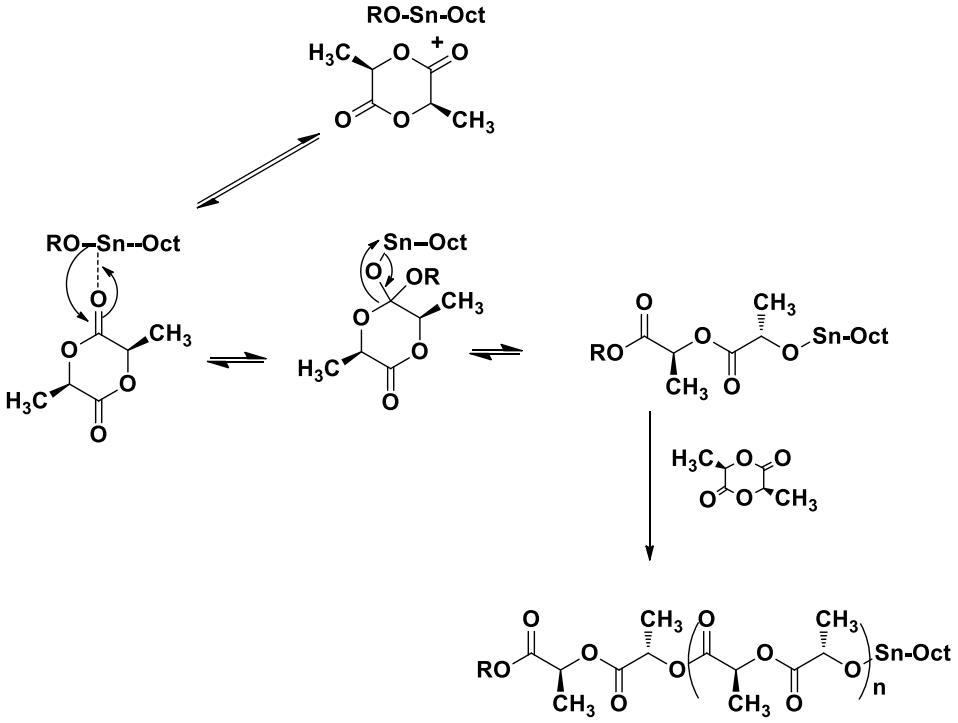

Another ideal approach to creating these BCPs by ROP is by using the organocatalyst triazabicyclodecene (TBD). The primary mechanism for this strategy in biodegradable monomers such as ε-caprolactone is through bifunctional nucleophilic attack (Scheme 1.2) using simultaneous acyl transfer and hydrogen bonding. Nucleophilic attack of the nitrogen imine at the carbonyl carbon generates an intermediate where the adjacent protonated nitrogen is ideally suited for proton transfer to the alkoxide to generate the TBD amide[205]. The incoming hydroxyl (from either alcohol cocatalyst or hydroxyl end group) can also participate by hydrogen bonding, which increases its nucleophilicity and helps to facilitate esterification, freeing the ester and reforming TBD[205]. By this mechanism, TBD functions as a bifunctional transesterification catalyst. Although this catalyst has sufficient reactivity without a hydroxyl

initiator in the reaction pot, initially due to its bifunctional nature, adding an initiator with a hydroxyl functionality improves reactivity.

Scheme 1.2 Dual activation of monomer and initiator by TBD.

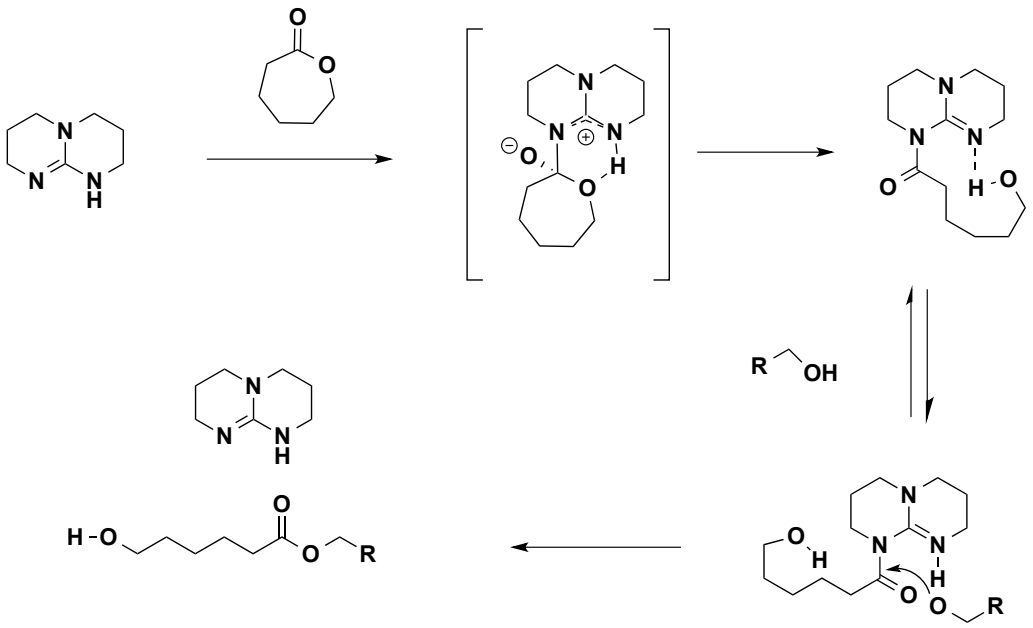

The principal synthetic strategy that was employed in our work to obtain the styrene majority phase polymer is atom transfer radical polymerization (ATRP). ATRP was developed by Matyjaszewski [206] and Sawamoto [207] in 1994 and is a form of controlled radical polymerization (CRP). There are many other forms that can be used for radical polymerizations such as anionic, cationic, and free radical, but ATRP is the technique utilized here to provide block copolymers due to its "living" nature and the ease of setup [208].

Most ATRP reactions require the formation of four essential components for an ATRP reaction to proceed (Figure 1.1). ATRP is based on an inner sphere electron transfer process which involves (1) a macroinitiator P_n-X, with at least one transferable halogen, frequently X = Cl or Br; (2) a transition metal, Mt^n, that can undergo a one electron reduction process; (3) a

ligand, L, that complexes to the transition metal to enhance the solubility of catalyst in its lower oxidative state (Mt^n/ligand); and (4) one or more radical monomers that can copolymerize[209]. The active radicals form with a rate constant of activation, k_{act}, and generally undergo one of three processes. The radical can propagate with monomer, k_p, reversibly deactivate, k_{deact}, or terminate with a rate constant, k_t. The use of these four components enables a synthetic pathway that allows for precise control of the propagation of monomer in order to derive low dispersity polymers with controlled molecular weights and a reduction in the termination pathways that create uncontrolled kinetics.

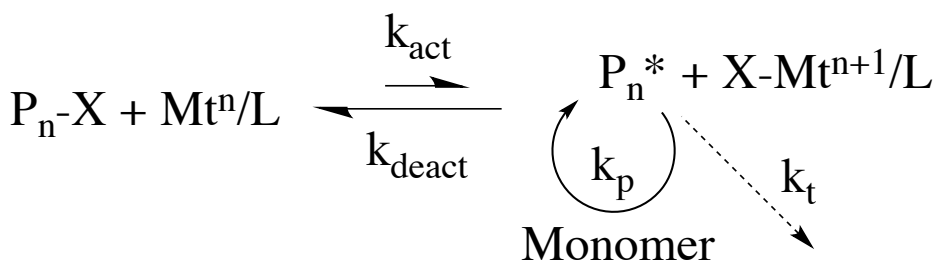

Figure 1.1 Reaction mechanism for an ATRP reaction.

Polymer Brushes:

Polymer brushes are a unique class of polymers that are generally attached to a pendant group that is covalently bound to a surface. Tethering a molecule to the surface can be done in several ways. The first is by physisorption, which is the attachment to a surface by noncovalent interactions such as hydrogen bonding or electrostatic interactions. Although this technique is commonly used to create polymer layers on surfaces, the polymer is easily removed by weathering due to its weak interaction with the surface. Paint flaking on the side of an old barn is

a good example of weather adversely affecting the integrity of the physisorbed polymer coating. The next two methods offer a more robust mechanism for surface attachment through chemisorption. Covalently attached brushes are synthesized by attaching the polymer to a surface using "grafting from" and "grafting to" methodologies, as shown in Figure 1.2.

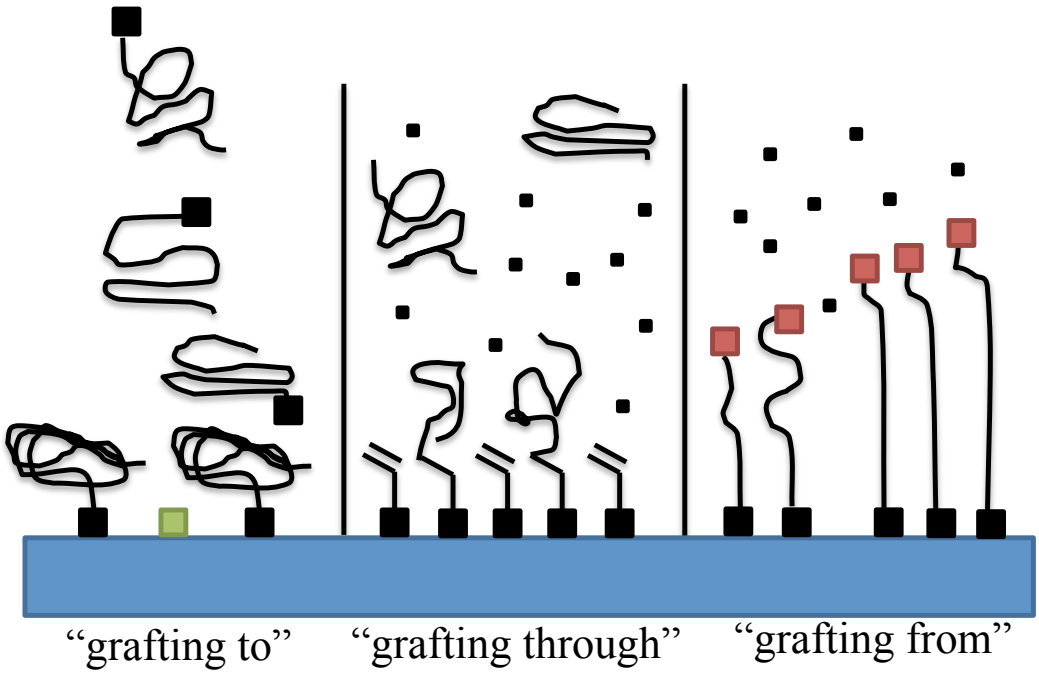

Figure 1.2 An illustration of the different techniques to immobilize polymers on a surface.

Grafting to methods utilize a polymer synthesized in solution with either a single or multiple reactive groups attached to the polymer backbone. The polymer matrix can then be spin coated or drop cast onto a surface, after which the complementary functionalities undergo covalent attachment. However, due to the polymer favoring its natural random coil configuration, the grafting density (the number of chains per unit area, usually defined as chains/nm^2) is generally very low. The low grafting density is generally referred to as the mushroom regime and can be attributed to the diffusion limited process that prevents the chains

from extending perpendicular to the surface[210]. These non-interacting random coils block availability to reactive sites that are in close proximity, which also hinders the packing density of the polymer. It should be noted that typical grafted to polymers that are subjected to favorable solvents yield thicknesses that are directly proportional to their degree of polymerization. In most cases, a polymer layer is covalently attached to the surface in order to create an anchoring layer for the grafting of the solution-prepared polymer. A common anchoring technique utilized for silicon substrates involves the epoxide-containing polymer poly(glycidyl methacrylate) (PGMA) [211]. The epoxide can be ring opened by thermal annealing in the presence of hydroxyl groups on the silicon substrate to form a thin anchoring layer used in many "grafting to" approaches.

The grafting from approach produces covalently attached tethered polymers through polymerization from surface-bound initiators, which is often referred to as surface-initiated polymerization. This approach is an ideal technique for synthesizing thick, high grafting density brushes to fabricate polymer thin films. Because of the density of initiators on the surface, the chains are highly stretched as a result of steric crowding and excluded volume limitations, which promotes the formation of polymer brushes (also known as the brush regime) (see the "grafted from" brush regime in Figure 1.2). The polymer chains in the brush regime generally have superior interfacial properties than the less densely packed mushroom regime. Introducing stimuli such as light, solvent, and temperature to the film allows for easily manipulation over the polymer brush microenvironment to alter polymer conformation, thickness and morphology.

The modification of surfaces with polymers of high grafting density is a popular technique to produce surface-bound films with tunable properties, which gives rise to a myriad of applications, such as the manipulation of interfacial forces [212-218], investigation and development of biomaterials [219-227], surface coatings [228-230], and nanoparticle

encapsulation [231-235]. Factors such as grafting density, chain length, and thickness of the film directly influence the interfacial properties of the substrate [236, 237], illustrating the need for polymerization methodologies that afford control over these parameters [238]. Some common polymerization techniques found in the literature that offer control of these parameters are ring-opening metathesis polymerization (ROMP) [239], nitroxide-mediated polymerization (NMP) [240], atom transfer radical polymerization (ATRP) [241], single-electron-transfer living radical polymerization (SET-LRP) [242], and reversible addition fragmentation chain transfer (RAFT) polymerization [243].

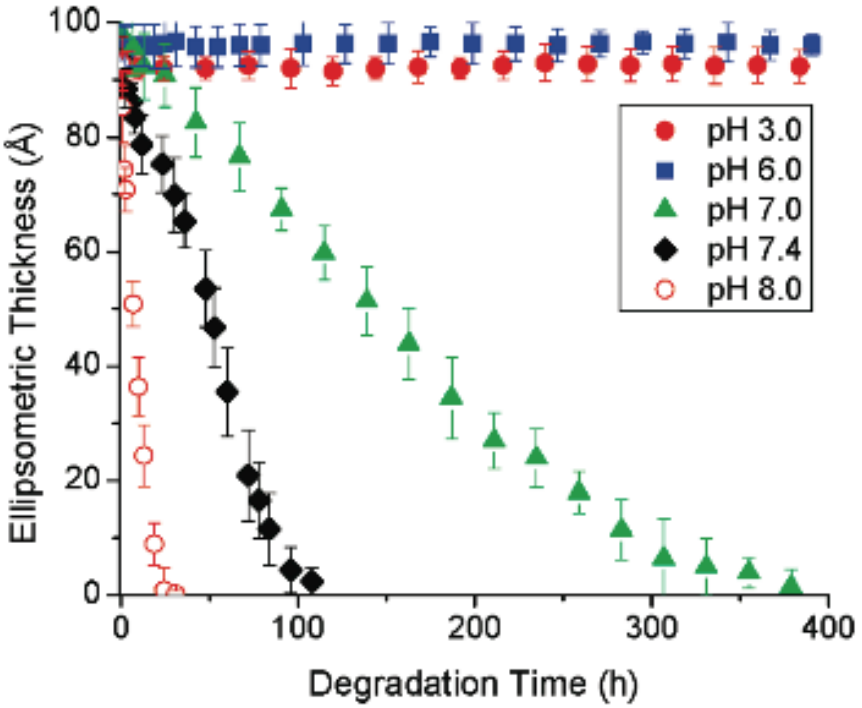

Figure 1.3 Film degradation of PLA brushes in different pH conditions. Reprinted with permission from Macromolecules reference [244]. Copyright 2011 American Chemical Society.

In addition, surface-initiated ring-opening polymerization (SI-ROP) is a chain growth polymerization technique that offers great promise in controlling these parameters for polymer brush generation. The coordination/insertion mechanism in which the metal catalyst coordinates to the ester carbonyl, allowing the initiator to insert, has allowed the polymerization of monomers such as lactide and lactones (Scheme 1.1). This mechanism has been adopted for the ring-opening polymerization of cyclic esters in solution and on the surface using a metal catalyst. Although SI-ROP has been utilized over the past decade to generate biodegradable polymer brushes from lactide and ε-caprolactone, this technique has only provided ultrathin coatings of 15 nm or less [245-252], which is a potential limitation to their practical utility as evident by the 10 nm thickness and degradation rates reported by Xu in degradation studies of PLA brushes (Figure 1.3)[244]. Recently, Pratt and Dove reviewed the use of a more reactive organocatalyst, triazabicyclodecene (TBD)[205], as an alternative to the common metal catalysts utilized in ring-opening polymerization, which showed promise in using organocatalysis for SI-ROP [253]. Martello et al. proved that TBD can be used to successfully synthesize δ-decalactone at low temperatures with fast kinetics, as shown in Scheme 1.3 [254]. This work provided evidence that TBD was a better catalyst for certain lactone polymerizations and offered increased reactivity over metal catalysts in low temperature systems.

Scheme 1.3 Synthetic scheme of δ-decalactone polymerized by TBD

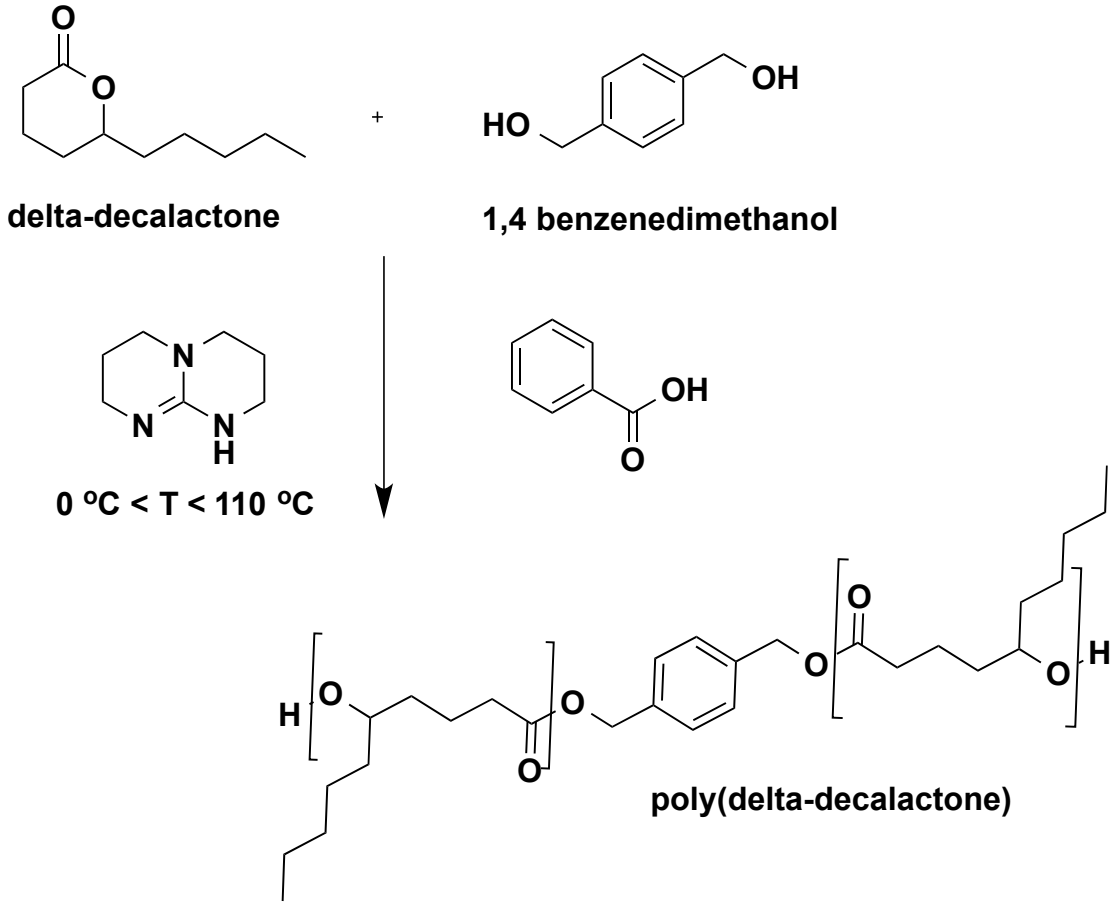

Block Copolymer Phase Separation:

Block copolymers are a high-end class of polymers with a wide range of physical and chemical properties that can be tailored for many specific applications. Block copolymers are complex soft materials that have been used in diverse industrial and scientific capacities [255]. While block copolymers are found in everyday items such as adhesives, shoe soles, and chewing gum [256, 257], they have also been employed to understand interesting and broadly important physical phenomena in ordered soft materials. The predictable self-assembly and wide array of accessible block morphologies have enabled scientific and technologically relevant advances using these hybrid materials. Examples of relevant applications include the preparation of

interesting materials such as patterned templates [258-267] and nanoporous membranes [255, 268-277]. With respect to the latter materials, block copolymers are ideal precursors for the formation of ordered nanoporous organic polymers.

The self-organization of block copolymers is driven by the immiscibility of constituent blocks. Several classes of phase-separated morphologies are exhibited by block copolymers. The most abundant and rich of these morphologies are lamellae, cylinders, spheres, and gyroids. For such morphologies to be present, two important factors must be met: the Hansen solubility parameter for each block must be significantly different and the volume fraction of the minority phase must correspond to that required for a specific morphology (Figure 1.4). For example, if the desire morphology is hexagonal (cylinder), the volume fraction of the minority phase must be around 20-35%. Although this is true for most cases, the phase diagram shown in Figure 1.4 is only a basic template. If both blocks are miscible or have similar solubility parameters, no phase-separated morphology will be exhibited. Figure 1.4 also illustrates the difference in block copolymer morphologies based on volume fraction and degree of polymerization of the minority block [278].

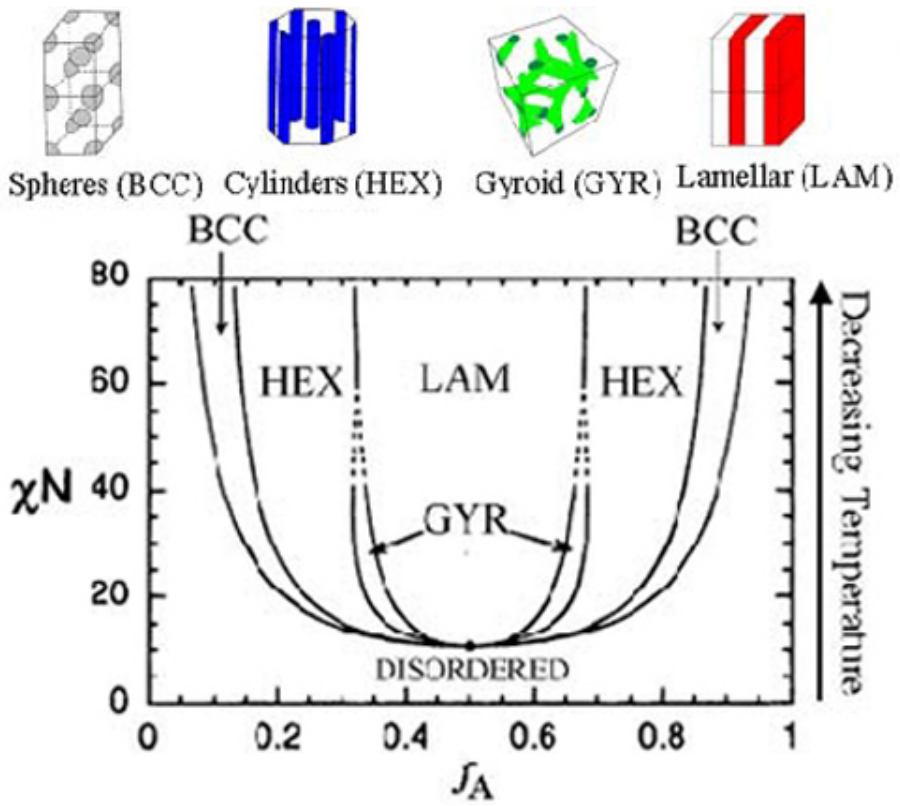

Figure 1.4 Phase separation diagram for block copolymers. Reproduced from Chemical Communications reference [278] with permission of The Royal Chemistry Society.

Block copolymers have a well established utility as self-organizing soft materials for nanolithography applications [279]. Cylinder-forming diblock copolymers are particularly useful in this regard if the cylinders can be oriented perpendicular to the substrate interface and then subsequently removed by a selective etching process to leave a nanoporous film [255, 268, 270-272, 274, 276]. These types of films have been utilized as masks for the patterning of metallic nanodots and for nanopattern transfer [262, 266]. There are three key requirements for the practical use of cylinder-forming block copolymers: the cylinders should be easily oriented perpendicular to the substrate, the cylinders should be easily etched away without compromising the film, and the nanopores should traverse through the entire thickness of the film. Also, long-

range order should be obtained to ensure a uniform film. There are two common methods used in the literature to achieve long-range order and perpendicular orientation for block copolymer phase separation. Solvent annealing is a very useful and a simple method to generate both perpendicular orientation and highly organized cylinders [280]. Films that are composed of polystyrene (PS) and polylactide (PLA) are easily annealed through the use of THF vapor to achieve highly ordered morphologies, as evidenced from the work of Vayer et al. shown in Figure 1.5[280].

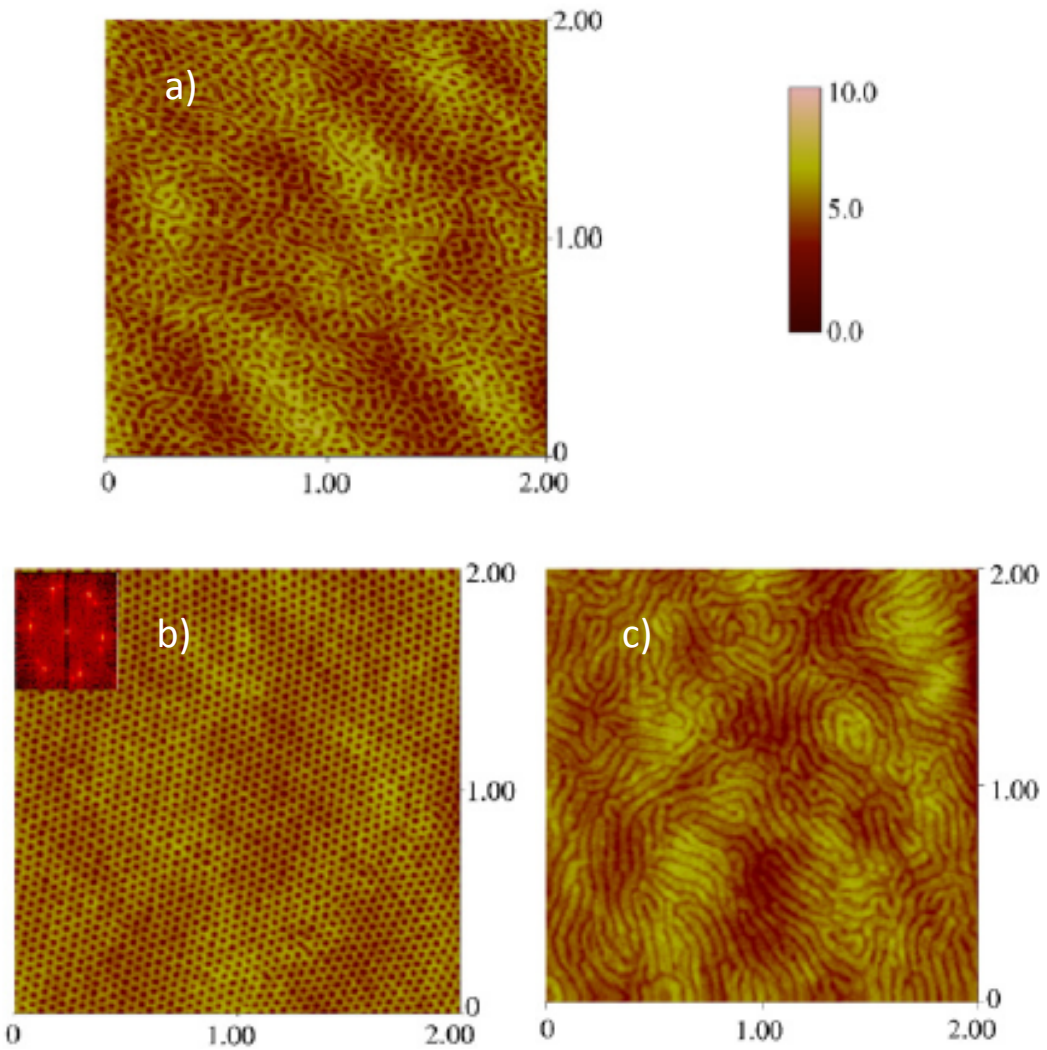

Figure 1.5 AFM images of the orientation and order obtained by solvent annealing where the scale bar is in nm. a) initial film spin coated from chlorobenzene, b) after exposure to THF vapors for 4 h, and c) after exposure to THF vapors for 7 h. Reprinted with permission from Thin Solid Films reference [280]. Copyright 2009 Elsevier.

Thermal annealing is another useful way to obtain perpendicular orientation and long-range order; see for example the work of Olayo-Valles et al. (Figure 1.6)[281]. However, thermal annealing has been shown to cause degradation issues in some block copolymer systems. PLA is

a common block copolymer system that shows degradation issues because of its hydrolytic stability and/or backbiting. At an annealing temperature of about 240 °C, PLA has previously been observed to undergo degradation [281].

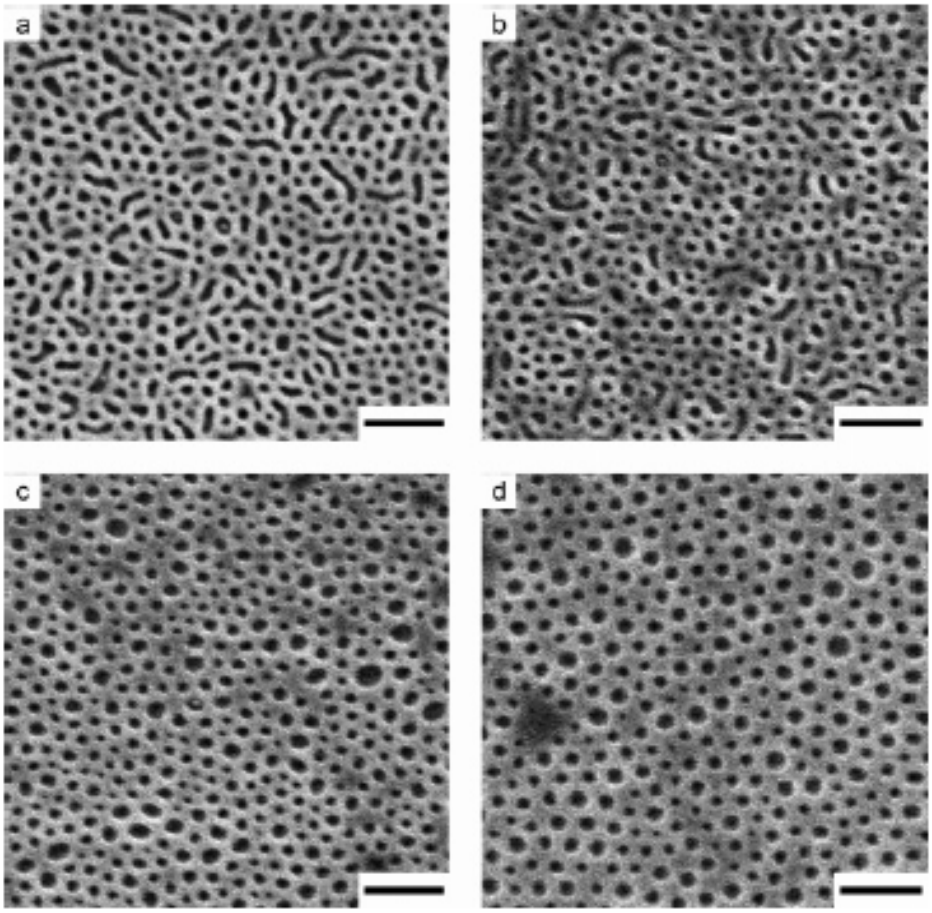

Figure 1.6 AFM phase images of ordered cylinders in a thermally annealed block copolymer. a) No order initially exists within the spin coated film annealed at 130 °C for 12 h. As the annealing temperature is increased to b) 170, c) 210, and d) 240 °C, the polymer forms ordered cylinders after 12 h. The black smudge in d) is the degradation of PLA. Reprinted with permission from Macromolecules reference [281]. Copyright 2005 American Chemical Society

PLA-containing block copolymers are very useful in the formation of nanoporous materials and thin films due to the ability of PLA to be removed through hydrolysis using basic solution. Thin films of PLA BCPs have been fabricated in the literature with perpendicularly oriented cylindrical domains and have been effectively utilized in many lab-scale applications. Two practical applications of BCP cylinder porous membranes are in water filtration [272, 282, 283] and drug delivery [272, 284].

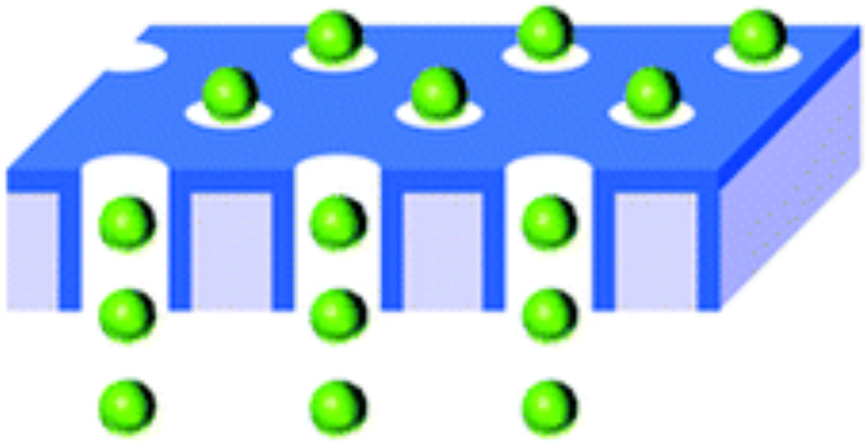

Figure 1.7 Nanochannels made by etching of cylinder domains as a route to drug delivery. Reprinted with permission from ACS Nano reference [284]. Copyright 2010 American Chemical Society.

Yang et al. have developed diffusion-based nanochannels for the controlled delivery of protein-based drugs, as shown schematically in Figure 1.7 [284]. The fabricated device showed good stability over a 3-week period along with good throughput for the single file loading of protein drugs. Although drug delivery applications are being heavily researched, water filtration is a growing need as we strive to develop technologies that will enable better quality drinking

water. Many advancements have been made, and the utility of block copolymer membranes has been hypothesized as a potential solution (Figure 1.8), but there is still a lot of work left to be done. Membranes can now be created with high efficiency and excellent quality, but there are still limitations in robustness for high throughput applications such as water filtration. Another drawback to these highly specialized architectures is the number of steps involved in obtaining a fully fabricated device, and whether this is a scalable technology.

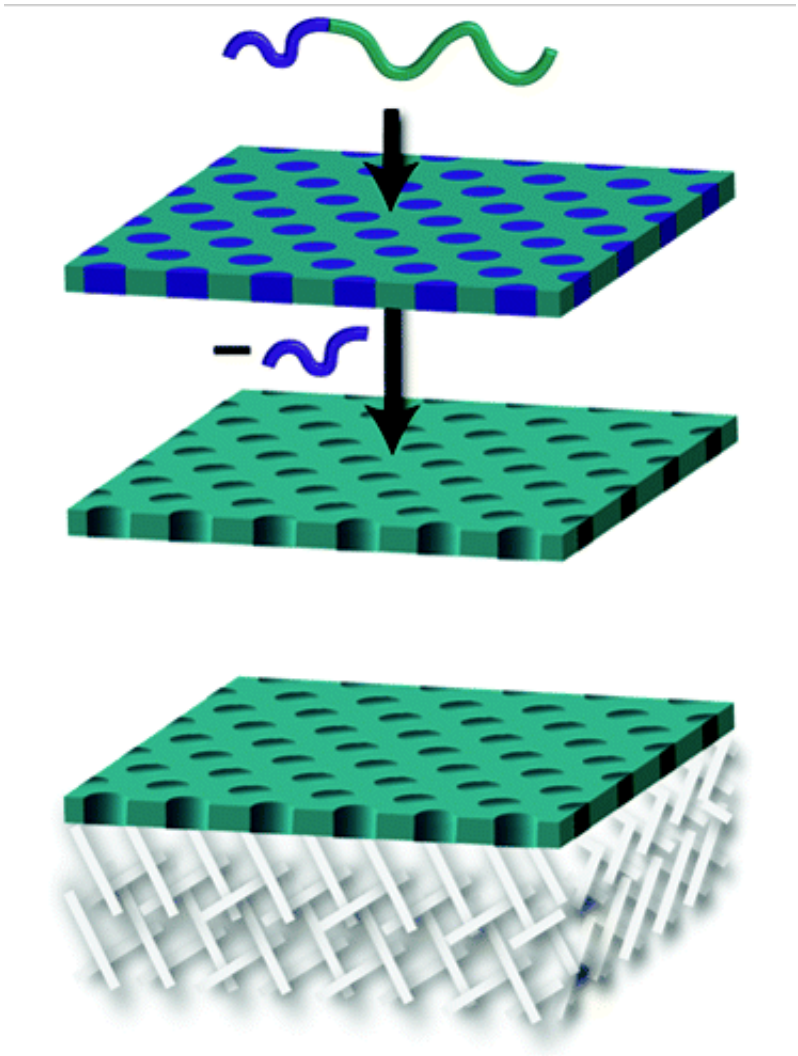

Figure 1.8 Nanoporous membrane illustration with a macroporous support layer. Reprinted with permission from ACS Nano reference [272]. Copyright 2010 American Chemical Society.

Objectives and Dissertation Outline:

In this dissertation, surface-initiated ring-opening polymerization (SI-ROP), atom transfer radical polymerization (ATRP), and ring-opening polymerization (ROP) are used to generate covalent and noncovalently attached biodegradable polymer thin films on silicon oxide substrates. The objectives herein are as follows: 1) fabricate "grafted from" polycaprolactone (PCL) homopolymer brushes with increased thickness using the organocatalyst TBD, 2) graft PCL homopolymers to a poly(glycidyl methacrylate) anchoring layer in order to compare the degradation kinetics, 3) chain extend PCL brushes using a zirconium catalyst to produce block copolymer brushes, 4) utilize a methanol/water pH 14 solution in order to selectively degrade the block copolymer brushes to improve the degradation kinetics, 5) synthesize block copolymers consisting of polystyrene and polylactide to create microphase separated morphologies that enable uniform and reproducible perpendicular cylinders through solvent annealing, 6) produce polymer thin films with varying thicknesses in order to compare the effect of thickness on the long-range order during solvent annealing, and 7) fabricate PS-b-PLLA brushes in order to probe the effect of a crystalline block in phase separation and annealing.

Chapter 2 of this dissertation discusses the production of biodegradable polyester brushes using SI-ROP to produce PCL and PCL-b-PLA brushes. Grafting to and grafting from techniques were used to generate these coatings. High grafting density PCL homopolymer brushes were prepared using a TBD catalyst in order to retain the hydroxyl end groups for subsequent polymerizations. Lower grafting density brushes were prepared using a PGMA anchoring layer to provide more accessible functionalities for covalent attachment. The PCL-b-PLA brushes were synthesized by chain extension from the hydroxyl end of PCL. Degradation

studies were carried out using a solvent-based pH 14 solution in an attempt to increase the rate of degradation for thicker films and to compare rates between the two.

Chapter 3 of this dissertation investigates the synthesis of PS-b-PDLLA and PS-b-PLLA polymers as a route to produce nanoporous membranes. ATRP and ROP were used as controlled polymerization techniques to produce low dispersity, exact molecular weight blocks. The BCP thin films were spin coated on silicon substrates to various thicknesses in order to understand the effect of thickness and crystallinity on the microscale and nanoscale ordering. Solvent annealing using THF was employed to precisely control the ordering of the cylindrical morphologies. The films were exposed to a pH 14 methanol/water solution to selectively etch the PLA cylinders, leaving a honeycomb matrix of PS.

Chapter 4 summarizes the chapters of this dissertation and offers an outlook as to the possible future directions of these projects.

References

1. Al-Itry, R., K. Lamnawar, and A. Maazouz, *Improvement of thermal stability, rheological and mechanical properties of PLA, PBAT and their blends by reactive extrusion with functionalized epoxy.* Polymer Degradation and Stability, 2012. **97**(10): p. 1898-1914.
2. Al-Itry, R., K. Lamnawar, and A. Maazouz, *Reactive extrusion of PLA, PBAT with a multi-functional epoxide: Physico-chemical and rheological properties.* European Polymer Journal, 2014. **58**(0): p. 90-102.
3. Almeida, C.R., et al., *Impact of 3-D printed PLA- and chitosan-based scaffolds on human monocyte/macrophage responses: Unraveling the effect of 3-D structures on inflammation.* Acta Biomaterialia, 2014. **10**(2): p. 613-622.
4. Amass, A.J., et al., *Polylactic acids produced from l- and dl-lactic acid anhydrosulfite: stereochemical aspects.* Polymer, 1999. **40**(18): p. 5073-5078.
5. Anderson, J.M. and M.S. Shive, *Biodegradation and biocompatibility of PLA and PLGA microspheres.* Advanced Drug Delivery Reviews, 1997. **28**(1): p. 5-24.
6. Anselme, K., et al., *Fate of bioresorbable poly(lactic acid) microbeads implanted in artificial bone defects for cortical bone augmentation in dog mandible.* Biomaterials, 1993. **14**(1): p. 44-50.
7. Armentano, I., et al., *Multifunctional nanostructured PLA materials for packaging and tissue engineering.* Progress in Polymer Science, 2013. **38**(10–11): p. 1720-1747.
8. Arrieta, M.P., et al., *PLA-PHB/cellulose based films: Mechanical, barrier and disintegration properties.* Polymer Degradation and Stability, 2014. **107**(0): p. 139-149.

9. Arrieta, M.P., et al., *Ternary PLA–PHB–Limonene blends intended for biodegradable food packaging applications.* European Polymer Journal, 2014. **50**(0): p. 255-270.

10. As'habi, L., et al., *Non-isothermal crystallization behavior of PLA/LLDPE/nanoclay hybrid: Synergistic role of LLDPE and clay.* Thermochimica Acta, 2013. **565**(0): p. 102-113.

11. B, A., S. Suin, and B.B. Khatua, *Highly exfoliated eco-friendly thermoplastic starch (TPS)/poly (lactic acid)(PLA)/clay nanocomposites using unmodified nanoclay.* Carbohydrate Polymers, 2014. **110**(0): p. 430-439.

12. Badrinarayanan, P., et al., *Investigation of the effect of clay nanoparticles on the thermal behavior of PLA using a heat flux rapid scanning rate calorimeter.* Polymer Testing, 2014. **35**(0): p. 1-9.

13. Bao, L., et al., *Gas permeation properties of poly(lactic acid) revisited.* Journal of Membrane Science, 2006. **285**(1–2): p. 166-172.

14. Belbella, A., et al., *In vitro degradation of nanospheres from poly(D,L-lactides) of different molecular weights and polydispersities.* International Journal of Pharmaceutics, 1996. **129**(1–2): p. 95-102.

15. Bilbao-Sainz, C., et al., *Solution blow spun poly(lactic acid)/hydroxypropyl methylcellulose nanofibers with antimicrobial properties.* European Polymer Journal, 2014. **54**(0): p. 1-10.

16. Bitinis, N., et al., *Poly(lactic acid)/natural rubber/cellulose nanocrystal bionanocomposites. Part II: Properties evaluation.* Carbohydrate Polymers, 2013. **96**(2): p. 621-627.

17. Bondeson, D. and K. Oksman, *Polylactic acid/cellulose whisker nanocomposites modified by polyvinyl alcohol.* Composites Part A: Applied Science and Manufacturing, 2007. **38**(12): p. 2486-2492.

18. Breitenbach, A., Y.X. Li, and T. Kissel, *Branched biodegradable polyesters for parenteral drug delivery systems.* Journal of Controlled Release, 2000. **64**(1–3): p. 167-178.

19. Brekke, J.H., et al., *Influence of polylactic acid mesh on the incidence of localized osteitis.* Oral Surgery, Oral Medicine, Oral Pathology, 1983. **56**(3): p. 240-245.

20. Cadar, O., et al., *Biodegradation behaviour of poly(lactic acid) and (lactic acid-ethylene glycol-malonic or succinic acid) copolymers under controlled composting conditions in a laboratory test system.* Polymer Degradation and Stability, 2012. **97**(3): p. 354-357.

21. Cao, X., et al., *DSC study of biodegradable poly(lactic acid) and poly(hydroxy ester ether) blends.* Thermochimica Acta, 2003. **406**(1–2): p. 115-127.

22. Carrasco, F., et al., *Processing of poly(lactic acid)/organomontmorillonite nanocomposites: Microstructure, thermal stability and kinetics of the thermal decomposition.* Chemical Engineering Journal, 2011. **178**(0): p. 451-460.

23. Carrasco, F., et al., *Processing of poly(lactic acid): Characterization of chemical structure, thermal stability and mechanical properties.* Polymer Degradation and Stability, 2010. **95**(2): p. 116-125.

24. Chavalitpanya, K. and S. Phattanarudee, *Poly(Lactic Acid)/Polycaprolactone Blends Compatibilized with Block Copolymer.* Energy Procedia, 2013. **34**(0): p. 542-548.

25. Chen, B.-K., et al., *Ductile polylactic acid prepared with ionic liquids.* Chemical Engineering Journal, 2013. **215–216**(0): p. 886-893.

26. Chen, R.-y., et al., *Poly(lactic acid)/poly(butylene succinate)/calcium sulfate whiskers biodegradable blends prepared by vane extruder: Analysis of mechanical properties, morphology, and crystallization behavior.* Polymer Testing, 2014. **34**(0): p. 1-9.

27. Choi, K.-m., et al., *Plasticization of poly(lactic acid) (PLA) through chemical grafting of poly(ethylene glycol) (PEG) via in situ reactive blending.* European Polymer Journal, 2013. **49**(8): p. 2356-2364.

28. Cifuentes, S.C., et al., *Novel PLLA/magnesium composite for orthopedic applications: A proof of concept.* Materials Letters, 2012. **74**(0): p. 239-242.

29. Csizmadia, R., et al., *PLA/wood biocomposites: Improving composite strength by chemical treatment of the fibers.* Composites Part A: Applied Science and Manufacturing, 2013. **53**(0): p. 46-53.

30. Dadbin, S. and Y. Kheirkhah, *Gamma irradiation of melt processed biomedical PDLLA/HAP nanocomposites.* Radiation Physics and Chemistry, 2014. **97**(0): p. 270-274.

31. Debien, I.C.N., et al., *High-pressure phase equilibrium data for the l-lactic and the l-lactic acid systems.* The Journal of Supercritical Fluids, 2013. **79**(0): p. 27-31.

32. Dey, P. and P. Pal, *Direct production of l (+) lactic acid in a continuous and fully membrane-integrated hybrid reactor system under non-neutralizing conditions.* Journal of Membrane Science, 2012. **389**(0): p. 355-362.

33. Dey, P. and P. Pal, *Modelling and simulation of continuous L (+) lactic acid production from sugarcane juice in membrane integrated hybrid-reactor system.* Biochemical Engineering Journal, 2013. **79**(0): p. 15-24.

34. dos Santos Almeida, A., et al., *Development of hybrid nanocomposites based on PLLA and low-field NMR characterization.* Polymer Testing, 2012. **31**(2): p. 267-275.

35. Duarte, A.R.C., J.F. Mano, and R.L. Reis, *Novel 3D scaffolds of chitosan–PLLA blends for tissue engineering applications: Preparation and characterization.* The Journal of Supercritical Fluids, 2010. **54**(3): p. 282-289.

36. Duncanson, W.J., et al., *Targeted binding of PLA microparticles with lipid-PEG-tethered ligands.* Biomaterials, 2007. **28**(33): p. 4991-4999.

37. Fan, Y., et al., *Thermal degradation behaviour of poly(lactic acid) stereocomplex.* Polymer Degradation and Stability, 2004. **86**(2): p. 197-208.

38. Finkenstadt, V.L., et al., *Poly(lactic acid) green composites using oilseed coproducts as fillers.* Industrial Crops and Products, 2007. **26**(1): p. 36-43.

39. Freitas, M.N. and J.M. Marchetti, *PLA microspheres as a potential sustained release system for the treatment of inflammatory diseases.* International Journal of Pharmaceutics, 2005. **295**(1–2): p. 201-211.

40. Fukushima, K., et al., *Biotic degradation of poly(dl-lactide) based nanocomposites.* Polymer Degradation and Stability, 2012. **97**(8): p. 1278-1284.

41. Fukushima, K., D. Tabuani, and G. Camino, *Poly(lactic acid)/clay nanocomposites: effect of nature and content of clay on morphology, thermal and thermo-mechanical properties.* Materials Science and Engineering: C, 2012. **32**(7): p. 1790-1795.

42. Gao, X., et al., *Lectin-conjugated PEG–PLA nanoparticles: Preparation and brain delivery after intranasal administration.* Biomaterials, 2006. **27**(18): p. 3482-3490.

43. Ghofar, A., S. Ogawa, and T. Kokugan, *Production of L-lactic acid from fresh cassava roots slurried with tofu liquid waste by Streptococcus bovis.* Journal of Bioscience and Bioengineering, 2005. **100**(6): p. 606-612.

44. Gordobil, O., et al., *Physicochemical properties of PLA lignin blends.* Polymer Degradation and Stability, 2014. **108**(0): p. 330-338.

45. Gorrasi, G. and R. Pantani, *Effect of PLA grades and morphologies on hydrolytic degradation at composting temperature: Assessment of structural modification and kinetic parameters.* Polymer Degradation and Stability, 2013. **98**(5): p. 1006-1014.

46. Grizzi, I., et al., *Hydrolytic degradation of devices based on poly(dl-lactic acid) size-dependence.* Biomaterials, 1995. **16**(4): p. 305-311.

47. Gupta, B., N. Revagade, and J. Hilborn, *Poly(lactic acid) fiber: An overview.* Progress in Polymer Science, 2007. **32**(4): p. 455-482.

48. Haafiz, M.K.M., et al., *Properties of polylactic acid composites reinforced with oil palm biomass microcrystalline cellulose.* Carbohydrate Polymers, 2013. **98**(1): p. 139-145.

49. Hakkarainen, M., S. Karlsson, and A.C. Albertsson, *Rapid (bio)degradation of polylactide by mixed culture of compost microorganisms—low molecular weight products and matrix changes.* Polymer, 2000. **41**(7): p. 2331-2338.

50. Hashima, K., S. Nishitsuji, and T. Inoue, *Structure-properties of super-tough PLA alloy with excellent heat resistance.* Polymer, 2010. **51**(17): p. 3934-3939.

51. He, Y., et al., *Unique crystallization behavior of poly(l-lactide)/poly(d-lactide) stereocomplex depending on initial melt states.* Polymer, 2008. **49**(26): p. 5670-5675.

52. Heald, C.R., et al., *Self-consistent field modelling of poly(lactic acid)–poly(ethylene glycol) particles.* Colloids and Surfaces A: Physicochemical and Engineering Aspects, 2001. **179**(1): p. 79-91.

53. Huang, Y.-Y., T.-W. Chung, and T.-w. Tzeng, *Drug release from PLA/PEG microparticulates.* International Journal of Pharmaceutics, 1997. **156**(1): p. 9-15.

54. Iovino, R., et al., *Biodegradation of poly(lactic acid)/starch/coir biocomposites under controlled composting conditions.* Polymer Degradation and Stability, 2008. **93**(1): p. 147-157.

55. Ishida, N., et al., *d-Lactic acid production by metabolically engineered Saccharomyces cerevisiae.* Journal of Bioscience and Bioengineering, 2006. **101**(2): p. 172-177.

56. Jeevitha, D. and K. Amarnath, *Chitosan/PLA nanoparticles as a novel carrier for the delivery of anthraquinone: Synthesis, characterization and in vitro cytotoxicity evaluation.* Colloids and Surfaces B: Biointerfaces, 2013. **101**(0): p. 126-134.

57. Jin, H.-J., et al., *Blending of poly(L-lactic acid) with poly(cis-1,4-isoprene).* European Polymer Journal, 2000. **36**(1): p. 165-169.

58. Jompang, L., et al., *Poly(lactic acid) and poly(butylene succinate) blend fibers prepared by melt spinning technique.* Energy Procedia, 2013. **34**(0): p. 493-499.

59. Jung, Y., et al., *A poly(lactic acid)/calcium metaphosphate composite for bone tissue engineering.* Biomaterials, 2005. **26**(32): p. 6314-6322.

60. Kadowakil, S., et al., *Application of poly(L-lactic acid) particles for the suppression of genetic resistance to bone marrow allografts by reticuloendothelial system-blockade.* Biomedicine & Pharmacotherapy, 1993. **47**(9): p. 385-391.

61. Kang, Y., et al., *Preparation of PLLA/PLGA microparticles using solution enhanced dispersion by supercritical fluids (SEDS).* Journal of Colloid and Interface Science, 2008. **322**(1): p. 87-94.

62. Kathuria, A., M.G. Abiad, and R. Auras, *Toughening of poly(l-lactic acid) with Cu3BTC2 metal organic framework crystals.* Polymer, 2013. **54**(26): p. 6979-6986.

63. Kim, J.-W., et al., *Preparation of poly(L-lactic acid) honeycomb monolith structure by unidirectional freezing and freeze-drying.* Chemical Engineering Science, 2008. **63**(15): p. 3858-3863.

64. Kouya, T., et al., *Microporous membranes of PLLA/PCL blends for periosteal tissue scaffold.* Materials Letters, 2013. **95**(0): p. 103-106.

65. Kumar, B., M. Castro, and J.F. Feller, *Poly(lactic acid)–multi-wall carbon nanotube conductive biopolymer nanocomposite vapour sensors.* Sensors and Actuators B: Chemical, 2012. **161**(1): p. 621-628.

66. Lebourg, M., J.S. Antón, and J.L.G. Ribelles, *Porous membranes of PLLA–PCL blend for tissue engineering applications.* European Polymer Journal, 2008. **44**(7): p. 2207-2218.

67. Lehermeier, H.J., J.R. Dorgan, and J.D. Way, *Gas permeation properties of poly(lactic acid).* Journal of Membrane Science, 2001. **190**(2): p. 243-251.

68. Lim, L.T., R. Auras, and M. Rubino, *Processing technologies for poly(lactic acid).* Progress in Polymer Science, 2008. **33**(8): p. 820-852.

69. Lopes, M.S., A.L. Jardini, and R.M. Filho, *Poly (lactic acid) production for tissue engineering applications.* Procedia Engineering, 2012. **42**(0): p. 1402-1413.

70. Lucke, A., et al., *Biodegradable poly(d,l-lactic acid)-poly(ethylene glycol)-monomethyl ether diblock copolymers: structures and surface properties relevant to their use as biomaterials.* Biomaterials, 2000. **21**(23): p. 2361-2370.

71. Mai, F., et al., *Poly(lactic acid)/carbon nanotube nanocomposites with integrated degradation sensing.* Polymer, 2013. **54**(25): p. 6818-6823.

72. McLauchlin, A.R., O. Ghita, and A. Gahkani, *Quantification of PLA contamination in PET during injection moulding by in-line NIR spectroscopy.* Polymer Testing, 2014. **38**(0): p. 46-52.

73. Monticelli, O., et al., *Impact of synthetic talc on PLLA electrospun fibers.* European Polymer Journal, 2013. **49**(9): p. 2572-2583.

74. Murariu, M., et al., *Polylactide (PLA)–CaSO4 composites toughened with low molecular weight and polymeric ester-like plasticizers and related performances.* European Polymer Journal, 2008. **44**(11): p. 3842-3852.

75. Najafi, N., et al., *Control of thermal degradation of polylactide (PLA)-clay nanocomposites using chain extenders.* Polymer Degradation and Stability, 2012. **97**(4): p. 554-565.

76. Notta-Cuvier, D., et al., *Tailoring polylactide (PLA) properties for automotive applications: Effect of addition of designed additives on main mechanical properties.* Polymer Testing, 2014. **36**(0): p. 1-9.

77. Oksman, K., M. Skrifvars, and J.F. Selin, *Natural fibres as reinforcement in polylactic acid (PLA) composites.* Composites Science and Technology, 2003. **63**(9): p. 1317-1324.

78. Padee, S., et al., *Preparation of poly(lactic acid) and poly(trimethylene terephthalate) blend fibers for textile application.* Energy Procedia, 2013. **34**(0): p. 534-541.

79. Persson, M., et al., *Effect of bioactive extruded PLA/HA composite films on focal adhesion formation of preosteoblastic cells.* Colloids and Surfaces B: Biointerfaces, 2014. **121**(0): p. 409-416.

80. Pivsa-Art, W., et al., *Preparation of polymer blends between poly (l-lactic acid), poly (butylene succinate-co-adipate) and poly (butylene adipate-co-terephthalate) for blow film industrial application.* Energy Procedia, 2011. **9**(0): p. 581-588.

81. Plackett, D., et al., *Biodegradable composites based on l-polylactide and jute fibres.* Composites Science and Technology, 2003. **63**(9): p. 1287-1296.

82. Raquez, J.-M., et al., *Polylactide (PLA)-based nanocomposites.* Progress in Polymer Science, 2013. **38**(10–11): p. 1504-1542.

83. Rasal, R.M., A.V. Janorkar, and D.E. Hirt, *Poly(lactic acid) modifications.* Progress in Polymer Science, 2010. **35**(3): p. 338-356.

84. Re, G.L., et al., *Stereocomplexed PLA nanocomposites: From in situ polymerization to materials properties.* European Polymer Journal, 2014. **54**(0): p. 138-150.

85. Saeidlou, S., et al., *Poly(lactic acid) crystallization.* Progress in Polymer Science, 2012. **37**(12): p. 1657-1677.

86. Samuel, C., J.-M. Raquez, and P. Dubois, *PLLA/PMMA blends: A shear-induced miscibility with tunable morphologies and properties?* Polymer, 2013. **54**(15): p. 3931-3939.

87. Sasatsu, M., H. Onishi, and Y. Machida, *Preparation of a PLA–PEG block copolymer using a PLA derivative with a formyl terminal group and its application to nanoparticulate formulation.* International Journal of Pharmaceutics, 2005. **294**(1–2): p. 233-245.

88. Sébastien, F., et al., *Novel biodegradable films made from chitosan and poly(lactic acid) with antifungal properties against mycotoxinogen strains.* Carbohydrate Polymers, 2006. **65**(2): p. 185-193.

89. Shogren, R.L., et al., *Biodegradation of starch/polylactic acid/poly(hydroxyester-ether) composite bars in soil.* Polymer Degradation and Stability, 2003. **79**(3): p. 405-411.

90. Siebold, M., et al., *Comparison of the production of lactic acid by three different lactobacilli and its recovery by extraction and electrodialysis.* Process Biochemistry, 1995. **30**(1): p. 81-95.

91. Song, X., et al., *Methanolysis of poly(lactic acid) (PLA) catalyzed by ionic liquids.* Polymer Degradation and Stability, 2013. **98**(12): p. 2760-2764.

92. Spiridon, I., et al., *Evaluation of PLA–lignin bioplastics properties before and after accelerated weathering.* Composites Part B: Engineering, 2015. **69**(0): p. 342-349.

93. Stoyanova, N., et al., *Poly(l-lactide) and poly(butylene succinate) immiscible blends: From electrospinning to biologically active materials.* Materials Science and Engineering: C, 2014. **41**(0): p. 119-126.

94. Tomita, K., et al., *Degradation of poly(l-lactic acid) by a newly isolated thermophile.* Polymer Degradation and Stability, 2004. **84**(3): p. 433-438.

95. Vert, M., J. Mauduit, and S. Li, *Biodegradation of PLA/GA polymers: increasing complexity.* Biomaterials, 1994. **15**(15): p. 1209-1213.

96. Wang, M., et al., *Synthesis and characterization of PLLA–PLCA–PEG multiblock copolymers and their applications in modifying PLLA porous scaffolds.* European Polymer Journal, 2007. **43**(11): p. 4683-4694.

97. Agarwal, S. and C. Speyerer, *Degradable blends of semi-crystalline and amorphous branched poly(caprolactone): Effect of microstructure on blend properties.* Polymer, 2010. **51**(5): p. 1024-1032.

98. Ángeles Corres, M., et al., *Effect of crystallization on morphology–conductivity relationship in polypyrrole/poly(ε-caprolactone) blends.* Polymer, 2006. **47**(19): p. 6759-6764.

99. Annabi, N., et al., *Fabrication of porous PCL/elastin composite scaffolds for tissue engineering applications.* The Journal of Supercritical Fluids, 2011. **59**(0): p. 157-167.

100. Arbelaiz, A., et al., *Mechanical properties of short flax fibre bundle/poly(ε-caprolactone) composites: Influence of matrix modification and fibre content.* Carbohydrate Polymers, 2006. **64**(2): p. 224-232.

101. Armentano, I., et al., *Biodegradable polymer matrix nanocomposites for tissue engineering: A review.* Polymer Degradation and Stability, 2010. **95**(11): p. 2126-2146.

102. Bao, T.-Q., R.A. Franco, and B.-T. Lee, *Preparation and characterization of a novel 3D scaffold from poly(ε-caprolactone)/biphasic calcium phosphate hybrid composite microspheres adhesion.* Biochemical Engineering Journal, 2012. **64**(0): p. 76-83.

103. Bianco, A., et al., *Electrospun poly(ε-caprolactone)/Ca-deficient hydroxyapatite nanohybrids: Microstructure, mechanical properties and cell response by murine embryonic stem cells.* Materials Science and Engineering: C, 2009. **29**(6): p. 2063-2071.

104. Bikiaris, D.N., et al., *Miscibility and enzymatic degradation studies of poly(ε-caprolactone)/poly(propylene succinate) blends.* European Polymer Journal, 2007. **43**(6): p. 2491-2503.

105. Bogdanov, B., et al., *Synthesis and thermal properties of poly(ethylene glycol)-poly(ϵ-caprolactone) copolymers.* Polymer, 1998. **39**(8–9): p. 1631-1636.

106. Buma, P., et al., *Tissue engineering of the meniscus.* Biomaterials, 2004. **25**(9): p. 1523-1532.

107. Calil, M.R., et al., *Enzymatic degradation of poly (ε-caprolactone) and cellulose acetate blends by lipase and α-amylase.* Polymer Testing, 2007. **26**(2): p. 257-261.

108. Calvert, J.W., L.E. Weiss, and M.J. Sundine, *New frontiers in bone tissue engineering.* Clinics in Plastic Surgery, 2003. **30**(4): p. 641-648.

109. Casper, M.E., et al., *Tissue engineering of cartilage using poly-ε-caprolactone nanofiber scaffolds seeded in vivo with periosteal cells.* Osteoarthritis and Cartilage, 2010. **18**(7): p. 981-991.

110. Chen, B. and K. Sun, *Poly (ε-caprolactone)/hydroxyapatite composites: effects of particle size, molecular weight distribution and irradiation on interfacial interaction and properties.* Polymer Testing, 2005. **24**(1): p. 64-70.

111. Chen, H., et al., *Electrospun chitosan-graft-poly (ε-caprolactone)/poly (ε-caprolactone) cationic nanofibrous mats as potential scaffolds for skin tissue engineering.* International Journal of Biological Macromolecules, 2011. **48**(1): p. 13-19.

112. Cheng, Z. and S.-H. Teoh, *Surface modification of ultra thin poly (ε-caprolactone) films using acrylic acid and collagen.* Biomaterials, 2004. **25**(11): p. 1991-2001.

113. Chong, E.J., et al., *Evaluation of electrospun PCL/gelatin nanofibrous scaffold for wound healing and layered dermal reconstitution.* Acta Biomaterialia, 2007. **3**(3): p. 321-330.

114. Chong, M.S.K., C.N. Lee, and S.H. Teoh, *Characterization of smooth muscle cells on poly(ε-caprolactone) films.* Materials Science and Engineering: C, 2007. **27**(2): p. 309-312.

115. Choong, C., J.T. Triffitt, and Z.F. Cui, *Polycaprolactone scaffolds for bone tissue engineering: effects of a calcium phosphate coating layer on osteogenic cells.* Food and Bioproducts Processing, 2004. **82**(2): p. 117-125.

116. Cottam, E., et al., *Effect of sterilisation by gamma irradiation on the ability of polycaprolactone (PCL) to act as a scaffold material.* Medical Engineering & Physics, 2009. **31**(2): p. 221-226.

117. Darcos, V., H.A. Tabchi, and J. Coudane, *Synthesis of PCL–graft–PS by combination of ROP, ATRP, and click chemistry.* European Polymer Journal, 2011. **47**(2): p. 187-195.

118. De Kesel, C., C.V. Wauven, and C. David, *Biodegradation of polycaprolactone and its blends with poly(vinylalcohol) by micro-organisms from a compost of house-hold refuse.* Polymer Degradation and Stability, 1997. **55**(1): p. 107-113.

119. de Matos, M.B.C., et al., *Dexamethasone-loaded poly(ε-caprolactone)/silica nanoparticles composites prepared by supercritical CO2 foaming/mixing and deposition.* International Journal of Pharmaceutics, 2013. **456**(2): p. 269-281.

120. Diban, N., et al., *Hollow fibers of poly(lactide-co-glycolide) and poly(ε-caprolactone) blends for vascular tissue engineering applications.* Acta Biomaterialia, 2013. **9**(5): p. 6450-6458.

121. Dorj, B., et al., *Functionalization of poly(caprolactone) scaffolds by the surface mineralization for use in bone regeneration.* Materials Letters, 2011. **65**(23–24): p. 3559-3562.

122. Elomaa, L., et al., *Preparation of poly(ε-caprolactone)-based tissue engineering scaffolds by stereolithography.* Acta Biomaterialia, 2011. **7**(11): p. 3850-3856.

123. Fukushima, K., et al., *Biodegradation trend of poly(ε-caprolactone) and nanocomposites.* Materials Science and Engineering: C, 2010. **30**(4): p. 566-574.

124. Gan, Z., et al., *Enzymatic degradation of poly(ε-caprolactone)/poly(dl-lactide) blends in phosphate buffer solution.* Polymer, 1999. **40**(10): p. 2859-2862.

125. Ghasemi-Mobarakeh, L., et al., *Electrospun poly(ε-caprolactone)/gelatin nanofibrous scaffolds for nerve tissue engineering.* Biomaterials, 2008. **29**(34): p. 4532-4539.

126. Gurarslan, A., J. Shen, and A.E. Tonelli, *Single-component poly(ε-caprolactone) composites.* Polymer, 2013. **54**(21): p. 5747-5753.

127. Han, J., C.J. Branford-White, and L.-M. Zhu, *Preparation of poly(ε-caprolactone)/poly(trimethylene carbonate) blend nanofibers by electrospinning.* Carbohydrate Polymers, 2010. **79**(1): p. 214-218.

128. Hsu, S.-H., C.-M. Tang, and C.-C. Lin, *Biocompatibility of poly(ε-caprolactone)/poly(ethylene glycol) diblock copolymers with nanophase separation.* Biomaterials, 2004. **25**(25): p. 5593-5601.

129. Huang, M.-H., S. Li, and M. Vert, *Synthesis and degradation of PLA–PCL–PLA triblock copolymer prepared by successive polymerization of ε-caprolactone and dl-lactide.* Polymer, 2004. **45**(26): p. 8675-8681.

130. Jian, C., et al., *Multifunctional comb copolymer ethyl cellulose-g-poly(ε-caprolactone)-rhodamine B/folate: Synthesis, characterization and targeted bonding application.* European Polymer Journal, 2014. **55**(0): p. 235-244.

131. Jones, D.S., et al., *Poly(ε-caprolactone) and poly(ε-caprolactone)-polyvinylpyrrolidone-iodine blends as ureteral biomaterials: characterisation of mechanical and surface properties, degradation and resistance to encrustation in vitro.* Biomaterials, 2002. **23**(23): p. 4449-4458.

132. Khor, H.L., et al., *Poly(ε-caprolactone) films as a potential substrate for tissue engineering an epidermal equivalent.* Materials Science and Engineering: C, 2002. **20**(1–2): p. 71-75.

133. Kiersnowski, A., et al., *Synthesis and structure of poly(ε-caprolactone)/synthetic montmorillonite nano-intercalates.* European Polymer Journal, 2004. **40**(11): p. 2591-2598.

134. Kim, J.K., K.I. Kim, and D.S. Huh, *Fabrication of honeycomb-patterned poly(ε-caprolactone) composite films containing chemically modified silver nanoparticles.* Materials Letters, 2014. **132**(0): p. 312-316.

135. La Cara, F., et al., *Biodegradation of poly-ε-caprolactone/poly-β-hydroxybutyrate blend.* Polymer Degradation and Stability, 2003. **79**(1): p. 37-43.

136. Lemoine, D., et al., *Stability study of nanoparticles of poly(ε-caprolactone), poly(d,l-lactide) and poly(d,l-lactide-co-glycolide).* Biomaterials, 1996. **17**(22): p. 2191-2197.

137. Li, L., et al., *Electrospun poly (ε-caprolactone)/silk fibroin core-sheath nanofibers and their potential applications in tissue engineering and drug release.* International Journal of Biological Macromolecules, 2011. **49**(2): p. 223-232.

138. Lin, W.-J., D.R. Flanagan, and R.J. Linhardt, *A novel fabrication of poly(ε-caprolactone) microspheres from blends of poly(ε-caprolactone) and poly(ethylene glycol)s.* Polymer, 1999. **40**(7): p. 1731-1735.

139. Lönnberg, H., et al., *Surface grafting of microfibrillated cellulose with poly(ε-caprolactone) – Synthesis and characterization.* European Polymer Journal, 2008. **44**(9): p. 2991-2997.

140. Lu, F., et al., *Effects of amphiphilic PCL–PEG–PCL copolymer addition on 5-fluorouracil release from biodegradable PCL films for stent application.* International Journal of Pharmaceutics, 2011. **419**(1–2): p. 77-84.

141. Malheiro, V.N., et al., *New poly(ε-caprolactone)/chitosan blend fibers for tissue engineering applications.* Acta Biomaterialia, 2010. **6**(2): p. 418-428.

142. Mattioli-Belmonte, M., et al., *Tuning polycaprolactone–carbon nanotube composites for bone tissue engineering scaffolds.* Materials Science and Engineering: C, 2012. **32**(2): p. 152-159.

143. Nava, D., et al., *Thermal properties and interactions in blends of poly(ε-caprolactone) with unsaturated polyester resins.* Journal of Materials Processing Technology, 2003. **143–144**(0): p. 171-174.

144. Ohtaki, A., N. Akakura, and K. Nakasaki, *Effects of temperature and inoculum on the degradability of poly-ε-caprolactone during composting.* Polymer Degradation and Stability, 1998. **62**(2): p. 279-284.

145. Oyane, A., et al., *Simple surface modification of poly(ε-caprolactone) for apatite deposition from simulated body fluid.* Biomaterials, 2005. **26**(15): p. 2407-2413.

146. Park, J.S., et al., *In vitro and in vivo test of PEG/PCL-based hydrogel scaffold for cell delivery application.* Journal of Controlled Release, 2007. **124**(1–2): p. 51-59.

147. Pintado-Sierra, M., et al., *Surface hierarchical porosity in poly (ε-caprolactone) membranes with potential applications in tissue engineering prepared by foaming in*

supercritical carbon dioxide. The Journal of Supercritical Fluids, 2014. **95**(0): p. 273-284.

148. Puga, A.M., et al., *Hot melt poly-ε-caprolactone/poloxamine implantable matrices for sustained delivery of ciprofloxacin.* Acta Biomaterialia, 2012. **8**(4): p. 1507-1518.

149. Reignier, J. and M.A. Huneault, *Preparation of interconnected poly(ε-caprolactone) porous scaffolds by a combination of polymer and salt particulate leaching.* Polymer, 2006. **47**(13): p. 4703-4717.

150. Rimmer, S. and M.H. George, *Differential scanning calorimetry of some well defined poly(ε-caprolactone-g-PMMA)-co-polyurethanes.* Polymer, 1994. **35**(10): p. 2123-2127.

151. Salerno, A., et al., *Novel 3D porous multi-phase composite scaffolds based on PCL, thermoplastic zein and ha prepared via supercritical CO2 foaming for bone regeneration.* Composites Science and Technology, 2010. **70**(13): p. 1838-1846.

152. Seretoudi, G., D. Bikiaris, and C. Panayiotou, *Synthesis, characterization and biodegradability of poly(ethylene succinate)/poly(ε-caprolactone) block copolymers.* Polymer, 2002. **43**(20): p. 5405-5415.

153. Shin, K.-H., et al., *Direct coating of bioactive sol–gel derived silica on poly(ε-caprolactone) nanofibrous scaffold using co-electrospinning.* Materials Letters, 2010. **64**(13): p. 1539-1542.

154. Sivalingam, G., S. Chattopadhyay, and G. Madras, *Enzymatic degradation of poly (ε-caprolactone), poly (vinyl acetate) and their blends by lipases.* Chemical Engineering Science, 2003. **58**(13): p. 2911-2919.

155. Sivalingam, G. and G. Madras, *Thermal degradation of poly (ε-caprolactone).* Polymer Degradation and Stability, 2003. **80**(1): p. 11-16.

156. Sivalingam, G. and G. Madras, *Oxidative degradation of poly (vinyl acetate) and poly (ε-caprolactone) and their mixtures in solution.* Chemical Engineering Science, 2004. **59**(7): p. 1577-1587.

157. Sousa, I., A. Mendes, and P.J. Bártolo, *PCL Scaffolds with Collagen Bioactivator for Applications in Tissue Engineering.* Procedia Engineering, 2013. **59**(0): p. 279-284.

158. Sousa, I., et al., *Collagen surface modified poly(ε-caprolactone) scaffolds with improved hydrophilicity and cell adhesion properties.* Materials Letters, 2014. **134**(0): p. 263-267.

159. Tasdelen, M.A., *Poly(epsilon-caprolactone)/clay nanocomposites via "click" chemistry.* European Polymer Journal, 2011. **47**(5): p. 937-941.

160. Toselli, M., et al., *Poly(ϵ-caprolactone)-poly(fluoroalkylene oxide)-poly(ϵ-caprolactone) block copolymers. 2. Thermal and surface properties.* Polymer, 2001. **42**(5): p. 1771-1779.

161. Urbanczyk, L., et al., *Synthesis of PCL/clay masterbatches in supercritical carbon dioxide.* Polymer, 2008. **49**(18): p. 3979-3986.

162. Wang, M., et al., *Polycaprolactone scaffolds or anisotropic particles: The initial solution temperature dependence in a gelatin particle-leaching method.* Polymer, 2013. **54**(1): p. 277-283.

163. Yang, X., et al., *Poly(ε-caprolactone)-based copolymers bearing pendant cyclic ketals and reactive acrylates for the fabrication of photocrosslinked elastomers.* Acta Biomaterialia, 2013. **9**(9): p. 8232-8244.

164. Zhang, Y., et al., *The effects of Runx2 immobilization on poly (ε-caprolactone) on osteoblast differentiation of bone marrow stromal cells in vitro.* Biomaterials, 2010. **31**(12): p. 3231-3236.

165. Zheng, X. and C.A. Wilkie, *Nanocomposites based on poly (ϵ-caprolactone) (PCL)/clay hybrid: polystyrene, high impact polystyrene, ABS, polypropylene and polyethylene.* Polymer Degradation and Stability, 2003. **82**(3): p. 441-450.

166. Abdal-hay, A., F.A. Sheikh, and J.K. Lim, *Air jet spinning of hydroxyapatite/poly(lactic acid) hybrid nanocomposite membrane mats for bone tissue engineering.* Colloids and Surfaces B: Biointerfaces, 2013. **102**(0): p. 635-643.

167. Bolland, B.J.R.F., et al., *The application of human bone marrow stromal cells and poly(dl-lactic acid) as a biological bone graft extender in impaction bone grafting.* Biomaterials, 2008. **29**(22): p. 3221-3227.

168. Cai, X., et al., *Preparation and characterization of homogeneous chitosan–polylactic acid/hydroxyapatite nanocomposite for bone tissue engineering and evaluation of its mechanical properties.* Acta Biomaterialia, 2009. **5**(7): p. 2693-2703.

169. Chen, M., et al., *Self-assembled composite matrix in a hierarchical 3-D scaffold for bone tissue engineering.* Acta Biomaterialia, 2011. **7**(5): p. 2244-2255.

170. Hong, Z., R.L. Reis, and J.F. Mano, *Preparation and in vitro characterization of scaffolds of poly(l-lactic acid) containing bioactive glass ceramic nanoparticles.* Acta Biomaterialia, 2008. **4**(5): p. 1297-1306.

171. Kang, Y., et al., *Preparation of poly(l-lactic acid)/β-tricalcium phosphate scaffold for bone tissue engineering without organic solvent.* Materials Letters, 2008. **62**(12–13): p. 2029-2032.

172. Leenslag, J.W., et al., *Resorbable materials of poly(l-lactide). VI. Plates and screws for internal fracture fixation.* Biomaterials, 1987. **8**(1): p. 70-73.

173. Li, X., Q. Feng, and F. Cui, *In vitro degradation of porous nano-hydroxyapatite/collagen/PLLA scaffold reinforced by chitin fibres.* Materials Science and Engineering: C, 2006. **26**(4): p. 716-720.

174. Argarate, N., et al., *Biodegradable Bi-layered coating on polymeric orthopaedic implants for controlled release of drugs.* Materials Letters, 2014. **132**(0): p. 193-195.

175. Biondi, M., et al., *Controlled drug delivery in tissue engineering.* Advanced Drug Delivery Reviews, 2008. **60**(2): p. 229-242.

176. Brannon-Peppas, L., *Recent advances on the use of biodegradable microparticles and nanoparticles in controlled drug delivery.* International Journal of Pharmaceutics, 1995. **116**(1): p. 1-9.

177. Chen, S., et al., *Poly (lactic acid)/chitosan hybrid nanoparticles for controlled release of anticancer drug.* Materials Science and Engineering: C, (0).

178. Dev, A., et al., *Preparation of poly(lactic acid)/chitosan nanoparticles for anti-HIV drug delivery applications.* Carbohydrate Polymers, 2010. **80**(3): p. 833-838.

179. Ekenseair, A.K., F.K. Kasper, and A.G. Mikos, *Perspectives on the interface of drug delivery and tissue engineering.* Advanced Drug Delivery Reviews, 2013. **65**(1): p. 89-92.

180. Lee, E.S., et al., *Tumor pH-responsive flower-like micelles of poly(l-lactic acid)-b-poly(ethylene glycol)-b-poly(l-histidine).* Journal of Controlled Release, 2007. **123**(1): p. 19-26.

181. Riley, T., et al., *Colloidal stability and drug incorporation aspects of micellar-like PLA–PEG nanoparticles.* Colloids and Surfaces B: Biointerfaces, 1999. **16**(1–4): p. 147-159.

182. Tan, H. and J. Ye, *Surface morphology and in vitro release performance of double-walled PLLA/PLGA microspheres entrapping a highly water-soluble drug.* Applied Surface Science, 2008. **255**(2): p. 353-356.

183. Verrecchia, T., et al., *Non-stealth (poly(lactic acid/albumin)) and stealth (poly(lactic acid-polyethylene glycol)) nanoparticles as injectable drug carriers.* Journal of Controlled Release, 1995. **36**(1–2): p. 49-61.

184. Zhang, C.Y., et al., *Self-assembled pH-responsive MPEG-b-(PLA-co-PAE) block copolymer micelles for anticancer drug delivery.* Biomaterials, 2012. **33**(26): p. 6273-6283.

185. Zhu, A., F. Li, and L. Ji, *Poly(lactic acid)/N-maleoylchitosan core–shell capsules: Preparation and drug release properties.* Colloids and Surfaces B: Biointerfaces, 2012. **91**(0): p. 162-167.

186. Baker, S.C., et al., *The relationship between the mechanical properties and cell behaviour on PLGA and PCL scaffolds for bladder tissue engineering.* Biomaterials, 2009. **30**(7): p. 1321-1328.

187. Chen, C.-H., et al., *Surface modification of polycaprolactone scaffolds fabricated via selective laser sintering for cartilage tissue engineering.* Materials Science and Engineering: C, 2014. **40**(0): p. 389-397.

188. Cleary, M.A., et al., *Vascular tissue engineering: the next generation.* Trends in Molecular Medicine, 2012. **18**(7): p. 394-404.

189. Cui, Z., et al., *Fabrication and characterization of injection molded poly (ε-caprolactone) and poly (ε-caprolactone)/hydroxyapatite scaffolds for tissue engineering.* Materials Science and Engineering: C, 2012. **32**(6): p. 1674-1681.

190. Dash, T.K. and V.B. Konkimalla, *Poly-ϵ-caprolactone based formulations for drug delivery and tissue engineering: A review.* Journal of Controlled Release, 2012. **158**(1): p. 15-33.

191. Declercq, H.A., et al., *Synergistic effect of surface modification and scaffold design of bioplotted 3-D poly-ε-caprolactone scaffolds in osteogenic tissue engineering.* Acta Biomaterialia, 2013. **9**(8): p. 7699-7708.

192. Driscoll, T.P., et al., *Fiber angle and aspect ratio influence the shear mechanics of oriented electrospun nanofibrous scaffolds.* Journal of the Mechanical Behavior of Biomedical Materials, 2011. **4**(8): p. 1627-1636.

193. Gautam, S., A.K. Dinda, and N.C. Mishra, *Fabrication and characterization of PCL/gelatin composite nanofibrous scaffold for tissue engineering applications by electrospinning method.* Materials Science and Engineering: C, 2013. **33**(3): p. 1228-1235.

194. Hoque, M.E., et al., *Fabrication and characterization of hybrid PCL/PEG 3D scaffolds for potential tissue engineering applications.* Materials Letters, 2014. **131**(0): p. 255-258.

195. Jiang, C.-P., Y.-Y. Chen, and M.-F. Hsieh, *Biofabrication and in vitro study of hydroxyapatite/mPEG–PCL–mPEG scaffolds for bone tissue engineering using air pressure-aided deposition technology.* Materials Science and Engineering: C, 2013. **33**(2): p. 680-690.

196. Johari, N., M.H. Fathi, and M.A. Golozar, *The effect of fluorine content on the mechanical properties of poly (ε-caprolactone)/nano-fluoridated hydroxyapatite scaffold for bone-tissue engineering.* Ceramics International, 2011. **37**(8): p. 3247-3251.

197. Johari, N., M.H. Fathi, and M.A. Golozar, *Fabrication, characterization and evaluation of the mechanical properties of poly (ε-caprolactone)/nano-fluoridated hydroxyapatite scaffold for bone tissue engineering.* Composites Part B: Engineering, 2012. **43**(3): p. 1671-1675.

198. Jonnalagadda, J.B. and I.V. Rivero, *Effect of cryomilling times on the resultant properties of porous biodegradable poly(e-caprolactone)/poly(glycolic acid) scaffolds for articular cartilage tissue engineering.* Journal of the Mechanical Behavior of Biomedical Materials, 2014. **40**(0): p. 33-41.

199. Neves, S.C., et al., *Chitosan/Poly(ε-caprolactone) blend scaffolds for cartilage repair.* Biomaterials, 2011. **32**(4): p. 1068-1079.

200. Pamuła, E., et al., *Hydrolytic degradation of porous scaffolds for tissue engineering from terpolymer of l-lactide, ε-caprolactone and glycolide.* Journal of Molecular Structure, 2005. **744–747**(0): p. 557-562.

201. Patrício, T., et al., *Characterisation of PCL and PCL/PLA Scaffolds for Tissue Engineering.* Procedia CIRP, 2013. **5**(0): p. 110-114.

202. Rajzer, I., et al., *Electrospun gelatin/poly(ε-caprolactone) fibrous scaffold modified with calcium phosphate for bone tissue engineering.* Materials Science and Engineering: C, 2014. **44**(0): p. 183-190.

203. Shalumon, K.T., et al., *Fabrication of chitosan/poly(caprolactone) nanofibrous scaffold for bone and skin tissue engineering.* International Journal of Biological Macromolecules, 2011. **48**(4): p. 571-576.

204. Zhang, Q., et al., *Fabrication of three-dimensional poly(ε-caprolactone) scaffolds with hierarchical pore structures for tissue engineering.* Materials Science and Engineering: C, 2013. **33**(4): p. 2094-2103.

205. Pratt, R.C., et al., *Triazabicyclodecene: A simple bifunctional organocatalyst for acyl transfer and ring-opening polymerization of cyclic esters.* Journal of the American Chemical Society, 2006. **128**(14): p. 4556-4557.

206. Wang, J.-S. and K. Matyjaszewski, *Controlled/"living" radical polymerization. atom transfer radical polymerization in the presence of transition-metal complexes.* Journal of the American Chemical Society, 1995. **117**(20): p. 5614-5615.

207. Kato, M., et al., *Polymerization of Methyl Methacrylate with the Carbon Tetrachloride/Dichlorotris- (triphenylphosphine)ruthenium(II)/Methylaluminum Bis(2,6-di-tert-butylphenoxide) Initiating System: Possibility of Living Radical Polymerization.* Macromolecules, 1995. **28**(5): p. 1721-1723.

208. Matyjaszewski, K. and J. Xia, *Atom Transfer Radical Polymerization.* Chemical Reviews, 2001. **101**(9): p. 2921-2990.

209. Matyjaszewski, K., *Atom transfer radical polymerization: from mechanisms to applications.* Israel Journal of Chemistry, 2012. **52**(3-4): p. 206-220.

210. Rühe, J., *Polymer Brushes: On the way to tailor-made surfaces*, in *polymer brushes*. 2005, Wiley-VCH Verlag GmbH & Co. KGaA. p. 1-31.

211. Iyer, K.S., et al., *Polystyrene layers grafted to macromolecular anchoring layer.* Macromolecules, 2003. **36**(17): p. 6519-6526.

212. Mei, Y., et al., *Tuning cell adhesion on gradient poly(2-hydroxyethyl methacrylate)-grafted surfaces.* Langmuir : the ACS journal of surfaces and colloids, 2005. **21**(26): p. 12309-12314.

213. Harris, B., et al., *Photopatterned polymer brushes promoting cell adhesion gradients.* Langmuir : the ACS journal of surfaces and colloids, 2006. **22**(10): p. 4467-4471.

214. Raynor, J.E., et al., *Controlling Cell Adhesion to Titanium: Functionalization of Poly[oligo(ethylene glycol)methacrylate] Brushes with Cell-Adhesive Peptides.* Advanced Materials, 2007. **19**.

215. Mukesh Kumar, V., et al., *Switching of friction by binary polymer brushes.* Soft Matter, 2008. **4**.

216. Limpoco, F.T., R.C. Advincula, and S.S. Perry, *Solvent Dependent Friction Force Response of Polystyrene Brushes Prepared by Surface Initiated Polymerization.* Langmuir, 2007. **23**(24): p. 12196-12201.

217. Landherr, L.J.T., et al., *Interfacial Friction and Adhesion of Polymer Brushes.* Langmuir, 2011. **27**(15): p. 9387-9395.

218. Sheparovych, R., M. Motornov, and S. Minko, *Adapting Low-Adhesive Thin Films from Mixed Polymer Brushes.* Langmuir, 2008. **24**(24): p. 13828-13832.

219. Roosjen, A., et al., *Inhibition of adhesion of yeasts and bacteria by poly(ethylene oxide)-brushes on glass in a parallel plate flow chamber.* Microbiology (Reading, England), 2003. **149**(Pt 11): p. 3239-3246.

220. Cringus-Fundeanu, I., et al., *Synthesis and characterization of surface-grafted polyacrylamide brushes and their inhibition of microbial adhesion.* Langmuir : the ACS journal of surfaces and colloids, 2007. **23**(9): p. 5120-5126.

221. Cullen, S., et al., *Polymeric brushes as functional templates for immobilizing ribonuclease A: study of binding kinetics and activity.* Langmuir : the ACS journal of surfaces and colloids, 2008. **24**(3): p. 913-920.

222. DeRouchey, J., et al., *Monomolecular assembly of siRNA and poly(ethylene glycol)-peptide copolymers.* Biomacromolecules, 2008. **9**(2): p. 724-732.

223. Matthew, T.B., et al., *Nonfouling polymer brushes via surface-initiated, two-component atom transfer radical polymerization.* Macromolecules, 2008. **41**.

224. Tugulu, S. and H.-A. Klok, *Stability and nonfouling properties of poly(poly(ethylene glycol) methacrylate) brushes under cell culture conditions.* Biomacromolecules, 2008. **9**(3): p. 906-912.

225. Jiang, H., et al., *Improvement of Hemocompatibility of Polycaprolactone Film Surfaces with Zwitterionic Polymer Brushes.* Langmuir, 2011. **27**(18): p. 11575-11581.

226. Yuan, S., et al., *Surface modification of polycaprolactone substrates using collagen-conjugated poly(methacrylic acid) brushes for the regulation of cell proliferation and endothelialisation.* Journal of Materials Chemistry, 2012. **22**(26): p. 13039-13049.

227. Arnold, R.M. and J. Locklin, *Self-Sorting click reactions that generate spatially controlled chemical functionality on surfaces.* Langmuir, 2013. **29**(19): p. 5920-5926.

228. Howarter, J.A. and J.P. Youngblood, *Self-Cleaning and anti-fog surfaces via stimuli-responsive polymer brushes.* Advanced Materials, 2007. **19**.

229. Thérien-Aubin, H., L. Chen, and C.K. Ober, *Fouling-resistant polymer brush coatings.* Polymer, 2011. **52**(24): p. 5419-5425.

230. Kobayashi, M., et al., *Wettability and antifouling behavior on the surfaces of superhydrophilic polymer brushes.* Langmuir, 2012. **28**(18): p. 7212-7222.

231. Leermakers, F.A.M., et al., *Effect of a polymer brush on capillary condensation.* Langmuir, 2001. **17**.

232. Smrati, G., et al., *Immobilization of silver nanoparticles on responsive polymer brushes.* Macromolecules, 2008. **41**.

233. Vivek, A.V., S.M. Pradipta, and R. Dhamodharan, *Synthesis of silver nanoparticles using a novel graft copolymer and enhanced particle stability via a "Polymer Brush Effect".* Macromolecular Rapid Communications, 2008. **29**.

234. Ohno, K., et al., *Synthesis of monodisperse silica particles coated with well-defined, high-density polymer brushes by surface-initiated atom transfer radical polymerization.* Macromolecules, 2005. **38**(6): p. 2137-2142.

235. Ohno, K., et al., *Fabrication of ordered arrays of gold nanoparticles coated with high-density polymer brushes.* Angewandte Chemie International Edition, 2003. **42**(24): p. 2751-2754.

236. Kohji, O., et al., *Suspensions of silica particles grafted with concentrated polymer brush: effects of graft chain length on brush layer thickness and colloidal crystallization.* Macromolecules, 2007. **40**.

237. Nagase, K., et al., *Effects of graft densities and chain lengths on separation of bioactive compounds by nanolayered thermoresponsive polymer brush surfaces.* Langmuir : the ACS journal of surfaces and colloids, 2008. **24**(2): p. 511-517.

238. Xu, L. and C.B. Gorman, *Poly(lactic acid) brushes grow longer at lower temperatures.* Journal of Polymer Science Part A: Polymer Chemistry, 2010. **48**(15): p. 3362-3367.

239. Jeon, N.L., et al., *Patterned polymer growth on silicon surfaces using microcontact printing and surface-initiated polymerization.* Applied Physics Letters, 1999. **75**(26): p. 4201-4203.

240. Husseman, M., et al., *Controlled synthesis of polymer brushes by "living" free radical polymerization techniques.* Macromolecules, 1999. **32**(5): p. 1424-1431.

241. Matyjaszewski, K., et al., *Polymers at interfaces: Using atom transfer radical polymerization in the controlled growth of homopolymers and block copolymers from silicon surfaces in the absence of untethered sacrificial initiator.* Macromolecules, 1999. **32**(26): p. 8716-8724.

242. Ding, S., J.A. Floyd, and K.B. Walters, *Comparison of surface confined ATRP and SET-LRP syntheses for a series of amino (meth)acrylate polymer brushes on silicon substrates.* Journal of Polymer Science Part A: Polymer Chemistry, 2009. **47**(23): p. 6552-6560.

243. Baum, M. and W.J. Brittain, *Synthesis of polymer brushes on silicate substrates via reversible addition fragmentation chain transfer technique.* Macromolecules, 2002. **35**(3): p. 610-615.

244. Xu, L., K. Crawford, and C.B. Gorman, *Effects of temperature and ph on the degradation of poly(lactic acid) brushes.* Macromolecules, 2011. **44**(12): p. 4777-4782.

245. Hu, X., et al., *Comparison of the growth and degradation of poly(glycolic acid) and poly(ε-caprolactone) brushes.* Journal of Polymer Science Part A: Polymer Chemistry, 2013. **51**(21): p. 4643-4649.

246. Choi, I.S. and R. Langer, *Surface-initiated polymerization of l-lactide: coating of solid substrates with a biodegradable polymer.* Macromolecules, 2001. **34**(16): p. 5361-5363.

247. Möller, M., et al., *Stannous(II) trifluoromethane sulfonate: a versatile catalyst for the controlled ring-opening polymerization of lactides: Formation of stereoregular surfaces from polylactide "brushes".* Journal of Polymer Science Part A: Polymer Chemistry, 2001. **39**(20): p. 3529-3538.

248. Carrot, G., et al., *Surface-initiated ring-opening polymerization: A versatile method for nanoparticle ordering.* Macromolecules, 2002. **35**(22): p. 8400-8404.

249. Lahann, J. and R. Langer, *Surface-initiated ring-opening polymerization of ε-caprolactone from a patterned poly(hydroxymethyl- p-xylylene).* Macromolecular Rapid Communications, 2001. **22**(12): p. 968-971.

250. Schmidt, A.M., *The synthesis of magnetic core-shell nanoparticles by surface-initiated ring-opening polymerization of ε-caprolactone.* Macromolecular Rapid Communications, 2005. **26**(2): p. 93-97.

251. Chen, F., et al., *Synthesis of magnetite core–shell nanoparticles by surface-initiated ring-opening polymerization of l-lactide.* Journal of Magnetism and Magnetic Materials, 2008. **320**(13): p. 1921-1927.

252. Chen, J., et al., *Controlled surface-initiated ring-opening polymerization of L-lactide from risedronate-anchored hydroxyapatite nanocrystals: Novel synthesis of biodegradable hydroxyapatite/poly(L-lactide) nanocomposites.* Journal of Polymer Science Part A: Polymer Chemistry, 2011. **49**(20): p. 4379-4386.

253. Dove, A.P., *Organic catalysis for ring-opening polymerization.* ACS Macro Letters, 2012. **1**(12): p. 1409-1412.

254. Martello, M.T., A. Burns, and M. Hillmyer, *Bulk ring-opening transesterification polymerization of the renewable δ-decalactone using an organocatalyst.* ACS Macro Letters, 2011. **1**(1): p. 131-135.

255. Zalusky, A.S., et al., *Ordered nanoporous polymers from polystyrene−polylactide block copolymers.* Journal of the American Chemical Society, 2002. **124**(43): p. 12761-12773.

256. Holden, G., E.T. Bishop, and N.R. Legge, *Thermoplastic elastomers.* Journal of Polymer Science Part C: Polymer Symposia, 1969. **26**(1): p. 37-57.

257. Holden, G., *Thermoplastic Elastomers*, in *Kirk-Othmer Encyclopedia of Chemical Technology*. 2000, John Wiley & Sons, Inc.

258. Fukuhira, Y., et al., *Biodegradable honeycomb-patterned film composed of poly(lactic acid) and dioleoylphosphatidylethanolamine.* Biomaterials, 2006. **27**(9): p. 1797-1802.

259. Ho, R.-M., et al., *Solvent-induced microdomain orientation in polystyrene-b-poly(l-lactide) diblock copolymer thin films for nanopatterning.* Polymer, 2005. **46**(22): p. 9362-9377.

260. Kuech, T.F. and L.J. Mawst, *Nanofabrication of III–V semiconductors employing diblock copolymer lithography.* Journal of Physics D: Applied Physics, 2010. **43**(18): p. 183001.

261. Park, C., J. Yoon, and E.L. Thomas, *Enabling nanotechnology with self assembled block copolymer patterns.* Polymer, 2003. **44**(22): p. 6725-6760.

262. Park, S., et al., *From nanorings to nanodots by patterning with block copolymers.* Nano Letters, 2008. **8**(6): p. 1667-1672.

263. Park, S.-M., et al., *Patterning sub-10 nm line patterns from a block copolymer hybrid.* Nanotechnology, 2008. **19**(45): p. 455304.

264. Perego, M., et al., *Collective behavior of block copolymer thin films within periodic topographical structures.* Nanotechnology, 2013. **24**(24): p. 245301.

265. Segalman, R.A., *Patterning with block copolymer thin films.* Materials Science and Engineering: R: Reports, 2005. **48**(6): p. 191-226.

266. Xiao, S., et al., *Aligned nanowires and nanodots by directed block copolymer assembly.* Nanotechnology, 2011. **22**(30): p. 305302.

267. Yoshida, S., T. Ono, and M. Esashi, *Conductive polymer patterned media fabricated by diblock copolymer lithography for scanning multiprobe data storage.* Nanotechnology, 2008. **19**(47): p. 475302.

268. Bang, J., et al., *Defect-free nanoporous thin films from abc triblock copolymers.* Journal of the American Chemical Society, 2006. **128**(23): p. 7622-7629.

269. Chen, L., et al., *Robust nanoporous membranes templated by a doubly reactive block copolymer.* Journal of the American Chemical Society, 2007. **129**(45): p. 13786-13787.

270. Gruber, M.F., L. Schulte, and S. Ndoni, *Nanoporous materials modified with biodegradable polymers as models for drug delivery applications.* Journal of Colloid and Interface Science, 2013. **395**(0): p. 58-63.

271. Hillmyer, M., *Nanoporous materials from block copolymer precursors*, in *block copolymers II*, V. Abetz, Editor. 2005, Springer Berlin Heidelberg. p. 137-181.

272. Jackson, E.A. and M.A. Hillmyer, *Nanoporous membranes derived from block copolymers: from drug delivery to water filtration.* ACS Nano, 2010. **4**(7): p. 3548-3553.

273. Kang, J. and K.J. Beers, *Macromolecular transport through nanostructured and porous hydrogels synthesized using the amphiphilic copolymer, PCL-b-PEO-b-PCL.* European Polymer Journal, 2009. **45**(11): p. 3004-3009.

274. Pitet, L.M., M.A. Amendt, and M.A. Hillmyer, *Nanoporous linear polyethylene from a block polymer precursor.* Journal of the American Chemical Society, 2010. **132**(24): p. 8230-8231.

275. Sperschneider, A., et al., *Towards nanoporous membranes based on abc triblock terpolymers.* Small, 2007. **3**(6): p. 1056-1063.

276. Wang, Y., et al., *Nanoporous metal membranes with bicontinuous morphology from recyclable block-copolymer templates.* Advanced Materials, 2010. **22**(18): p. 2068-2072.

277. Yang, S.Y., et al., *Virus Filtration membranes prepared from nanoporous block copolymers with good dimensional stability under high pressures and excellent solvent resistance.* Advanced Functional Materials, 2008. **18**(9): p. 1371-1377.

278. Huck, W.T.S., *Effects of nanoconfinement on the morphology and reactivity of organic materials.* Chemical Communications, 2005(33): p. 4143-4148.

279. Bang, J., et al., *Block copolymer nanolithography: Translation of molecular level control to nanoscale patterns.* Advanced Materials, 2009. **21**(47): p. 4769-4792.

280. Vayer, M., et al., *Perpendicular orientation of cylindrical domains upon solvent annealing thin films of polystyrene-b-polylactide.* Thin Solid Films, 2010. **518**(14): p. 3710-3715.

281. Olayo-Valles, R., et al., *Perpendicular domain orientation in thin films of polystyrene−polylactide diblock copolymers.* Macromolecules, 2005. **38**(24): p. 10101-10108.

282. Phillip, W.A., et al., *Self-assembled block copolymer thin films as water filtration membranes.* ACS Applied Materials & Interfaces, 2010. **2**(3): p. 847-853.

283. Wandera, D., et al., *Modification of ultrafiltration membranes with block copolymer nanolayers for produced water treatment: The roles of polymer chain density and polymerization time on performance.* Journal of Membrane Science, 2012. **403–404**(0): p. 250-260.

284. Yang, S.Y., et al., *Single-file diffusion of protein drugs through cylindrical nanochannels.* ACS Nano, 2010. **4**(7): p. 3817-3822.

CHAPTER 2

DEGRADABLE POLYCAPROLACTONE AND POLYLACTIDE HOMOPOLYMER AND BLOCK COPOLYMER BRUSHES PREPARED BY SURFACE INITIATED POLYMERIZATION UTILIZING TRIAZABICYCLODECENE AND ZIRCONIUM CATALYSTS[1]

[1]Joe B. Grubbs III, Rachelle M. Arnold, Anandi Roy, Karson Brooks, Jenna A. Bilbrey, Jing Gao, and Jason Locklin. To be submitted to *Langmuir*

Abstract

Surface-initiated ring-opening polymerization (SI-ROP) of polycaprolactone (PCL) and polylactide (PLA) polymer brushes with controlled degradation rates were prepared on oxide substrates. PCL brushes were polymerized from hydroxyl-terminated monolayers utilizing triazabicyclodecene (TBD) as the polymerization catalyst. A consistent brush thickness of 40 nm could be achieved with a reproducible unique crystalline morphology. The organocatalyzed PCL brushes were chain extended using lactide in the presence of zirconium n-butoxide to successfully grow PCL/PLA block copolymer (PCL-b-PLA) brushes with a final thickness of 55 nm. The degradation properties of "grafted from" PCL brush and the PCL-b-PLA brush were compared to "grafted to" PCL brushes, and we observed that the brush density plays a major role in degradation kinetics. Solutions of methanol/water at pH 14 were used to better solvate the brushes and increase the kinetics of degradation. This framework enables a control of degradation that allows for the precise removal of these coatings.

Introduction

Modification of surfaces with polymers of high grafting density is a popular technique to produce surface-bound films with tunable properties, which gives rise to a myriad of applications, such as manipulation of interfacial forces,[1-7] investigation and development of biomaterials,[8-16] surface coatings,[17-19] and nanoparticle encapsulation[20-24]. Factors such as grafting density, chain length, and thickness of the film directly influence the interfacial properties of the substrate,[25, 26] illustrating the need for polymerization methodologies that afford control over these parameters[27].

Surface-initiated ring-opening polymerization (SI-ROP) is a chain growth polymerization technique that offers great promise in control over these parameters. The predetermined coordination/insertion mechanism in which the metal catalyst coordinates to the ester carbonyl, allowing the initiator to insert, has allowed the polymerization of monomers such as lactide and lactones. Polycaprolactones (PCL) and polylactide (PLA) have garnered attention over the past decade due to their biodegradability and ever expanding uses in the medical field.[28-31] PCL brushes can be prepared by SI-ROP of ε-caprolactone using an alcohol pendant group attached to the surface[32]. These brushes allow the modulation of controlled release kinetics, as well as the ability to tune the degradation rate by increasing or decreasing diffusion, crystallinity, and glass transition (Tg). Although SI-ROP has been utilized over the past decade to generate biodegradable polymer brushes from lactide and ε-caprolactone, this technique has only provided ultrathin coatings of 15 nm or less [32-39], which is a potential limitation to their practical utility.

In this study, a synthetic strategy was developed to produce grafted from PCL brushes through SI-ROP from oxide surfaces through the use of a more active organocatalyst,

triazabicyclodecene (TBD), under mild temperatures[40]. This methodology affords the reproducible fabrication of films up to 40 nm in thickness. By using TBD catalyst, the hydroxyl end groups of PCL are retained and available for block copolymer formation. Chain extension of the PCL brushes was carried out using meso-lactide in the presence of zirconium n-butoxide, generating final film thicknesses of about 55 nm. Grafted to brushes were prepared by spin coating a PCL homopolymer to a PGMA anchored monolayer on a silicon substrate. The 25 nm PCL thin film was covalently attached to the PGMA layer by thermal annealing. Solvent-induced degradation behavior using a high pH methanol/water mixture was used to compare the "grafted from" and "grafted to" polymer films to prove densely packed brushes slow down the degradation kinetics. It was observed that the polymer brushes with higher grafting densities degraded 6-10 times slower than those with lower grafting densities. To further tune degradation solvent annealing of the BCP films was studied to decrease film roughness and promote orientation.

Experimental

Materials

Tetrahydrofuran (THF), toluene, and dichloromethane (DCM), were purified in a MBraun solvent purification system (SPS). Methanol, acetone, and isopropanol (IPA) were used as received from Fisher Scientific. E-caprolactone was received from Aldrich and dried over molecular sieves (0.4 nm) for at least 2 weeks. 1,6-hexanediol was received from Alfa Aesar and placed under 25 mtorr vacuum for 2 days prior to use. TBD was purified by refluxing in THF over calcium hydride. Meso-lactide and zirconium n-butoxide were received as a gift from DaniMer Scientific and used without purification. Silicon wafers (orientation <100>, native

oxide) were purchased from University Wafer. All other chemicals were purchased from Alfa Aesar, Sigma Aldrich, or TCI, and were used as received.

Preparation of Initiator Layers

Silicon wafers were cut into 10 x 20 mm^2 pieces and sonicated in hexane, isopropanol, acetone, and deionized water for 15 minutes each. The substrates were then dried using a stream of nitrogen and subjected to argon plasma (Harrick Plasma, PDC-32-G, 0.8 mbar, 18 W) for 5 minutes. A 10 mM stock solution of 7-octenyltrichlorosilane was made using 20 mL of dry toluene. The initiator solution was added to the substrates and allowed to sit for 16 hours. The substrates were then removed, rinsed with toluene, and dried under a stream of nitrogen. The alkene-functionalized substrates were placed in a Schlenk flask that was subsequently purged with N_2, and 2.0 mL of borane/THF complex (1.0 M soln) was added to the flask. After 16 hours, the substrates were removed and rinsed multiple times with THF. An 8.0 mL solution of 30% hydrogen peroxide/0.1 M NaOH (1:1 v/v) was added to the substrates for four hours and yielded a homogenous monolayer with hydroxyl functionality through an anti-Markovnikov addition.

Surface-Initiated Ring Opening Polymerization of PCL

The hydroxyl terminated monolayer substrates were placed in a large Schlenk flask followed by the addition of 45.1 mmol of ε-caprolactone and 80 μmol of TBD. The reaction was carried out at room temperature for 16 hours using a homemade teflon slide holder to reduce agitation of the substrate while stirring vigorously under a blanket of argon. The substrates were then removed, rinsed and sonicated in THF, chloroform, and acetone for 10 minutes each, and dried using a stream of nitrogen. The film thickness after sonication was 40 nm as measured by spectroscopic ellipsometry. To ensure that only covalently grafted polymer was present on the

surface after sonication, a Scotch Tape™ (3M) test was performed. The thickness after removing the tape remained 40 nm.

Chain Extension of PCL

The PCL brushes were placed in a large Schlenk flask with 13.9 mmol of lactide and purged with nitrogen/vacuum three times. Zirconium n-butoxide, 7.8 μmol, was added to 5.0 mL of toluene and syringed into the flask. The solution was heated at 105 °C overnight. After 18 hours, the substrate was removed and washed with copious amounts of DCM. The film thickness increased to 55 nm indicating successful generation of a block copolymer brush.

PGMA monolayer formation

Methyl ethyl ketone (MEK, 8.70 mL) and glycidyl methacrylate (3.73 mL) were added to a round bottom flask and degassed for 30 minutes, followed by heating to 60 °C. Azobisisobutyronitrile (AIBN, 23 mg) and MEK (1.00 mL) were placed in a small test tube capped with a rubber septum and degassed for 30 minutes. The initiator solution was added to the round bottom flask and stirred for 16 hours. The glassy polymer was then dissolved in MEK by refluxing at 80 °C for 30 minutes. Afterwards, the supernatant was removed and precipitated in cold methanol. The precipitated polymer was filtered and dried under reduced pressure.

Silicon slides were cut (10 x 20 mm^2) and sonicated in acetone, water, and IPA for 15 minutes each. The slides were immersed in 50/50 NH_3OH/H_2O_2 solution (base piranha) for 30 minutes, rinsed with water, sonicated with IPA, dried under nitrogen, and ozone cleaned using NOVASCAN PSD-UV ozone cleaner for 15 minutes. WARNING: Base piranha solution should be handled with caution. A solution 10 mg/mL solution of 75 kDa PGMA in MEK was prepared and passed through a 0.2 μm nylon filter. The cleaned silicon slides were spincoated with 35 μL of the PGMA solution at a speed of 3000 rpm, followed by annealing at 150 °C overnight in an

inert atmosphere. After rinsing with copious amounts of MEK and drying, thickness measurements of 5 nm were determined by ellipsometry.

PCL grafted to a PGMA monolayer

Silicon substrates with an anchor monolayer of PGMA were used to graft PCL to the surface. PCL was prepared for the "grafting to" approach by performing a neat ring-opening polymerization of ε-caprolactone in the presence of tin II ethylhexanoate and 1,6-hexanediol. A 12 kDa PCL homopolymer was synthesized by placing 44 mmol ε-caprolactone, 0.40 mmol 1,6 hexanediol, and 10 μmol tin II ethylhexanoate in a large schlenk flask. The reaction was allowed to stir at room temperature under a blanket of nitrogen overnight. After dissolving the polymer in minimal DCM and precipitating it in methanol, a pure white powder was obtained at 98% yield. A 60 μL aliquot of a 15 mg/mL PCL solution in chlorobenzene was spincoated at 2000 rpm onto a PGMA substrate. The substrate was thermally treated at 150°C for 1 hour. After covalent attachment, the substrate was rinsed and sonicated with copious amounts of DCM. The film thickness after sonication was 25 nm.

Solvent annealing the block copolymer (BCP) film

The BCP substrate was placed in a vacuum desiccator along with an aluminum pan filled with approximately 2 mL of THF. The pressure was reduced inside the desiccator to completely blanket the substrate with THF vapor. The substrate was removed at various time points to check for morphology changes exhibited by the brush using AFM.

Degradation studies of PCL brushes

A grafted from PCL substrate and a grafted to PCL/PCL-b-PLA substrate were placed into capped, flat bottom Schlenk flasks. A 10 mL aliquot of a 0.5 M NaOH methanol/water (60/40 v/v) solution was added to each flask. After various time points, the substrates were

removed and rinsed with copious amounts of DCM. After drying under a stream of nitrogen, thickness measurements were taken. This procedure was repeated until the PCL layer was completely removed.

Characterization

Thickness was determined on a J. A. Woollam M-2000V spectroscopic ellipsometer with a white light source at three angles of incidence (65°, 70°, and 75°) to the silicon wafer normal. A Cauchy model was used to fit the film thickness of the polymer brush layer. FTIR measurements were taken on a Nicolet Model 6700 with a grazing angle attenuated total reflectance (GATR) accessory at 256 scans with a 4 cm^{-1} resolution. Static contact angle measurements were taken on a Krüss DSA 100 using a 1 μL drop of 18 MΩ water (pH 7). For each trial, three drops were recorded for the substrate and averaged together. AFM images were taken in tapping mode on a Multimode NanoScope 8 (Veeco Metrology) using a silicon AFM probe with a spring constant of 48 N/m and resonant frequency of 190 kHz.

Results and Discussion

The effect of a metal catalyst versus a metal-free catalyst on PCL film thickness was investigated via SI-ROP using a hydroxyl terminated SAM. The SAM was prepared by covalently attaching 7-octenyltrichlorosilane to a silicon substrate, then using borane in THF to generate the terminal hydroxyl by hydroboration oxidation. Following the work of Cheshmedzhieva *et al*.[41] on various metal-based catalysts as well as metal-free catalysts for ring-opening polymerization, and Dove *et al.[42]* on the use of organocatalysis as an approach for ring-opening polymerization, two commercially available and easily accessible catalysts were utilized for polymerizations: zirconium n-butoxide, and TBD. After several side-by-side studies,

the more active TBD organocatalyst yielded consistently thicker films of PCL through SI-ROP. However, using a zirconium catalyst generated a thicker layer of PLA in the synthesis of the BCP. In this work, TBD was chosen as the catalyst for the SI-ROP of PCL, and zirconium n-butoxide was used in the synthesis of PLA.

Table 2.1. List of all substrates fabricated with thickness and contact angle data.

	Thickness (nm)	**Contact Angle °**
PGMA	5.5	58
PCL graft to PGMA	20.2	75
Alkene SAM	2.4	91
Hydroxyl SAM	2.5	63
PCL Brush	41.2	79
PLA Block	14.3	82
PCL-b-PLA Annealed	55.5	91

In order to achieve consistent thicknesses, the self-assembled monolayer (SAM) with terminal hydroxyls must be densely and uniformly packed on the surface. This was achieved by submerging the substrate in a 10 mM solution of 7-octenyltrichlorosilane in toluene under inert atmosphere overnight. The SAM thickness was determined to be 2.4 nm by ellipsometry (Table 2.1). The terminal alkenes were then converted to hydroxyls through hydroboration[43]. Contact angle measurements yielded a 28° reduction from the 91° of the alkene monolayer (Table 2.1), which is consistent with the conversion of alkene to hydroxyl functionality (Figure 2.1A). Once a completely homogenous hydroxyl layer was obtained, poly (ε-caprolactone) was synthesized in the presence of TBD as shown in Scheme 2.1.

Scheme 2.1. Organocatalyzed SI-ROP of PCL polymer brushes on a silicon oxide surface.

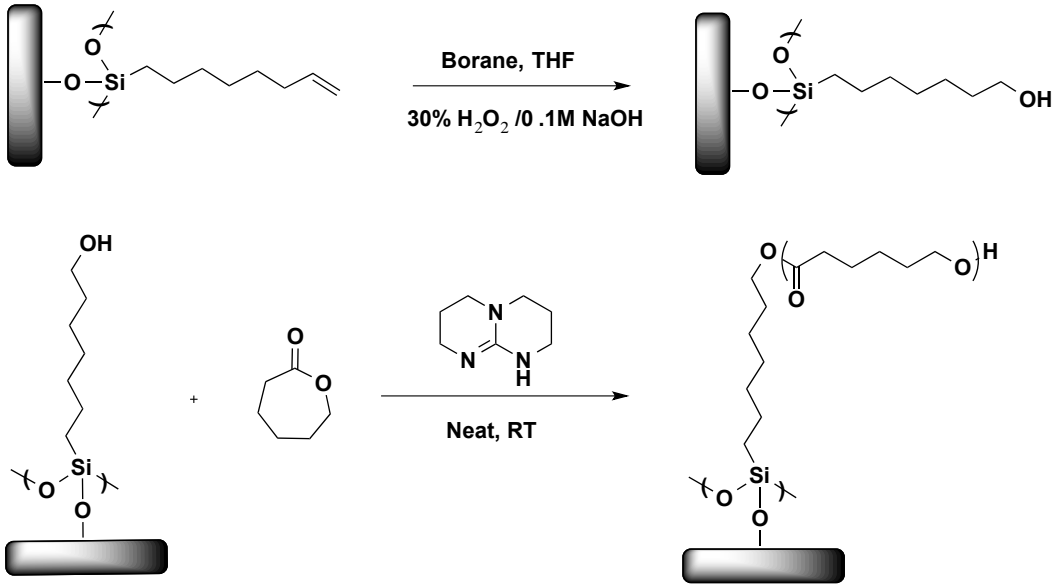

SI-ROP of PCL was performed under neat conditions by placing the hydroxyl-functionalized silicon substrate in a large Schlenk flask, then adding 5 mL of dry ε-caprolactone along with 0.2% by weight TBD. The reaction was carried out at room temperature stirring vigorously overnight. After 18 hours the reaction solution became a white solid due to simultaneous acyl transfer and hydrogen bonding from TBD acting as a bifunctional catalyst, resulting in PCL formation on the surface and in solution[44]. This organocatalyst limits the growth of PCL polymer brushes to 40 nm due to the consumption of monomer through polymerization in solution. We varied the solvent concentration, and several dilute reactions were carried out in toluene to reduce the viscosity allowing for longer reaction time, however the film thickness was comparable in each case. Figure 2.1B shows the ATR-FTIR spectra of the organocatalyzed PCL brush with a prominent carbonyl stretch at 1727 cm^{-1}, symmetric CH_2 stretch at 2865 cm^{-1}, and asymmetric CH_2 stretch at 2949 cm^{-1}.

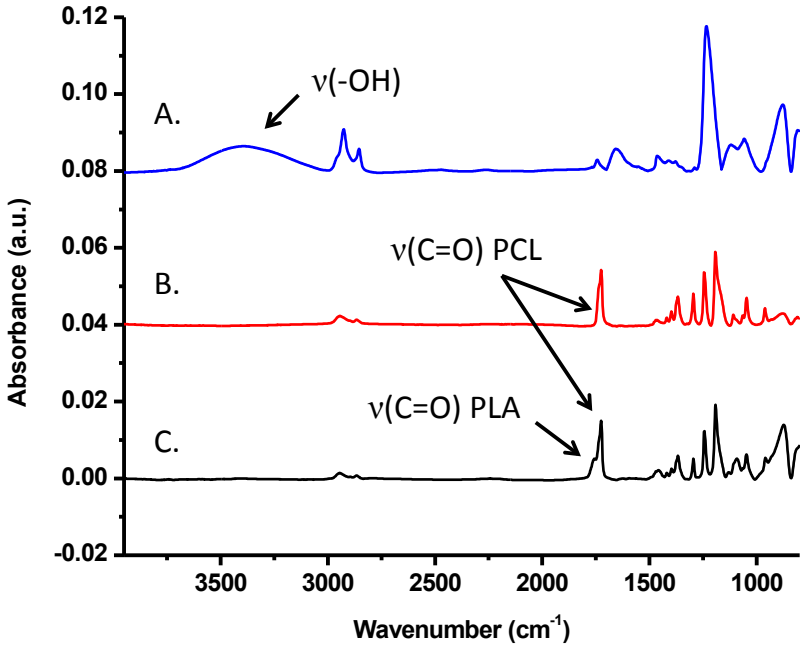

Figure 2.1. FTIR Spectra A) Hydroxyl functionalized monolayer. B) PCL homopolymer brush. C) PCL-b-PLA brush.

After successful reproduction of 40 nm brushes over several experiments, the morphology of the brushes was probed using AFM. It was determined that the brush had an RMS roughness of about 5.13 nm with an unique surface architecture (Figure 2.2). Using AFM for particle analysis the 5 μm image had crystalline domains with an average height of 2.78 nm an average diameter of 58 nm. The interesting topology can be attributed to the semi-crystalline nature of PCL and the densely packed nature of the polymer brush.

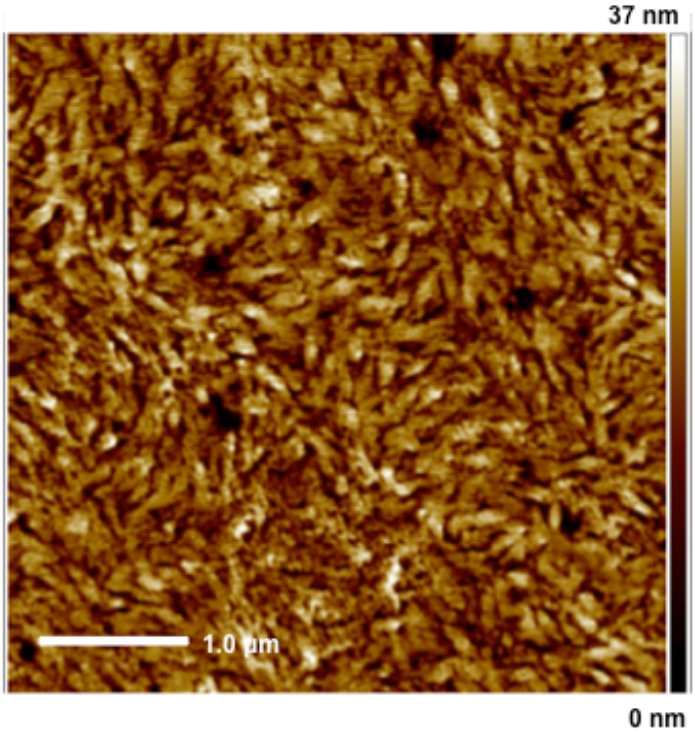

Figure 2.2. 5 µm AFM height image of SI-ROP polymer brush of PCL.

Chain extension of the 40 nm PCL brush was carried out via SI-ROP of lactide in solution using zirconium n-butoxide as illustrated in Scheme 2.2. Unlike the organocatalyzed PCL brush, no polymer was generated in solution due to the need for a hydroxyl functionality in the coordination-insertion mechanism of the zirconium catalyst.

Scheme 2.2: Metal catalyzed SI-ROP of PLA on PCL brushes

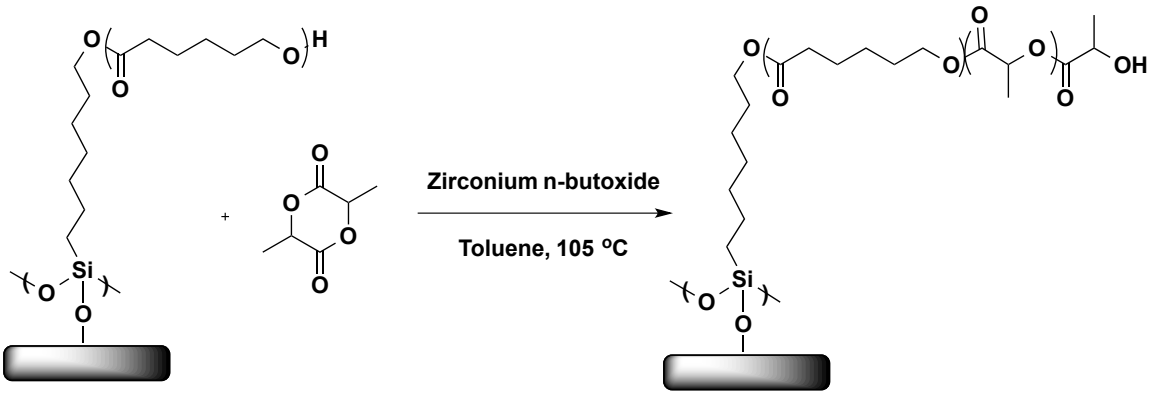

The PCL-b-PLA brush exhibited a 3° change in contact angle from 79° to 82° after chain extension, as well as a change in morphology due to the less crystalline PLA and roughness of the film (Figure 2.3a). The RMS roughness of the film increased to 10.7 nm, suggesting that the chain extension was not homogenous throughout the film, possibly due to the bulky catalyst and inadequate space for ROP. FTIR was also used to confirm the successful generation of the BCP brush (Figure 2.1C) with the appearance of a shoulder on the PCL carbonyl stretch corresponding to PLA carbonyl stretch at about 1761 cm^{-1}.

However, after annealing the BCP brush under a blanket of dry THF for 60 minutes in a desiccator, a significant change in the topology was observed. As seen in Figure 2.3b, solvent annealing the brush produced cylinder shape pillars throughout the image as well as a decrease in roughness to 6.96 nm. The cylindrical pillars have an average height of about 10 nm and a diameter of 78 nm. An increase in contact angle to 91° was also observed. This can be attributed to the crystalline nature of PCL which gives rise to these crystallized architectures and increased roughness.

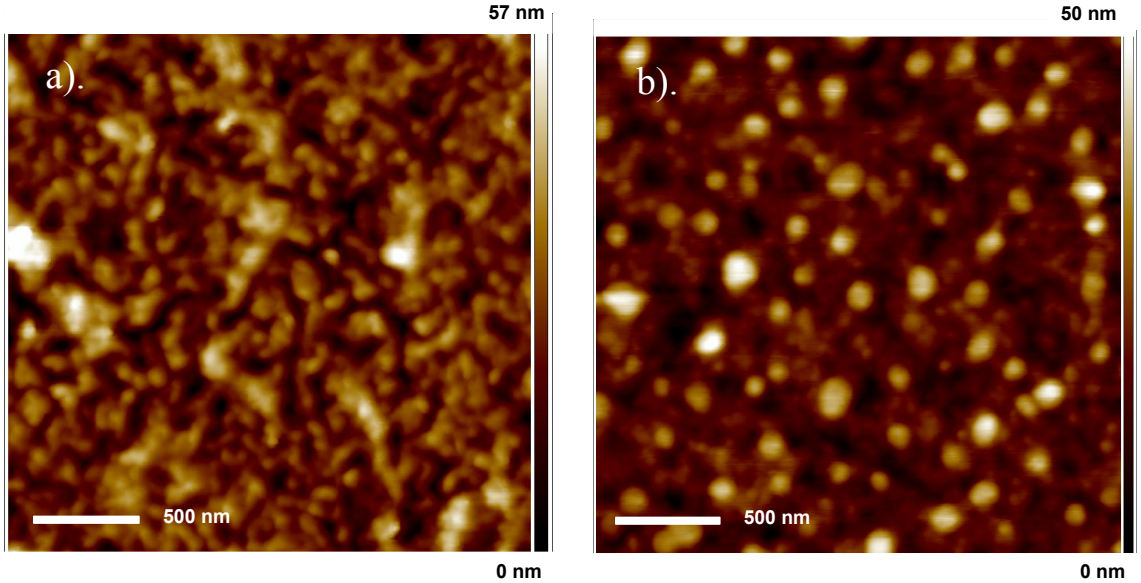

Figure 2.3. a). AFM height image of a SI-ROP PCL-b-PLA polymer brush. b). AFM height image of a SI-ROP PCL-b-PLA polymer brush annealed under a blanket of THF.

After successfully developing a grafting from methodology, a grafting to approach was used to compare degradation and surface topology of the subsequent brushes. Bulk PCL was synthesized using ROP with tin catalyst and 1,6-hexanediol at room temperature overnight, resulting in a polymer with a molecular weight of 12 kDa and a dispersity (Đ) of 1.21. In order to graft PCL to the surface, a monolayer of PGMA[45] was annealed to a silicon oxide surface to covalently attach the monolayer as shown in Scheme 2.3.

Scheme 2.3. PCL grafted to PGMA on a silicon oxide surface

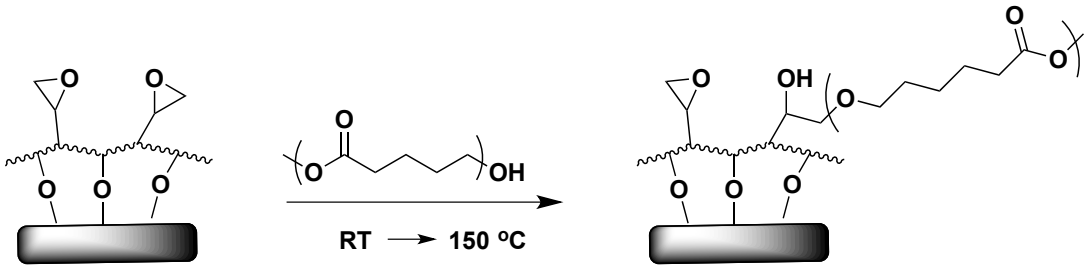

AFM shows the PGMA layer to be completely homogenous with a thickness of about 5 nm (Figure 2.4). The RMS roughness of the PGMA film was <1 nm and had a contact angle of 58° which correlated to a uniform, hydrophilic surface. The PCL was dissolved in chlorobenzene to form a 15 mg/mL solution; 60 μL was spin coated at 2000 rpm onto a PGMA anchoring substrate.

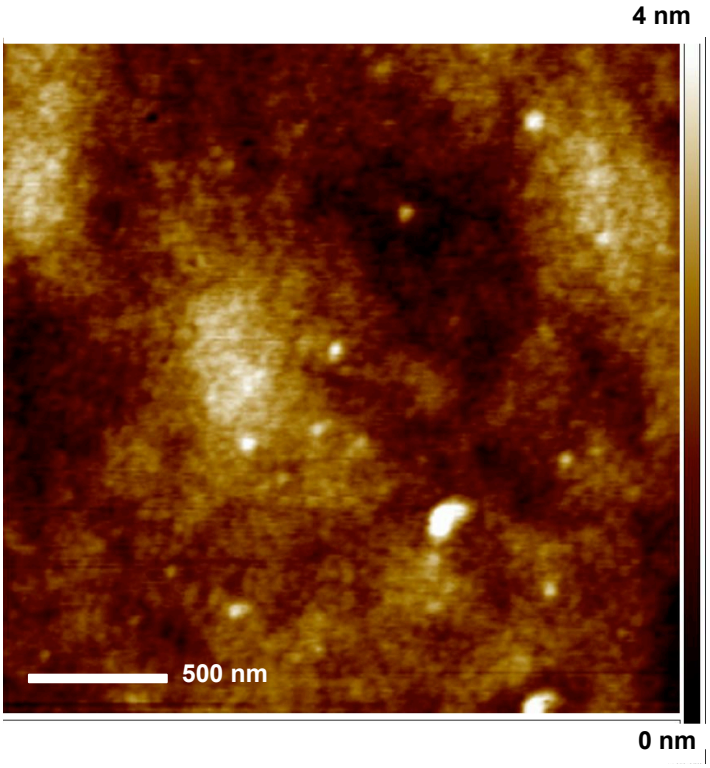

Figure 2.4. AFM height image of PGMA anchoring layer attached to a silicon oxide surface via thermal annealing.

The substrate was thermally treated at 150 °C for 1 hour. After covalent attachment, the substrate was rinsed and sonicated with copious amounts of DCM to remove physisorbed

polymer. The contact angle of the grafted to PCL was 75° across the entire 25 nm film, which suggests a homogeneous polymer layer (Figure 2.5).

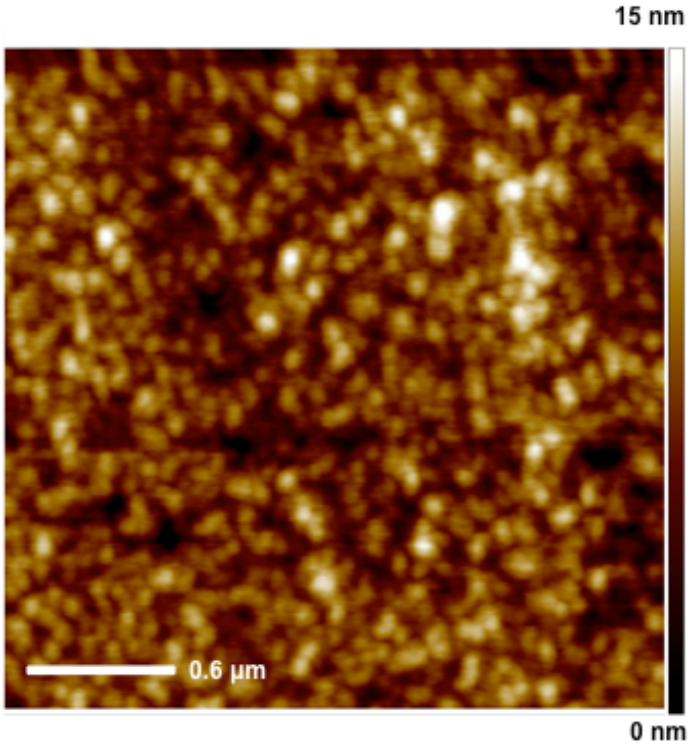

Figure 2.5. AFM 3µm height image of PCL grafted to PGMA on a silicon oxide surface.

After successful fabrication of both the grafted from and grafted to polymer brushes, the degradation behavior of each substrate was evaluated. In a previous study by Xu *et al.[46]*, PLA brushes 10 nm in thickness were exposed to aqueous solutions with pHs ranging from 3 to 8 in order to monitor the degradation rate. At pH 8, more than 24 hours was needed for complete degradation of the PLA brushes[46]. Based on the similarities between PLA and PCL, similar degradation results under similar conditions were anticipated. The degradation kinetics of the Xu and Hu[33] systems would take significant time to degrade our thicker brushes, so we wanted to expedite the degradation in order to compare the systems. We accomplished this by adding a

favorable solvent to the polymers and increasing the pH to improve the degradation kinetics, by encouraging hydrolysis over backbiting.

The grafted from and grafted to substrates were added to a capped, flat bottom Schlenk flask along with the degradation solution and removed at various time points. After thoroughly rinsing with DCM and drying under a stream of nitrogen, thickness measurements were taken using spectroscopic ellipsometry. This technique was repeated until both substrates were completely etched. In order to confirm the grafted to polymer was being completely etched, the thickness measurements were monitored by ellipsometry. The contact angle for the grafted to PCL was initially 79° and after degradation was 59°, which correlates to the contact angle of the PGMA anchoring layer (Table 2.1). As hypothesized, the solvent assisted degradation at higher pH provided faster degradation kinetics than previous results[33, 46]. Also, the grafted from polymer degraded much slower than the grafted to polymers, most likely due to the increased packing density of the brushes (Figure 2.6). The annealed BCP brush showed improved degradation resistance with interesting degradation results. The brush showed an initial 8% change in thickness that plateaued for approximately 50 minutes before degradation started to follow a trend similar to PCL degradation. This trend can be attributed to the change in morphology where PCL and PLA are both present at the interface and the increase in crystallinity and roughness of the BCP brush after annealing.

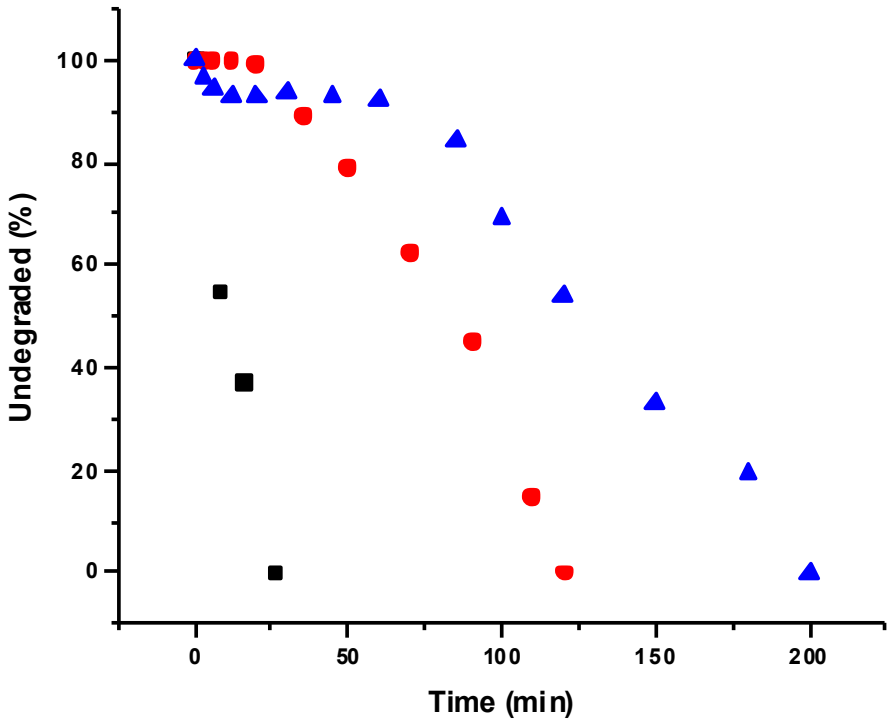

Figure 2.6. Grafted to and grafted from degradation studies using 0.5 M NaOH methanol/water (40/60 v/v). The black squares represent grafted to PCL polymer brush, the red circles represent grafted from PCL brush, and the blue triangles represent the annealed PCL-b-PLA grafted to brush.

Conclusions

In conclusion, TBD catalyzed SI-ROP of PCL polymer brushes that were 40 nm in thicknesses were consistently generated. Creating a uniform, well-packed monolayer enabled the synthesis of a densely packed PCL brush layer with unique, crystalline topology. The use of TBD catalyst enabled retention of end groups on the PCL homopolymer brush and allowed for chain extension using a zirconium catalyst to successfully generate a PLA layer. The topology of

the BCP underwent changes with the addition of PLA and an increase in surface roughness from 5.1 to 10.7 nm. The BCP annealed film also showed significant changes in topology with the appearance of cylindrical pillars of around 78 nm in diameter throughout the film. The roughness of the film after annealing changed to about 6.96 nm due to PCL permeating up through the PLA. This increase in roughness and crystallinity of the film suggested an increase in the hydrophobicity of the BCP film. We have demonstrated in this work a successful route to generate 40 nm PCL films with an organocatalyst and chain extension to produce PCL/PLA BCP brushes that can be annealed to change some of its physical properties as noted above.

It has also been demonstrated in this work that the degradation kinetics can accelerated by adding methanol to solvate the polymer brush and increasing pH to 14. The grafted to PCL brush degradation was 6x faster than the grafted from PCL homopolymer brush while the annealed BCP brush exhibited even slower kinetics than the homopolymer. Utilizing this degradation technique is ideal for protective coatings that require a degradable layer that can be quickly and easily removed.

References

1. Mei, Y., et al., *Tuning cell adhesion on gradient poly(2-hydroxyethyl methacrylate)-grafted surfaces.* Langmuir : the ACS journal of surfaces and colloids, 2005. **21**(26): p. 12309-12314.
2. Harris, B., et al., *Photopatterned polymer brushes promoting cell adhesion gradients.* Langmuir : the ACS journal of surfaces and colloids, 2006. **22**(10): p. 4467-4471.
3. Raynor, J.E., et al., *Controlling cell adhesion to titanium: Functionalization of poly[oligo(ethylene glycol)methacrylate] brushes with cell-adhesive peptides.* Advanced Materials, 2007. **19**.
4. Mukesh Kumar, V., et al., *Switching of friction by binary polymer brushes.* Soft Matter, 2008. **4**.
5. Limpoco, F.T., R.C. Advincula, and S.S. Perry, *Solvent dependent friction force response of polystyrene brushes prepared by surface initiated polymerization.* Langmuir, 2007. **23**(24): p. 12196-12201.
6. Landherr, L.J.T., et al., *Interfacial friction and adhesion of polymer brushes.* Langmuir, 2011. **27**(15): p. 9387-9395.
7. Sheparovych, R., M. Motornov, and S. Minko, *Adapting low-adhesive thin films from mixed polymer brushes.* Langmuir, 2008. **24**(24): p. 13828-13832.
8. Roosjen, A., et al., *Inhibition of adhesion of yeasts and bacteria by poly(ethylene oxide)-brushes on glass in a parallel plate flow chamber.* Microbiology (Reading, England), 2003. **149**(Pt 11): p. 3239-3246.

9. Cringus-Fundeanu, I., et al., *Synthesis and characterization of surface-grafted polyacrylamide brushes and their inhibition of microbial adhesion.* Langmuir : the ACS journal of surfaces and colloids, 2007. **23**(9): p. 5120-5126.

10. Cullen, S., et al., *Polymeric brushes as functional templates for immobilizing ribonuclease A: study of binding kinetics and activity.* Langmuir : the ACS journal of surfaces and colloids, 2008. **24**(3): p. 913-920.

11. DeRouchey, J., et al., *Monomolecular assembly of siRNA and poly(ethylene glycol)-peptide copolymers.* Biomacromolecules, 2008. **9**(2): p. 724-732.

12. Matthew, T.B., et al., *Nonfouling polymer brushes via surface-initiated, two-component atom transfer radical polymerization.* Macromolecules, 2008. **41**.

13. Tugulu, S. and H.-A. Klok, *Stability and nonfouling properties of poly(poly(ethylene glycol) methacrylate) brushes under cell culture conditions.* Biomacromolecules, 2008. **9**(3): p. 906-912.

14. Jiang, H., et al., *Improvement of hemocompatibility of polycaprolactone film surfaces with zwitterionic polymer brushes.* Langmuir, 2011. **27**(18): p. 11575-11581.

15. Yuan, S., et al., *Surface modification of polycaprolactone substrates using collagen-conjugated poly(methacrylic acid) brushes for the regulation of cell proliferation and endothelialisation.* Journal of Materials Chemistry, 2012. **22**(26): p. 13039-13049.

16. Arnold, R.M. and J. Locklin, *Self-sorting click reactions that generate spatially controlled chemical functionality on surfaces.* Langmuir, 2013. **29**(19): p. 5920-5926.

17. Howarter, J.A. and J.P. Youngblood, *Self-cleaning and anti-fog surfaces via stimuli-responsive polymer brushes.* Advanced Materials, 2007. **19**.

18. Thérien-Aubin, H., L. Chen, and C.K. Ober, *Fouling-resistant polymer brush coatings.* Polymer, 2011. **52**(24): p. 5419-5425.

19. Kobayashi, M., et al., *Wettability and antifouling behavior on the surfaces of superhydrophilic polymer brushes.* Langmuir, 2012. **28**(18): p. 7212-7222.

20. Leermakers, F.A.M., et al., *Effect of a polymer brush on capillary condensation.* Langmuir, 2001. **17**.

21. Smrati, G., et al., *Immobilization of silver nanoparticles on responsive polymer brushes.* Macromolecules, 2008. **41**.

22. Vivek, A.V., S.M. Pradipta, and R. Dhamodharan, *Synthesis of silver nanoparticles using a novel graft copolymer and enhanced particle stability via a "Polymer Brush Effect".* Macromolecular Rapid Communications, 2008. **29**.

23. Ohno, K., et al., *Synthesis of monodisperse silica particles coated with well-defined, high-density polymer brushes by surface-initiated atom transfer radical polymerization.* Macromolecules, 2005. **38**(6): p. 2137-2142.

24. Ohno, K., et al., *Fabrication of ordered arrays of gold nanoparticles coated with high-density polymer brushes.* Angewandte Chemie International Edition, 2003. **42**(24): p. 2751-2754.

25. Kohji, O., et al., *Suspensions of silica particles grafted with concentrated polymer brush: Effects of graft chain length on brush layer thickness and colloidal crystallization.* Macromolecules, 2007. **40**.

26. Nagase, K., et al., *Effects of graft densities and chain lengths on separation of bioactive compounds by nanolayered thermoresponsive polymer brush surfaces.* Langmuir : the ACS journal of surfaces and colloids, 2008. **24**(2): p. 511-517.

27. Xu, L. and C.B. Gorman, *Poly(lactic acid) brushes grow longer at lower temperatures.* Journal of Polymer Science Part A: Polymer Chemistry, 2010. **48**(15): p. 3362-3367.

28. Nair, L.S. and C.T. Laurencin, *Biodegradable polymers as biomaterials.* Progress in Polymer Science, 2007. **32**(8–9): p. 762-798.

29. Robert, D., et al., *Polymeric and biomacromolecular brush nanostructures: progress in synthesis, patterning and characterization.* Soft Matter, 2008. **4**.

30. Wei, X., et al., *Biodegradable poly(ε-caprolactone)–poly(ethylene glycol) copolymers as drug delivery system.* International Journal of Pharmaceutics, 2009. **381**(1): p. 1-18.

31. Woodruff, M.A. and D.W. Hutmacher, *The return of a forgotten polymer—Polycaprolactone in the 21st century.* Progress in Polymer Science, 2010. **35**(10): p. 1217-1256.

32. Carrot, G., et al., *Surface-initiated ring-opening polymerization: A versatile method for nanoparticle ordering.* Macromolecules, 2002. **35**(22): p. 8400-8404.

33. Hu, X., et al., *Comparison of the growth and degradation of poly(glycolic acid) and poly(ε-caprolactone) brushes.* Journal of Polymer Science Part A: Polymer Chemistry, 2013. **51**(21): p. 4643-4649.

34. Choi, I.S. and R. Langer, *Surface-initiated polymerization of l-lactide: Coating of solid substrates with a biodegradable polymer.* Macromolecules, 2001. **34**(16): p. 5361-5363.

35. Möller, M., et al., *Stannous(II) trifluoromethane sulfonate: a versatile catalyst for the controlled ring-opening polymerization of lactides: Formation of stereoregular surfaces from polylactide "brushes".* Journal of Polymer Science Part A: Polymer Chemistry, 2001. **39**(20): p. 3529-3538.

36. Lahann, J. and R. Langer, *Surface-initiated ring-opening polymerization of ε-caprolactone from a patterned poly(hydroxymethyl- p-xylylene).* Macromolecular Rapid Communications, 2001. **22**(12): p. 968-971.

37. Schmidt, A.M., *The synthesis of magnetic core-shell nanoparticles by surface-initiated ring-opening polymerization of ε-Caprolactone.* Macromolecular Rapid Communications, 2005. **26**(2): p. 93-97.

38. Chen, F., et al., *Synthesis of magnetite core–shell nanoparticles by surface-initiated ring-opening polymerization of l-lactide.* Journal of Magnetism and Magnetic Materials, 2008. **320**(13): p. 1921-1927.

39. Chen, J., et al., *Controlled surface-initiated ring-opening polymerization of L-lactide from risedronate-anchored hydroxyapatite nanocrystals: Novel synthesis of biodegradable hydroxyapatite/poly(L-lactide) nanocomposites.* Journal of Polymer Science Part A: Polymer Chemistry, 2011. **49**(20): p. 4379-4386.

40. Olivier, A., et al., *Semi-crystalline poly(ε-caprolactone) brushes on gold substrate via "grafting from" method: New insights with AFM characterization.* European Polymer Journal, 2011. **47**(1): p. 31-39.

41. Cheshmedzhieva, D., et al., *Initiation of ring-opening polymerization of lactide: The effect of metal alkoxide catalyst.* Computational and Theoretical Chemistry, 2012. **995**(0): p. 8-16.

42. Dove, A.P., *Organic catalysis for ring-opening polymerization.* ACS Macro Letters, 2012. **1**(12): p. 1409-1412.

43. Wasserman, S.R., Y.T. Tao, and G.M. Whitesides, *Structure and reactivity of alkylsiloxane monolayers formed by reaction of alkyltrichlorosilanes on silicon substrates.* Langmuir, 1989. **5**(4): p. 1074-1087.

44. Pratt, R.C., et al., *Triazabicyclodecene: A simple bifunctional organocatalyst for acyl transfer and ring-opening polymerization of cyclic esters.* Journal of the American Chemical Society, 2006. **128**(14): p. 4556-4557.

45. Iyer, K.S., et al., *Polystyrene layers grafted to macromolecular anchoring layer.* Macromolecules, 2003. **36**(17): p. 6519-6526.

46. Xu, L., K. Crawford, and C.B. Gorman, *Effects of temperature and ph on the degradation of poly(lactic acid) brushes.* Macromolecules, 2011. **44**(12): p. 4777-4782

CHAPTER 3

MORPHOLOGICAL COMPARISONS OF SOLVENT ANNEALED POLYLACTIDE BLOCK COPOLYMER THIN FILMS USING ATOM TRANSFER RADICAL POLYMERIZATION AND RING-OPENING POLYMERIZATION[1]

[1]Joe B. Grubbs III, Evan N. White, Rachelle M. Arnold, Gareth Shepard, Jenna A. Bilbrey, and Jason Locklin. To be submitted to *Journal of Polymer Science A: Polymer Chemistry*

Abstract

Polystyrene block copolymers (BCPs) using polylactide as a biodegradable sacrificial component (PS-b-PLA) were investigated as precursors for nanoporous membranes. The PS-b-PLA polymers were prepared using the bifunctional initiator 2-hydroxyethyl 2-bromoisobutyrate (HEBIB). Atom transfer radical polymerization (ATRP) was used to synthesize the PS macroinitiator with low dispersity from the bromine end of HEBIB, using gas chromatography to monitor conversion. PLA was then synthesized using the hydroxyl end of HEBIB to fabricate the diblock copolymer. Solvent annealing using THF was employed to create the ordered cylinder domains needed to develop nanopores. Film thicknesses ranging from 20 to 130 nm were investigated to elucidate the role of thickness in the long-range ordering of cylinders during annealing. In addition, two stereoisomers of lactide were studied as sacrificial components to probe morphological changes in the thin films. Degradation studies were carried out using a high pH methanol/water solution in order to promote degradation by hydrolysis.

Introduction

Block copolymer (BCPs) were described by Bates and Fredrickson in 1990 as macromolecules composed of sequences of distinct homopolymers linked by covalent bonds[1]. BCPs have been studied extensively since the turn of the century due to their unique ability to form ordered nanostructures over large areas[2-30]. These highly ordered self-assembled structures have enabled the exploration of nanoporous membranes[8, 31-38] and fabrication of patterned templates[18, 39-45]. Although BCP thin films have the ability to self assemble, they often require an additional process, such as thermal[12] or solvent annealing[23, 46], to achieve the desired long-range order. The development of these tunable architectures must be met with precise control over parameters such as volume fraction of majority/minority phase, film thickness, and annealing conditions to achieve desirable results.

The volume fraction of the constituent blocks can be controlled through chain-growth polymerizations such as ATRP and ring-opening polymerization (ROP). These polymerization techniques allow for the retention of end groups as well as provide low dispersities and exact control over the molecular weight, which is crucial to developing single phase morphologies. ATRP, developed by Matyjaszewski[47] and Sawamoto,[48] is a form of controlled radical polymerization (CRP) that affords precise control of the volume fraction. ROP is another technique that offers high control of this parameter and it also allows for polymerization of monomers that are biodegradable such as lactide. The predetermined coordination/insertion mechanism in which the metal catalyst coordinates to the ester carbonyl, allowing the initiator to insert, is ideal for bio-monomers such as lactide. ATRP and ROP can be used simultaneously in a one-pot polymerization[24] or in the more common two-step manner[22].

In this study, the fabrication of BCPs of PS and PLA was achieved using ATRP and ROP methodologies to produce cylindrical micro-phase separated morphologies. This methodology allows for precise control over the molecular weight, which enables tuning of the volume fractions for control of the specific morphology. The two-step approach employed here utilized the bifunctional initiator HEBIB to polymerize styrene from the bromine end group to a controlled molecular weight and dispersity. The PS-OH macroinitiator was then used to ROP lactide to a controlled molecular weight, achieving a volume fraction of the majority phase around 70.0%. A 70.0% volume fraction of the majority phase allows for horizontal or perpendicular cylinder formation. After the successful generation of 70/30 PS-b-PLA polymers, spin coated films were produced to probe the morphologies exhibited by the two stereoisomers present in the chiral lactide. To develop ordered perpendicular cylinders, we used solvent annealing, which has been successfully used by several groups[7, 10, 16, 19, 23, 46]. In addition, studies were performed on 20, 60, and 130 nm thick films to determine the ideal thickness of BCP films of polystyrene and poly(D, L-lactide) (PDLLA) (PS-b-PDLLA) films to achieve uniform perpendicular cylinders upon solvent annealing. In our studies, 20 and 60 nm films achieved more homogeneous orders than thicker films of amorphous PS-b-PDLLA, whereas the BCP films of PS and poly(l-lactide) (PS-b-PLLA) made with l-lactide produced a crystallized film when annealed under THF. The PS-b-PLLA films completely dewetted when annealed for longer than 45 min.

Experimental

Materials

Tetrahydrofuran (THF), toluene, and dichloromethane (DCM) solvents were purified using a MBraun solvent purification system, while methanol, chlorobenzene, and isopropanol (IPA) were used as received from Fisher Scientific. Ethylene glycol was purchased from Aldrich and dried over molecular sieves (0.4 nm) for at least 2 weeks prior to use. L-Lactide and meso-lactide were received from Purac and placed under a 250 mTorr vacuum for 2 days prior to use. Silicon wafers (orientation <100>, native oxide) were purchased from University Wafer. All other chemicals were purchased from Alfa Aesar, Sigma Aldrich, or TCI and were used as received.

Synthesis of HEBIB

Dry ethylene glycol (30.32 mL, 543.8 mmol) was added to a 250 mL 3-neck round bottom flask that had been dried in a 90 °C oven for 1 h, followed by purging of the flask with N_2 for 10 min. The flask was equipped with an addition funnel, magnetic stir bar, and two rubber septums. The flask was cooled to 0 °C by submerging in an ice bath. Bromoisobutyryl bromide (2.7 mL, 21.7 mmol) was added slowly to the ethylene glycol. The reaction was allowed to stir overnight. The reaction was quenched with 100 mL H_2O and extracted with 100 mL $CHCl_3$ six times. The extracts were dried over anhydrous $MgSO_4$ and filtered, followed by rotary evaporation to remove excess solvent. The initiator was then purified by distillation to yield a pure clear liquid[49].

Synthesis of the polystyrene macroinitiator (PS-OH)

Inhibitor free styrene (9.09 g, 87.3 mmol), *N*,*N*,*N′*,*N′*,*N″*-pentamethyldiethylenetriamine (PMDETA) (22.8 μL), HEBIB (15.8 μL), and methyl ethyl ketone (MEK, 7.0 mL) were placed

in an oven-dried schlenk flask. The components were degassed with Ar for 1.5 h at 0 °C to purge the solution. After degassing with Ar, the Schlenk flask was placed under a stream of N_2 for 10 min. After 10 min, copper bromide (CuBr, 15.7 mg, 109.4 μmol) was added to the degassed solution and immediately placed in a 70 °C oil bath to initiate the polymerization. The reaction was allowed to proceed for about 8 h with aliquots taken periodically to monitor conversion by gas chromatography (GC) to ensure a living-type polymerization was achieved. After reaching 40.0% conversion, the reaction was quenched by opening the flask to air. The product was precipitated in cold methanol to form a white precipitate with no visible trace of residual copper. The white solid was filtered and allowed to dry overnight under a 200 mTorr vacuum.

PS-OH synthesis of the block copolymer of PS-b-PDLLA

A pure white powder of 33,900 Da 1.10 Đ PS-OH (0.5g, 14.7 μmol), meso-lactide (0.48 mg, 3.3 mmol), and 5.0 mL of toluene was placed in a Schlenk flask. The flask was submerged into a temperature-controlled oil bath set to 120 °C. The components were allowed to stir until a homogeneous solution was obtained; then 1.0 μL of tin(II) 2-ethylhexanoate was added to the solution to initiate the polymerization. After 18 h, the reaction was removed from the oil bath and allowed to cool to room temperature. The viscous solution was precipitated 3 times in cold methanol and placed under high vacuum for 72 h to remove any impurities.

PS-OH synthesis of the block copolymer of PS-b-PLLA

A pure white powder of 31,585 Da 1.05 Đ PS-OH (0.5g, 15.8 μmol), meso-lactide (0.48 mg, 3.3 mmol), and 5.0 mL of toluene was polymerized under the exact same conditions as the above PS-b-PDLLA.

Spin coating BCP films on silicon substrates

Silicon wafers were cut into approximately 1×1 cm^2 squares, then sonicated in isopropanol (IPA) and dried with a stream of nitrogen gas. A chlorobenzene solution containing 10, 15, or 20 mg/mL BCP (filtered through a 0.2 μm poly(tetrafluoroethylene) filter) was spin-coated on a clean substrate at 1000, 1500, or 2000 rpm for 30 s (Chemat Technology KW-4A Spin Coater). The thicknesses of the films were varied from 20 to 130 nm for each experiment by changing the concentration and spin speed to reach the desired thicknesses to investigate morphology changes.

Solvent annealing BCP thin films

The BCP substrates were placed in a vacuum desiccator along with an aluminum pan filled with approximately 2 mL THF. The pressure was reduced inside the desiccator to completely cover each substrate with THF vapor. The substrates were removed at various times to check for morphological changes exhibited by the thin film using AFM.

Degradation studies of BCP thin films

PS-b-PLA substrates were placed into capped, flat bottom Schlenk flasks. A 10 mL aliquot of a 0.5 M NaOH methanol/water (60/40 v/v) solution was added to each flask. After various times, the substrates were removed and rinsed with copious amounts of DCM. After drying under a stream of nitrogen gas, AFM was performed to monitor the PLA removal. This procedure was repeated several times.

Characterization

Film thicknesses were determined on a J. A. Woollam M-2000V spectroscopic ellipsometer with a white light source at three angles of incidence (65°, 70°, and 75°) normal to the silicon wafer. A Cauchy model was used to fit the film thickness, extinction coefficient, and

refractive index of the polymer layer. Number and weight average molecular weights of all polymers were estimated using gel permeation chromatography (GPC, Viscotek, Malvern Inc.) with two high molecular weight columns (I-MBHMW-3078) and one low molecular weight column (I-MBLMW-3078). Triple point detection, consisting of refractive index, light scattering, and viscometry, was used. EasiCal polystyrene standards (580–377,500 Da) were used to determine the molecular weights obtained by universal calibration. Gas chromatography (GC) using a SRI 8610C gas chromatograph was used to monitor the polystyrene conversion. AFM images were taken in tapping mode on a Multimode NanoScope IIIa (Digital Instruments/Veeco Metrology) instrument using a silicon AFM probe with a spring constant of 48 N/m and resonant frequency of 190 kHz.

Results and Discussion

Fabrication of a BCP with a biodegradable sacrificial component is an excellent way to reduce the use of petroleum-based resources in high-end applications. To successfully fabricate a BCP using ATRP and ROP that meets the parameters for a homogeneous phase separated morphology, the initiator must be free of impurities. In order to successfully accommodate those two methodologies, an initiator that contains halogen and hydroxyl groups is needed. We identified HEBIB as our target initiator based on the work done by White et al. in 2006[49]. HEBIB was synthesized using a nucleophilic substitution reaction between bromoisobutyryl bromide and ethylene glycol at 0 °C (Scheme 3.1).

Scheme 3.1 Synthesis of 2-hydroxyethyl 2-bromoisobutyrate (HEBIB).

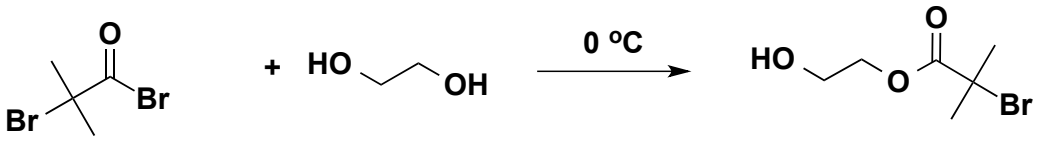

^{1}H NMR was used to track the purity of HEBIB before and after distillation (Figure 3.1). The disappearance of the methylene protons associated with ethylene glycol is crucial for the initiator to produce the homopolymer of PLA at a predetermined molecular weight with no impurities. A small amount of residual hydroxyl functionalities in the solution will hinder the quantitative conversion of lactide to reach the sufficient molecular weight.

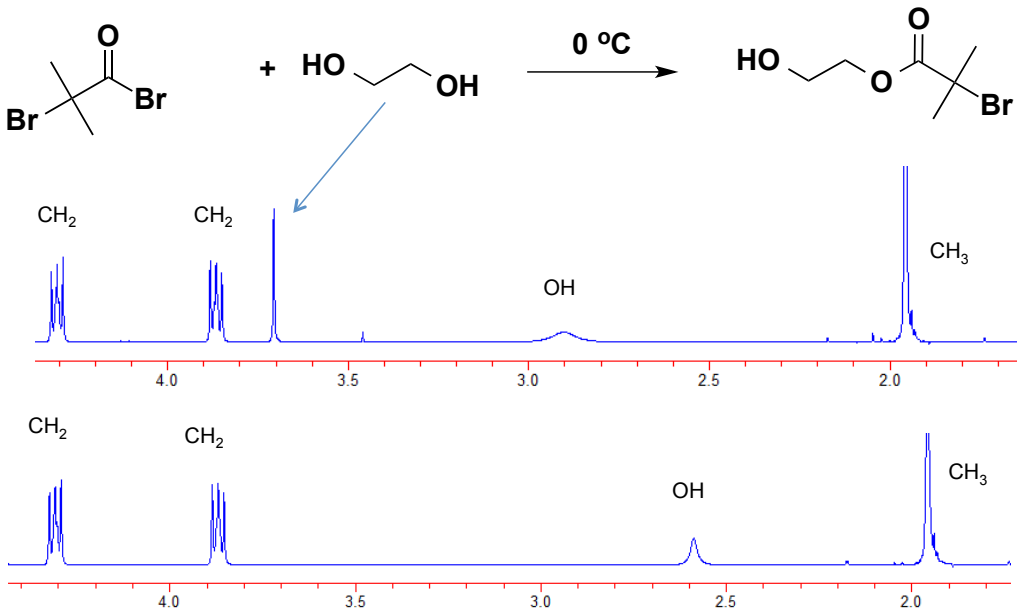

Figure 3.1 ^{1}H NMR (500 MHz) spectra of impure (top) and pure (bottom) HEBIB.

After the successful synthesis of a pure colorless HEBIB, we proceeded to make the PS macroinitiator. PS-OH was synthesized using ATRP, a type of chain-growth polymerization. The macroinitiator was synthesized by degassing inhibitor free styrene, HEBIB, PMDETA, and MEK (Scheme 3.2). The solution was placed in a Schlenk flask in the presence of CuBr at 75 °C to initiate the polymerization.

Scheme 3.2 Synthetic schemes for PS-OH and PS-b-PDLLA.

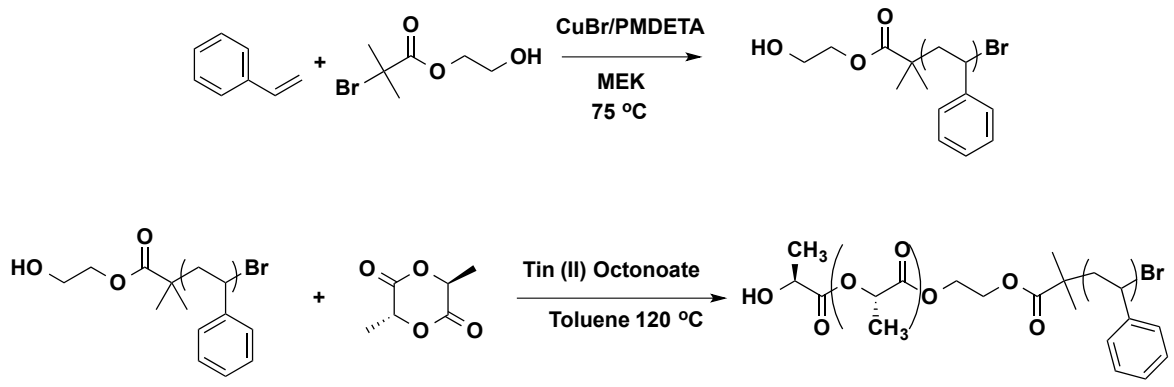

The polymerization kinetics were monitored using GC with a MEK internal standard to track the disappearance of the styrene monomer and determine the percent conversion, as shown by Colombani[50]. Tracking the percent conversion using an internal standard is an excellent way to control the molecular weight and dispersity in ATRP by monitoring the linear first order kinetics of the system (Figure 3.2). In order to ensure a low dispersity and a molecular weight that could be verified by additional techniques such as GPC, the polymerizations were stopped at about 40% conversion. This allowed for the retention of end groups, which could be used to fabricate more complex architectures using post-polymerization techniques such as click chemistry. PS-OH was characterized by GPC to obtain a relative number average molecular

weight (M_n) and dispersity (Đ). The M_n for PS-OH was 33,900 Da with 1.10 Đ, as shown in Figure 3.3.

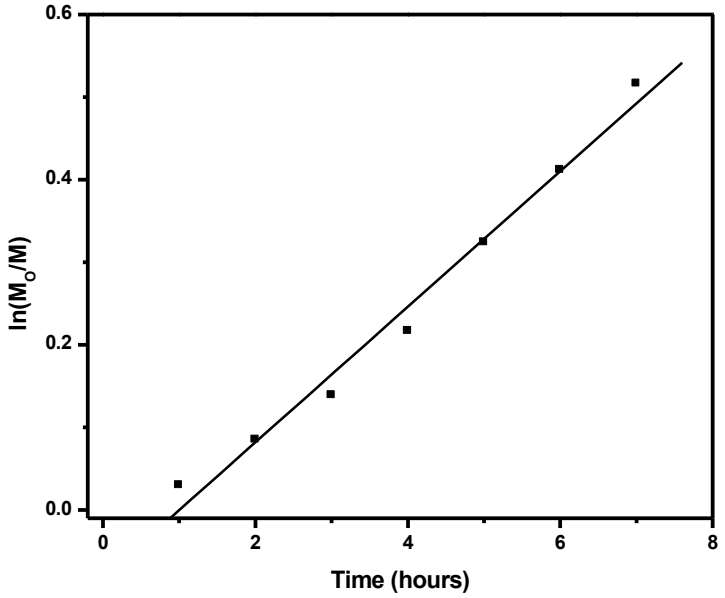

Figure 3.2 GC kinetic tracking of PS-OH during ATRP.

After the successful synthesis of PS-OH and purification of the 33,900 Da macroinitiator, we proceeded to polymerize a completely amorphous block copolymer using meso-lactide (Scheme 3.2). PS-OH, meso-lactide, and toluene were added to a large Schlenk flask, placed in an oil bath at 120 °C, and allowed to stir until a homogenous solution was obtained. The tin catalyst was then added to initiate the polymerization. The reaction was allowed to proceed overnight. After completion, the BCP was precipitated in cold methanol until a white powder was obtained, which was then dried under high vacuum overnight for analysis. GPC indicated that the BCP was formed by showing a single peak at an early elution time (Figure 3.3). The

dispersity remained low at 1.11 Đ and the M_n increased to 46,500 Da. The GPC data confirmed that the BCP theoretically should form the desired cylinders due to the volume fraction of the majority phase PS being about 70% and that of PDLLA being about 30%

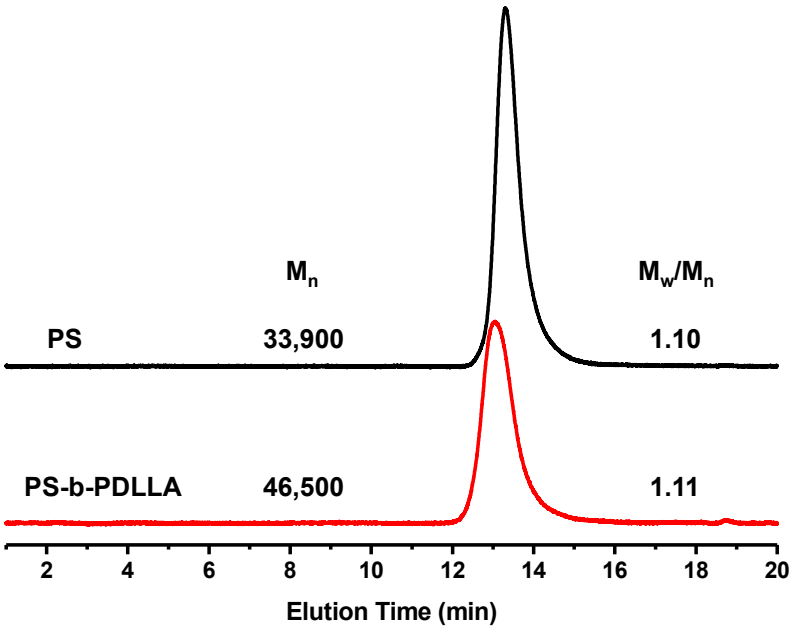

Figure 3.3 GPC traces of PS-OH and PS-b-PDLLA.

To further investigate polylactide BCP morphologies, we synthesized a semi-crystalline stereoisomer of lactide, L-lactide, which was chosen for its availability. The same approach used to synthesize the macroinitiator and PS-b-PDLLA was used to prepare the more crystalline PS-b-PLLA, as shown in Scheme 3.3. GPC yielded similar results when the PS-OH initiator of M_n = 31,585 Da and low 1.05 Đ was used. BCP generation was also confirmed by the peak shift to an earlier elution time and the single peak displayed in the GPC trace (Figure 3.4). The roughly 80 kDa BCP is about 70% PS and 30% PLLA. This consistency with PS-b-PDLLA is desirable because the similar physical properties enable more valid comparisons.

Scheme 3.3 Synthetic schemes for PS-OH and PS-b-PLLA.

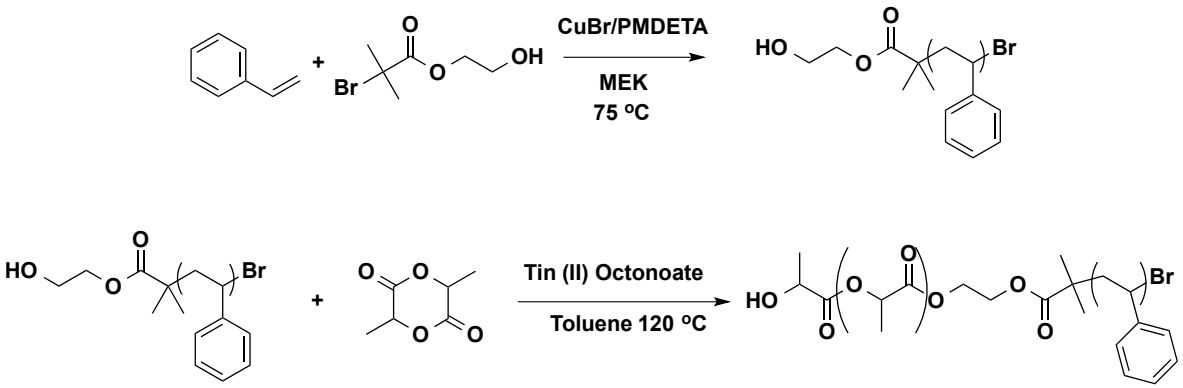

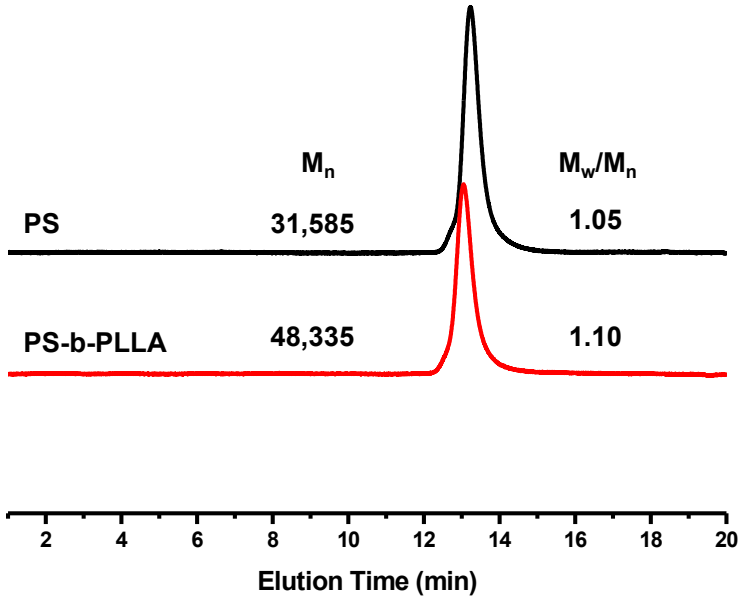

Figure 3.4 GPC traces of PS-OH and PS-b-PLLA.

Once all polymers were carefully synthesized and purified, thin films were spin coated on silicon oxide in order to compare morphological differences and adjust the film thicknesses for post-annealing studies. Film thicknesses were adjusted by varying the spin-coating concentration

in chlorobenzene from 10–20 mg/mL and spin speeds from 1000–2000 rpm. Chlorobenzene was chosen as the solvent because of the similar interaction with PS and PLA. Additionally, chlorobenzene is a high boiling solvent, which allows for longer evaporation times in order to provide time for micro-scale ordering before annealing. The BCP substrates were annealed in a vacuum desiccator under a blanket of THF. The substrates were removed at various times to determine any morphological changes. THF was found to be an ideal solvent for both PS and PLA, as shown in work by Vayer et al[23]. The group also examined solvents such as acetone, chlorobenzene, and THF for annealing PS-b-PLA and concluded that THF was the most favorable solvent[23]. Systems utilizing PLA as a BCP component for ordered nanostructures are prone to thermal degradation,[3, 12] which is another reason that solvent annealing is the ideal approach.

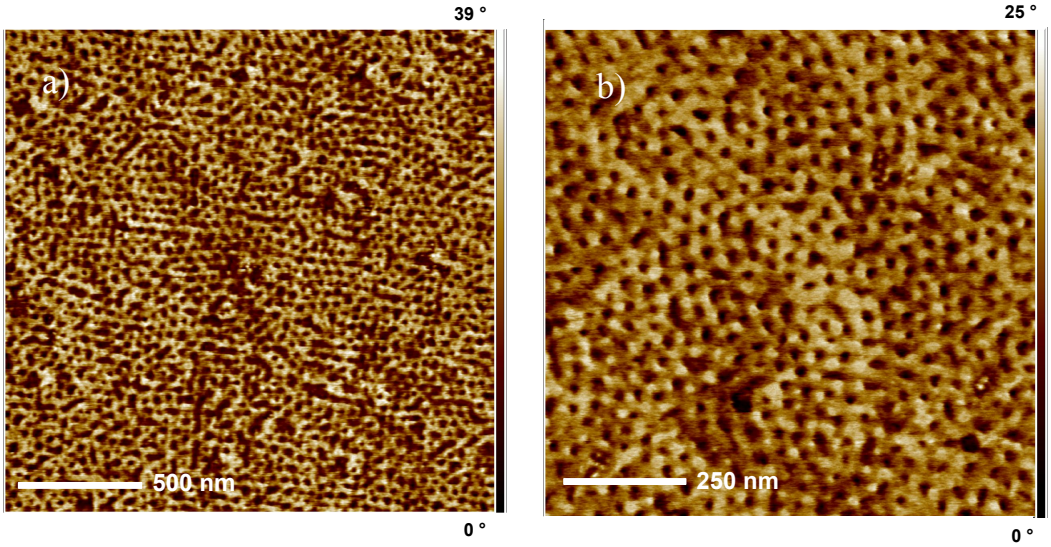

Figure 3.5 AFM phase images of a PS-b-PDLLA 20 nm film a) as spun from chlorobenzene and b) annealed under a blanket of THF for 20 min.

Solvent annealing using THF was employed to examine 20, 60, and 130 nm PS-b-PDLLA thin films and elucidate the role of thickness in achieving ordered perpendicular cylinders. The 20 nm films spun from chlorobenzene that were not subjected to annealing demonstrated perpendicular and horizontal cylinders after spin-coating of 10 mg/mL solutions at 3000 rpm. (Figure 3.5a). Due to this pre-structured morphology, the films were annealed under a blanket of THF for only 20 min. After 20 min, the morphology displayed a honeycomb appearance, which is indicative of homogeneous perpendicular cylinder phase separation, as shown in Figure 3.5b. The thin film has a root mean squared (RMS) roughness of about 3.98 nm with perpendicular PDLLA cylinders having average diameters of about 20 nm.

The 60 nm spin-coated films behaved slightly differently, taking about 2.5 times longer to reach the ordered perpendicular morphology (Figure 3.6). The films were spin-coated using a concentration of 15 mg/mL at 2000 rpm. Annealing the films under a blanket of THF for 25 min produced a morphology that displayed perpendicular and parallel cylinders in almost equal quantities, as shown in Figure 3.6b. The film was allowed to continue annealing for 75 min. The AFM image displayed ordered perpendicular cylinders with several parallel cylinders over a 2 μm x 2 μm area (Figure 3.6c). The film was exposed to THF for another 15 min to ensure the morphology had reached maximum order. From the AFM particle analysis, it was ascertained that the perpendicular cylinders were about 18.5 nm, which is consistent with the 20 nm film. The film roughness was about 4.57 nm, which was slightly higher than the thinner film.

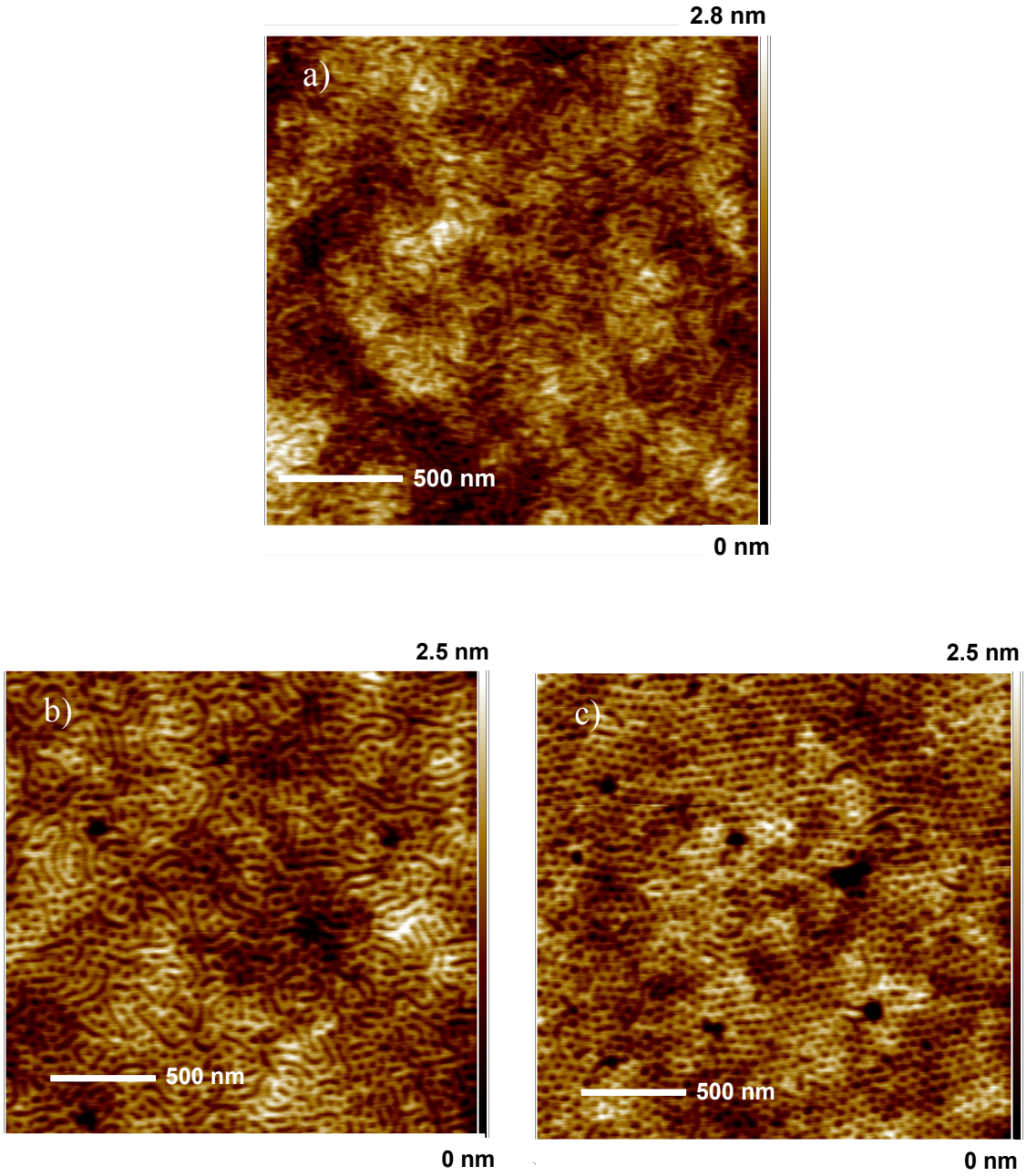

Figure 3.6 AFM height images of the 60 nm PS-b-PDLLA film a) as spun from chlorobenzene, b) annealed under a blanket of THF for 25 min, and c) annealed under a blanket of THF for 75 min.

A thicker 130 nm film was made in order to compare the three thicknesses and probe the ability to form ordered perpendicular cylinders through solvent annealing. To achieve the thicker film a 20 mg/mL concentration solution was used as well as a slower spin speed of 1000 rpm. The film as spun from chlorobenzene displayed almost all parallel cylinders (Figure 3.7a). The film was placed in a desiccator for 40 min under a blanket of THF. After 40 min, the film displayed the partial formation of perpendicular cylinders (Figure 3.7b) but still showed a significant amount of parallel domains. The film was exposed to THF vapors for an additional 180 min but never reached the uniform order required for patterning or membrane applications (Figure 3.7c). Vayer et al. showed that 100 nm films could be easily annealed to a uniform perpendicular morphology under THF[23], so a cut-off from obtaining homogeneous order in these thicker films may have been reached. The film roughness increased slightly to 5.72 nm, but the average diameter of the perpendicular cylinders remained constant.

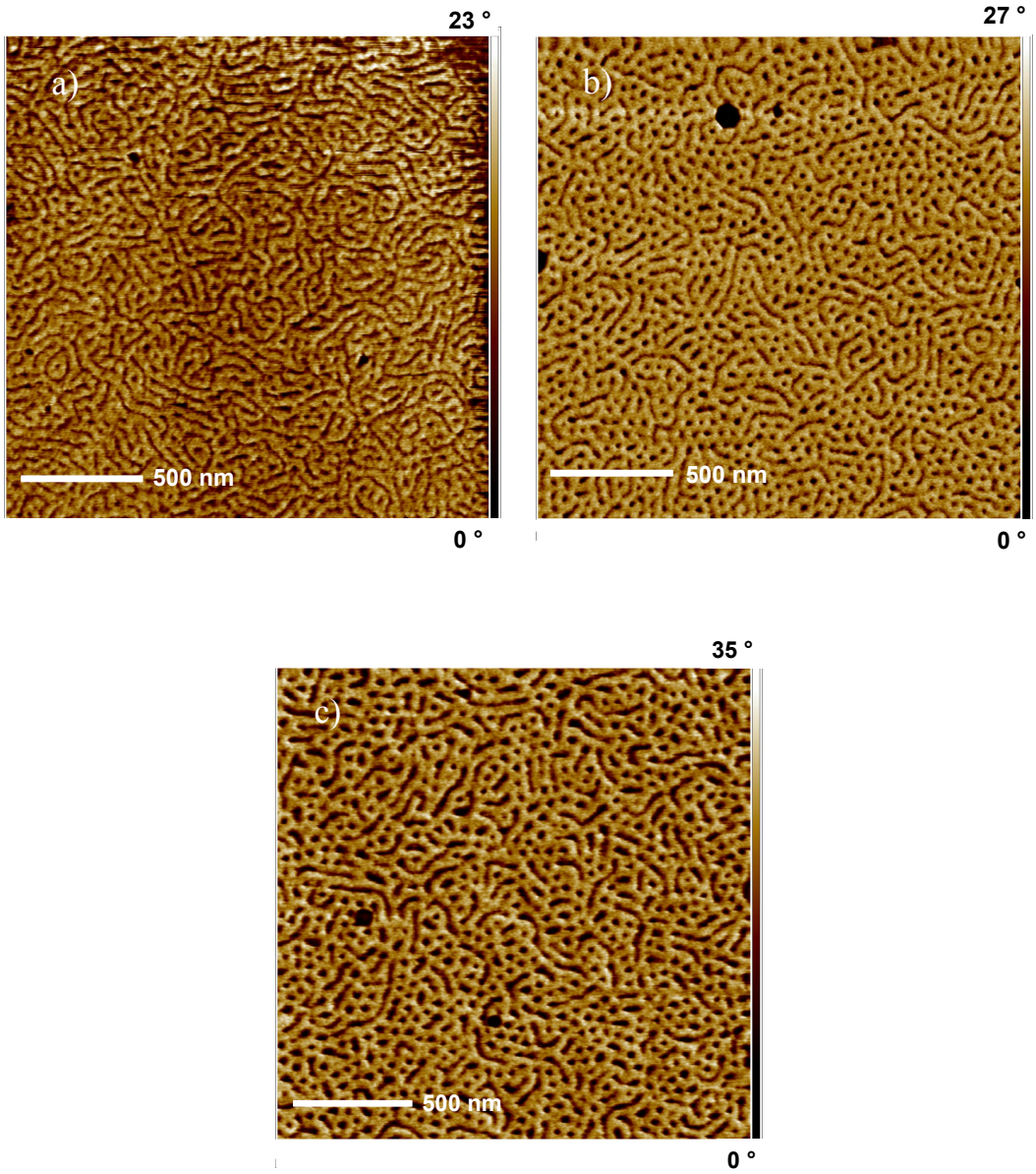

Figure 3.7 AFM phase images of 130 nm PS-b-PDLLA films a) as spun from chlorobenzene, b) annealed for 40 min under a blanket of THF, and c) annealed for 220 min under a blanket of THF.

After examining the formation of ordered nanostructures at various thicknesses, we examined a more crystalline BCP using l-lactide. It was our hypothesis that the films using l-lactide could not be annealed to an ordered morphology with THF. Ho et al.[5] synthesized

BCPs using l-lactide to create ordered morphologies from spin-coating but never annealed the films to examine the annealing-induced crystallization of the lactide block. The 65 nm film spin-coated from chlorobenzene failed to show a significant morphological distinction from the as-spun sample (Figure 3.8a). After exposing the film to THF vapors for 45 min, the film formed large crystallites that were about 650 nm in diameter (Figure 3.8b). The annealed film displayed a roughness of about 12.4 nm, which is indicative of crystalline behavior. The film was exposed to additional THF vapors for another 45 min, which caused the film to dewet, as illustrated in Figure 3.9.

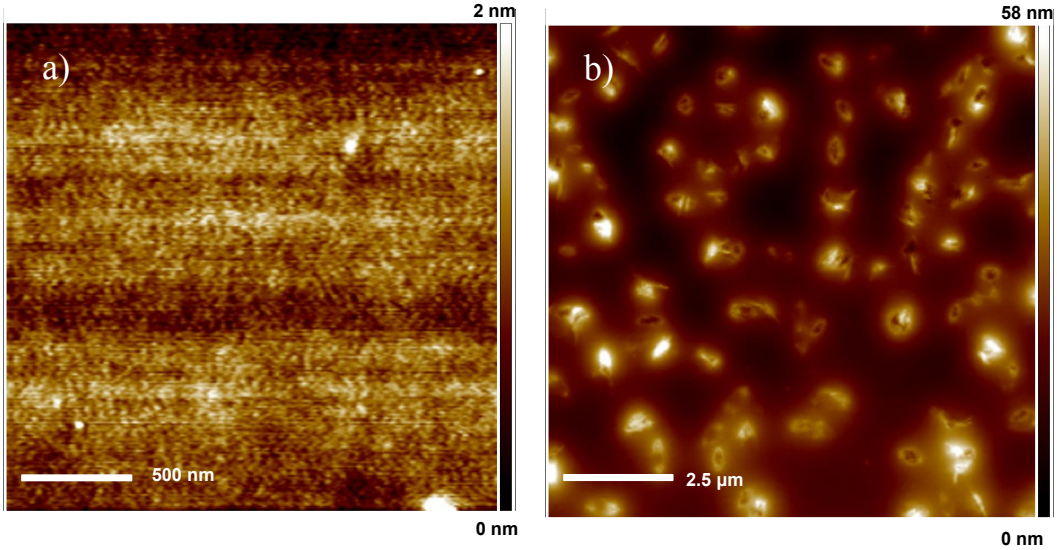

Figure 3.8 AFM height images of the 65 nm PS-b-PLLA film a) as spun from chlorobenzene and b) annealed under a blanket of THF for 45 min.

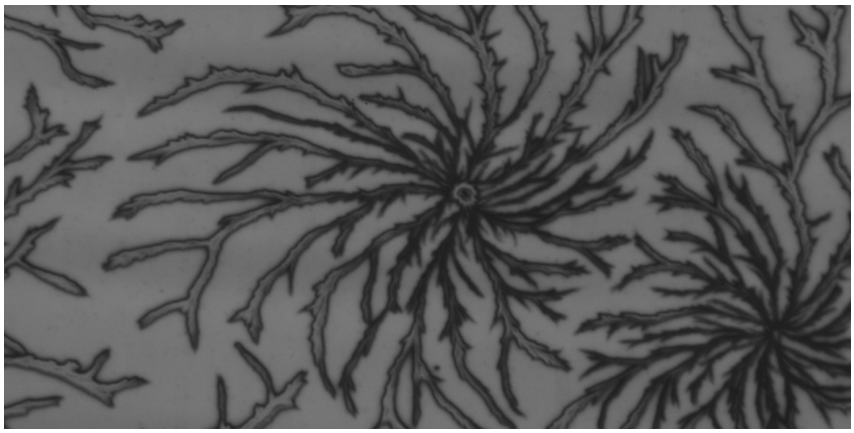

Figure 3.9 Optical image of dewetted PS-b-PLLA after annealing for 90 min in THF.

Once perpendicular ordered nanostructures of PS-b-PDLLA were obtained, degradation studies were carried out at room temperature. PS-b-PLA substrates were placed into a capped, flat bottom flask and a 10 mL aliquot of a 0.5 M NaOH methanol/water (60/40 v/v) solution was added[23]. The high pH solution assured that hydrolysis would be the primary mechanism for removal of the PLA cylinders. However, in our studies this technique proved to be unsuccessful in etching the PLA completely. The films were partially etched, and after 30 min, the films completely delaminated. We imaged the delaminated films by AFM as shown in Figure 3.10, but were unable to completely produce a porous membrane using the 0.5 M NaOH methanol/water (60/40 v/v) solution. However, this would be a good technique to float the film after complete etching was achieved.

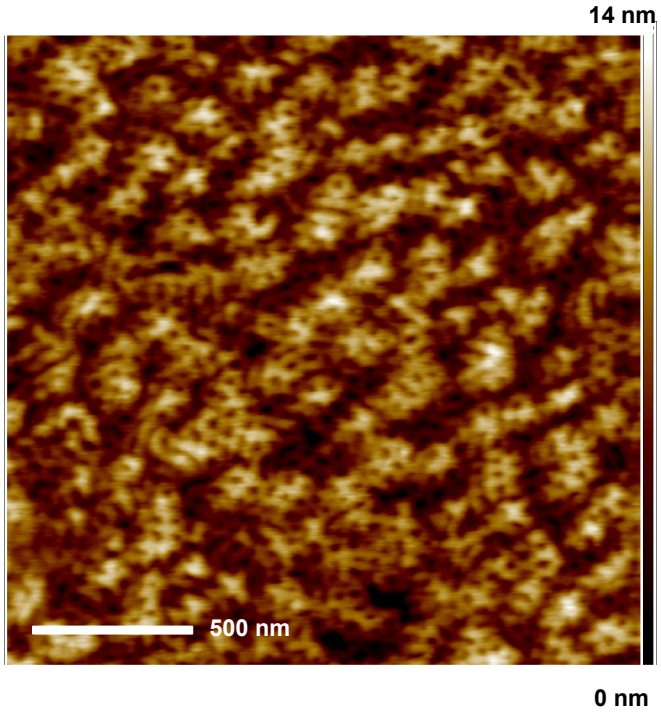

Figure 3.10 AFM image of PS-b-PDLLA etched and delaminated using a 0.5 M NaOH methanol/water (60/40 v/v) solution.

Conclusions

In conclusion, BCPs of PS and PLA were synthesized using the purified bifunctional initiator HEBIB to accommodate controlled polymerization by ATRP and ROP. ATRP and ROP allowed precise control over the molecular weight and dispersity, which are two key factors in BCP self assembly. Using these polymerization techniques, a BCP was successfully fabricated to provide a PS majority phase around 70% and a PLA minority phase around 30%. By synthesizing the BCP to a M_n around 80 kDa and a volume fraction around 70:30, ordered cylindrical phase separation was obtained. In this work, it was elucidated that films of 20 and 60

nm could be solvent annealed using THF to create a honeycomb morphology that achieved long-range order and displayed perpendicular cylinder domains with diameters of 20 nm. It was also shown that 20 nm films achieved long-range order with exposure to THF for only 20 min, which was significantly faster than the 60 nm film. Once the film reached 130 nm, it was unable to orient into perpendicular cylindrical domains that would be practical for membranes or patterning. It was also shown that 65 nm films containing a BCP using l-lactide as the minority phase developed crystallinity and dewetted after solvent annealing for more than 45 min. Films containing l-lactide have shown limitations in further inducing order due to the crystalline nature of the lactide. Therefore, crystalline films must be completely ordered by spin coating as opposed to inducing order through annealing.

References

1. Bates, F.S. and G.H. Fredrickson, *Block copolymer thermodynamics: Theory and experiment.* Annual Review of Physical Chemistry, 1990. **41**(1): p. 525-557.
2. Chakrabarti, A., R. Toral, and J.D. Gunton, *Microphase separation in block copolymers.* Physical Review Letters, 1989. **63**(24): p. 2661-2664.
3. Guo, S., et al., *Nanopore and nanobushing arrays from abc triblock thin films containing two etchable blocks.* Chemistry of Materials, 2006. **18**(7): p. 1719-1721.
4. Han, E., et al., *Perpendicular orientation of domains in cylinder-forming block copolymer thick films by controlled interfacial interactions.* Macromolecules, 2009. **42**(13): p. 4896-4901.
5. Ho, R.-M., et al., *Solvent-induced microdomain orientation in polystyrene-b-poly(l-lactide) diblock copolymer thin films for nanopatterning.* Polymer, 2005. **46**(22): p. 9362-9377.
6. Horechyy, A., et al., *Nanoparticle directed domain orientation in thin films of asymmetric block copolymers.* Colloid and Polymer Science, 2014. **292**(9): p. 2249-2260.
7. Huang, W.-H., P.-Y. Chen, and S.-H. Tung, *Effects of annealing solvents on the morphology of block copolymer-based supramolecular thin films.* Macromolecules, 2012. **45**(3): p. 1562-1569.
8. Jackson, E.A. and M.A. Hillmyer, *Nanoporous membranes derived from block copolymers: from drug delivery to water filtration.* ACS Nano, 2010. **4**(7): p. 3548-3553.
9. Kuech, T.F. and L.J. Mawst, *Nanofabrication of III–V semiconductors employing diblock copolymer lithography.* Journal of Physics D: Applied Physics, 2010. **43**(18): p. 183001.

10. Lee, D.H., et al., *Ordering evolution of block copolymer thin films upon solvent-annealing process.* Journal of Colloid and Interface Science, 2012. **383**(1): p. 118-123.

11. Nagpal, U., et al., *Free energy of defects in ordered assemblies of block copolymer domains.* ACS Macro Letters, 2012. **1**(3): p. 418-422.

12. Olayo-Valles, R., et al., *Perpendicular domain orientation in thin films of polystyrene−polylactide diblock copolymers.* Macromolecules, 2005. **38**(24): p. 10101-10108.

13. Park, S.-M., et al., *Patterning sub-10 nm line patterns from a block copolymer hybrid.* Nanotechnology, 2008. **19**(45): p. 455304.

14. Peinemann, K.-V., V. Abetz, and P.F.W. Simon, *Asymmetric superstructure formed in a block copolymer via phase separation.* Nat Mater, 2007. **6**(12): p. 992-996.

15. Perego, M., et al., *Collective behavior of block copolymer thin films within periodic topographical structures.* Nanotechnology, 2013. **24**(24): p. 245301.

16. Qiang, Z., et al., *A generalized method for alignment of block copolymer films: solvent vapor annealing with soft shear.* Soft Matter, 2014. **10**(32): p. 6068-6076.

17. Raman, V., et al., *Long-Range ordering of symmetric block copolymer domains by chaining of superparamagnetic nanoparticles in external magnetic fields.* Macromolecules, 2012. **45**(23): p. 9373-9382.

18. Segalman, R.A., *Patterning with block copolymer thin films.* Materials Science and Engineering: R: Reports, 2005. **48**(6): p. 191-226.

19. Stenbock-Fermor, A., et al., *Enhancing ordering dynamics in solvent-annealed block copolymer films by lithographic hard mask supports.* Macromolecules, 2014. **47**(9): p. 3059-3067.

20. Stuen, K.O., et al., *Graphoepitaxial assembly of asymmetric ternary blends of block copolymers and homopolymers.* Nanotechnology, 2010. **21**(49): p. 495301.

21. Stuparu, M.C., A. Khan, and C.J. Hawker, *Phase separation of supramolecular and dynamic block copolymers.* Polymer Chemistry, 2012. **3**(11): p. 3033-3044.

22. Tao, L., B. Luan, and C.-y. Pan, *Block and star block copolymers by mechanism transformation. VIII Synthesis and characterization of triblock poly(LLA-b-St-b-MMA) by combination of ATRP and ROP.* Polymer, 2003. **44**(4): p. 1013-1020.

23. Vayer, M., et al., *Perpendicular orientation of cylindrical domains upon solvent annealing thin films of polystyrene-b-polylactide.* Thin Solid Films, 2010. **518**(14): p. 3710-3715.

24. Wolf, F.F., N. Friedemann, and H. Frey, *Poly(lactide)-block-poly(hema) block copolymers: an orthogonal one-pot combination of rop and atrp, using a bifunctional initiator.* Macromolecules, 2009. **42**(15): p. 5622-5628.

25. Yoshida, S., T. Ono, and M. Esashi, *Conductive polymer patterned media fabricated by diblock copolymer lithography for scanning multiprobe data storage.* Nanotechnology, 2008. **19**(47): p. 475302.

26. Knoll, A., et al., *Phase behavior in thin films of cylinder-forming block copolymers.* Physical Review Letters, 2002. **89**(3): p. 035501.

27. Elhadj, S., et al., *Orientation of self-assembled block copolymer cylinders perpendicular to electric field in mesoscale film.* Applied Physics Letters, 2003. **82**(6): p. 871-873.

28. Leibler, L., *Theory of microphase separation in block copolymers.* Macromolecules, 1980. **13**(6): p. 1602-1617.

29. Kim, J.K., et al., *Functional nanomaterials based on block copolymer self-assembly.* Progress in Polymer Science, 2010. **35**(11): p. 1325-1349.

30. Darling, S.B., *Directing the self-assembly of block copolymers.* Progress in Polymer Science, 2007. **32**(10): p. 1152-1204.

31. Chen, L., et al., *Robust nanoporous membranes templated by a doubly reactive block copolymer.* Journal of the American Chemical Society, 2007. **129**(45): p. 13786-13787.

32. Hillmyer, M., *Nanoporous materials from block copolymer precursors*, in *block copolymers II*, V. Abetz, Editor. 2005, Springer Berlin Heidelberg. p. 137-181.

33. Phillip, W.A., et al., *Gas and water liquid transport through nanoporous block copolymer membranes.* Journal of Membrane Science, 2006. **286**(1–2): p. 144-152.

34. Yang, S.Y., et al., *Virus filtration membranes prepared from nanoporous block copolymers with good dimensional stability under high pressures and excellent solvent resistance.* Advanced Functional Materials, 2008. **18**(9): p. 1371-1377.

35. Phillip, W.A., et al., *Self-assembled block copolymer thin films as water filtration membranes.* ACS Applied Materials & Interfaces, 2010. **2**(3): p. 847-853.

36. Sperschneider, A., et al., *Towards nanoporous membranes based on abc triblock terpolymers.* Small, 2007. **3**(6): p. 1056-1063.

37. Nunes, S.P., et al., *Ultraporous films with uniform nanochannels by block copolymer micelles assembly.* Macromolecules, 2010. **43**(19): p. 8079-8085.

38. Bang, J., et al., *Defect-free nanoporous thin films from abc triblock copolymers.* Journal of the American Chemical Society, 2006. **128**(23): p. 7622-7629.

39. Park, C., J. Yoon, and E.L. Thomas, *Enabling nanotechnology with self assembled block copolymer patterns.* Polymer, 2003. **44**(22): p. 6725-6760.

40. Olson, D.A., L. Chen, and M.A. Hillmyer, *Templating nanoporous polymers with ordered block copolymers†.* Chemistry of Materials, 2007. **20**(3): p. 869-890.

41. Bang, J., et al., *Block copolymer nanolithography: Translation of molecular level control to nanoscale patterns.* Advanced Materials, 2009. **21**(47): p. 4769-4792.

42. Wang, Y., et al., *Nanoporous metal membranes with bicontinuous morphology from recyclable block-copolymer templates.* Advanced Materials, 2010. **22**(18): p. 2068-2072.

43. Park, S., et al., *A simple route to highly oriented and ordered nanoporous block copolymer templates.* ACS Nano, 2008. **2**(4): p. 766-772.

44. Lee, J.I., et al., *Highly aligned ultrahigh density arrays of conducting polymer nanorods using block copolymer templates.* Nano Letters, 2008. **8**(8): p. 2315-2320.

45. Park, S., et al., *From nanorings to nanodots by patterning with block copolymers.* Nano Letters, 2008. **8**(6): p. 1667-1672.

46. Cavicchi, K.A., K.J. Berthiaume, and T.P. Russell, *Solvent annealing thin films of poly(isoprene-b-lactide).* Polymer, 2005. **46**(25): p. 11635-11639.

47. Wang, J.-S. and K. Matyjaszewski, *Controlled/"living" radical polymerization. atom transfer radical polymerization in the presence of transition-metal complexes.* Journal of the American Chemical Society, 1995. **117**(20): p. 5614-5615.

48. Kato, M., et al., *Polymerization of methyl methacrylate with the carbon tetrachloride/dichlorotris- (triphenylphosphine)ruthenium(ii)/methylaluminum bis(2,6-di-tert-butylphenoxide) initiating system: Possibility of living radical polymerization.* Macromolecules, 1995. **28**(5): p. 1721-1723.

49. White, M.A., et al., *Toward the syntheses of universal ligands for metal oxide surfaces: Controlling surface functionality through click chemistry.* Journal of the American Chemical Society, 2006. **128**(35): p. 11356-11357.

50. Colombani, O., et al., *Polymerization kinetics: Monitoring monomer conversion using an internal standard and the key role of sample t0.* Journal of Chemical Education, 2010. **88**(1): p. 116-121.

CHAPTER 4

CONCLUSIONS AND OUTLOOK

Conclusions

This dissertation detailed the synthesis and investigation of biodegradable BCPs incorporating PLA and PCL as the degradable components. These materials were used as polymer coatings and thin films with tunable degradation rates and nanoscale phase separated morphologies. The manipulation of the BCP morphologies and interfacial properties have allowed for the generation of ordered cylinder domain patterns and the formation of tailored surface coatings.

In Chapter 2, the organocatalyst TBD was employed using SI-ROP of PCL polymer brushes that were 40 nm in thicknesses. The generation of thicknesses greater than 15 nm using a novel approach was described herein. Creating a uniform, well-packed monolayer enabled the synthesis of a densely packed PCL brush layer with unique, crystalline topology. The use of the TBD catalyst enabled the retention of end groups on the PCL homopolymer brush and allowed for chain extension using a zirconium catalyst to successfully generate the PLA layer. The fabrication of BCPs using SI-ROP in a two-pot synthetic strategy allowed for the first reported generation of these architectures. The topology of the BCP underwent changes after the addition of PLA and further changes were elucidated when the brushes were exposed to solvent annealing using THF. The annealed film showed significant changes in topology with the appearance of cylindrical pillars around 78 nm in diameter throughout the film. The generation of the cylinder

pillars increased the roughness and crystallinity of the film, which suggested an increase in the hydrophobicity of the BCP film. We have demonstrated in this chapter a successful route to generate 40 nm PCL films with an organocatalyst and chain extension to produce PCL-b-PLA BCP brushes that can be annealed to change its physical properties.

It has also been demonstrated in this work that the degradation kinetics can be accelerated by adding methanol to solvate the polymer brush and by increasing the pH of the etching solution to 14. The degradation of grafted to PCL brushes was 6 times faster than grafted from PCL homopolymer brushes, while the annealed BCP brush exhibited even slower kinetics than the homopolymer. Utilizing this degradation technique is ideal for protective coatings that require a degradable layer that can be quickly and easily removed.

In Chapter 3, BCPs of PS and PLA were synthesized using a prefabricated purified bifunctional initiator HEBIB with hydroxyl and bromine functional groups. Two controlled polymerization techniques were used to allow for precise control over volume fraction by tailoring the molecular weight and dispersity. ATRP and ROP satisfied the two specific requirements for BCP microscale self assembly for each respective monomer. Using these polymerization techniques, a BCP was successfully fabricated to provide a PS majority phase around 70% and a PLA minority phase around 30%. By synthesizing the BCP to a M_n around 80 kDa and a volume fraction around 70:30, ordered cylindrical phase separation was obtained. It was elucidated that films of 20 and 60 nm could be solvent annealed using THF to create a honeycomb morphology that achieved long-range order and displayed perpendicular cylinder domains with diameters of 20 nm. It was also shown that 20 nm films achieved long-range order with exposure to THF for only 20 min, which was significantly faster than the 60 nm film. Once the film reached 130 nm, the films were no longer able to orient into ordered perpendicular

cylindrical domains. In addition, 65 nm films containing a BCP using l-lactide as the minority phase developed large crystalline domains when exposed to THF vapors. After exposure to THF solvent annealing for more than 45 min, the films completely dewet from the substrate. Films containing the crystalline lactide stereoisomers have shown limitations in this work and for practical applications, no further ordering could be achieved. Therefore, crystalline films must be completely ordered by spin coating as opposed to inducing order through solvent annealing.

Future Outlook

Over the course of my PhD research a fundamental understanding of block copolymer synthesis has been demonstrated and studied extensively using systems that contain a biodegradable component. A library of different molecular weight polystyrene macroinitiators has been created to enable the synthesis of varying molecular weight block copolymer systems. This library will allow for the fine-tuning of PS-b-PLA polymers in order to obtain various volume fractions for phase separation and allow for variations in cylinder domain diameters. Although this project began with PS-b-PLA systems, the overall goal was to achieve more specialized systems after fabrication of these unique architectures.

Some of the new systems that we would like to investigate for potential membrane applications are block copolymers that use polylactide and various acrylates. It is our hypothesis that by utilizing ATRP to incorporate an acrylate into a block copolymer with PLA, we can fabricate more specialized polymers that will one day have the potential to be completely bio-sourced. Some of the potential acrylates that will be explored are butyl acrylate, butyl methacrylate, methyl methacrylate, tertbutyl methacrylate, and spiropyran methacrylate, a photochromic material (Scheme 4.1). These monomers were chosen because they have

significantly different solubility parameters than PLA, which should allow for the formation of cylinder phase separated morphologies. We hypothesize that by tailoring the volume fraction of these systems through controlling the molecular weight and dispersity, a porous membrane can be obtained after selective etching of PLA. It should be noted that although polystyrene block copolymer nanoporous systems are common in the literature, acrylate systems would allow for post-polymerization modification to enable the application specific sensing such as covalently attaching biocides for bacteria death efficacy. Also, the incorporation of spiropyran methacrylate into the block copolymer would allow for the production of the first light-switchable block copolymer membrane. This would allow for sensing to be turned on and off by light actuation.

Scheme 4.1: Conditions for spiropyran-co-butyl methacrylate macroinitiator synthesis and the addition of lactide to form a light-switchable block copolymer (PLA-b-SPMAcoBMA).

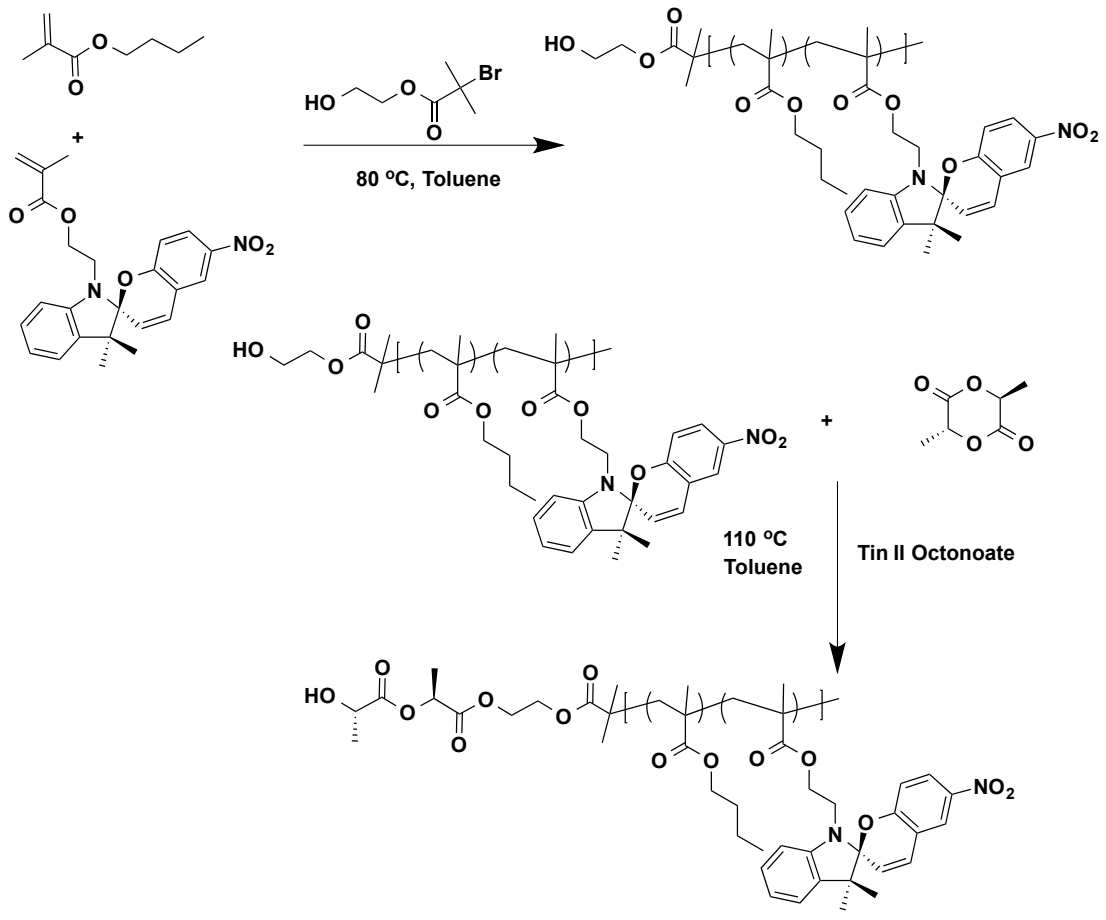

Although PLA and the acrylates have a lot of potential in the block copolymer membrane world, thermoresponsive polymers linked with PLA have the greatest potential in the near future. We plan to investigate a block copolymer system that uses PLA and *N*-isopropylacrylamide (NIPAM) (Scheme 4.2). We believe that due to the solubility difference and vastly different properties of these two blocks that this polymer could offer great promise. We hypothesize that with some tailoring PLA-b-PNIPAM membranes could offer an ideal solution to leaky baby diapers. Due to the thermal properties of NIPAM at human body temperature and the

temperature of urine when it passes, there may be potential for having a membrane in a diaper that may expand and contract as temperature changes. This could be very beneficial if one can tailor the properties for the pores to open when it is heated and collapse when it is cooled.

Scheme 4.2: Synthetic scheme for a *N*-isopropylacrylamide macroinitiator and addition of lactide to form a thermoresponsive block copolymer (PLA-b-PNIPAM).

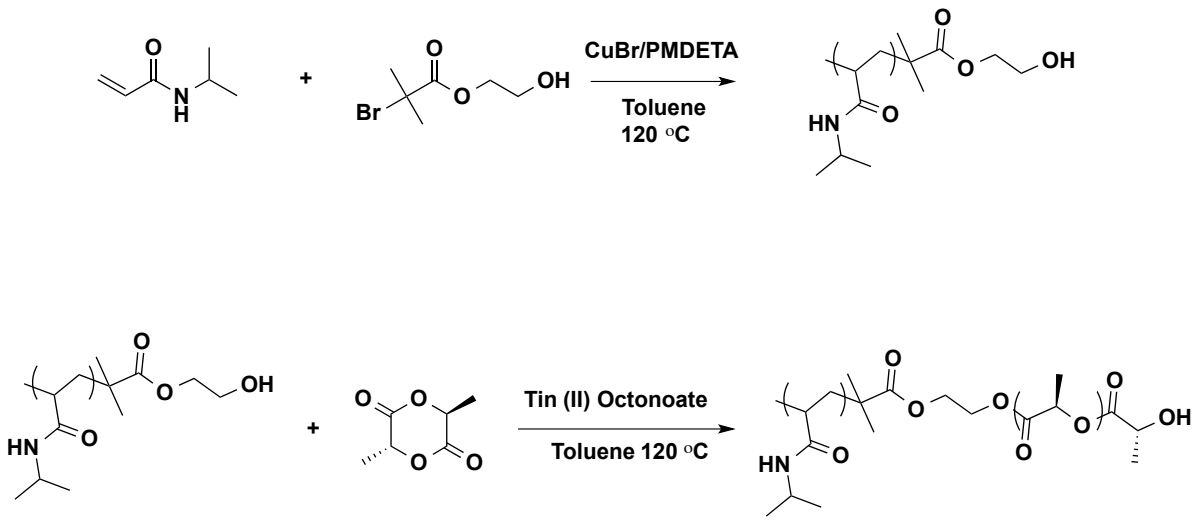

Although this project is just beginning, we believe that it has the potential to be continued by other talented students for years to come. Applications for thermoresponsive and light-switchable membranes offer great promise for directing future research. We look forward to developing porous membranes in this project and tailoring them to be suitable for a wide range of applications.

Final Remarks

In summary, this dissertation has expanded the capability of generating biodegradable homopolymer and BCP brushes to thicknesses not previously observed using the organocatalyst TBD. These brushes allow for tunable degradation rates as well as unique morphological changes when exposed to various solvent-based conditions. BCP thin films were also generated to fabricate phase separated morphologies. PS-b-PLA polymers were prepared to specific volume fractions to produce cylinder phase morphologies using ATRP and ROP. The morphologies were further tuned by solvent annealing with THF to achieve long-range order.

In conclusion, there are many practical applications for tailored tunable BCPs fabricated without the use of our petroleum resources. Biodegradable BCPs can be used to help modulate the time release of fertilizers and provide protection to stored devices through surface coatings. Also, BCP phase separated morphologies can be used to create patterned membranes for drug delivery by diffusion and water filtration through semipermeable membranes.